

1
2
3
4
5
6
7
8
9
10
11
12
13
14
15
16
17
18
19
20
21
22

Measurement report: Impact of domestic heating on dust
deposition sources in hyper-arid Qaidam Basin, northern
Qinghai-Xizang Plateau

Haixia Zhu^{abc}, Lufei Zhen^{abc}, Suping Zhao^{d*}, Xiying Zhang^{ab*}

^a Key Laboratory of Green and High-end Utilization of Salt Lake Resources, Qinghai Institute of Salt Lakes, Chinese Academy of Sciences, Xining, 810008, China.
^b Qinghai Provincial Key Laboratory of Geology and Environment of Salt Lakes, Qinghai Institute of Salt Lakes, Chinese Academy of Sciences, Xining, 810008, China.
^c University of the Chinese Academy of Sciences, Beijing, 100049, China
^d Key Laboratory of Cryospheric Science and Frozen Soil Engineering, Northwest Institute of Eco-Environment and Resources, Chinese Academy of Sciences, Lanzhou, 730000, China
** Corresponding author. E-mail address: xyzhchina@isl.ac.cn (Xiying Zhang) and zhaosp@lzb.ac.cn (Suping Zhao)*

23 **Highlights**

24 1. The temporal and spatial distribution of carbonaceous aerosols was analyzed using various carbon
25 indicators.

26 2. Domestic heating significantly increased atmospheric pollutants in rural areas.

27 3. The unique energy structure in Qaidam Basin significantly influenced the glaciers of the
28 Qinghai-Xizang Plateau and should not be overlooked.

29

30 Abstract

31 ~~Given the unique energy profile of the Qaidam Basin (QDB), it is crucial to examine the impacts of~~
32 ~~domestic heating on the Qinghai-Xizang Plateau (QXP) and global atmospheric systems. This study~~
33 ~~collected monthly dust deposition at six sites in the southern QDB between 2020 and 2023. We~~
34 ~~identified the sources of dust fall during domestic heating (HP) and non-heating periods (NHP) in~~
35 ~~urban and rural areas and its environmental effects. The results demonstrated that domestic heating~~
36 ~~increased the concentration of water-soluble ions in rural areas, trace elements in urban areas, and~~
37 ~~carbon emissions in both. Among various carbon indicators, organic carbon (OC) and element~~
38 ~~carbon (EC) levels rose during the HP, with Char-EC as the primary component of EC (80.44%).~~
39 ~~Char-EC concentrations were higher in urban areas (85.00%), while secondary organic carbon~~
40 ~~(68.17%), the main contributor to OC, was more prevalent in rural (73.92%). The OC/EC ratio in~~
41 ~~urban areas remained stable with an average of 2.16. In contrast, the rural OC/EC ratio was~~
42 ~~significantly higher during the NHP (7.27 ± 4.66) than during the HP (4.57 ± 3.02). Additionally,~~
43 ~~the char/soot ratio was elevated in the HP (5.06 ± 4.08) compared to the NHP (4.42 ± 3.09). The~~
44 ~~OC/EC and char-EC/soot-EC ratios, along with PMF results, indicated that coal combustion~~
45 ~~(17.28%) and biomass burning (32.50%) were the main contributors to dust deposition in rural areas,~~
46 ~~strongly influenced by domestic heating, whereas urban dust predominantly originated from traffic~~
47 ~~(44.43%) and industrial emissions (16.41%). Coal consumption in QDB was greater during the HP~~
48 ~~than that of other dust sources in the QXP. This increased consumption leads to higher emissions of~~
49 ~~atmospheric pollution, which may accelerate glacier melting in the region. Consequently,~~
50 ~~integrating QDB carbon aerosols into future environmental policies and climate models for the QXP~~
51 ~~is essential. This study provides a reference for investigating carbonaceous aerosols in climatically~~
52 ~~similar hyper-arid basins with intensive human activity and salt lake regions.~~

53 Given the unique energy structure of the Qaidam Basin (QDB), this study systematically reveals the
54 spatiotemporal variations in the chemical composition of atmospheric dust deposition and clarifies
55 the key contributions of coal and biomass burning to carbonaceous aerosols, as well as their potential
56 impacts on the Qinghai-Xizang Plateau (QXP) and global atmospheric systems. Monthly dust
57 deposition samples were collected at six sites in the southern QDB between 2020 and 2023. Results
58 indicated heightened carbon emissions and the higher char/soot ratio during the heating period (HP,

59 5.06 ± 4.08) than the non-heating period (NHP, 4.42 ± 3.09), indicating intensified seasonal solid
60 fuel consumption. Spatially, the organic carbon (OC) and elemental carbon (EC) ratio was
61 significantly lower in urban (3.97 ± 2.04) than that in rural areas (10.99 ± 10.00). Char-EC
62 dominated EC (80.44%), especially in urban areas (85.00%), while secondary organic carbon (SOC)
63 dominated OC (72.61%), particularly in rural areas (87.32%). The coal combustion (15.19%) and
64 biomass burning (33.55%) as major contributors in rural areas, strongly associated with domestic
65 heating, whereas urban dust predominantly originated from traffic (46.83%) and industrial
66 emissions (16.41%). Coal consumption in QDB was greater during the HP relative to other dust
67 sources on the QXP leads to increased atmospheric pollutant emissions, which may accelerate
68 regional glacier melting. Consequently, integrating QDB carbonaceous aerosols into future
69 environmental policies and climate models for the QXP is essential. This study provides a reference
70 for investigating carbonaceous aerosols in climatically similar hyper-arid basins with intensive
71 human activity and salt lake regions.

72 **Keywords:** Qinghai-Xizang Plateau; Qaidam Basin; Biomass burning; carbonaceous elements;
73 atmospheric dust deposition.

74

75 **Short summary**

76 This study collected dust samples from six sites in the Qaidam Basin over three years to investigate
77 the impact of domestic heating on atmospheric dust in hyper-arid region. Our results indicate that
78 rural dust is significantly influenced by heating, particularly from coal and biomass burning, which
79 accounts for over 70% of total sources. The unique energy structure here has resulted in distinct
80 environmental effects from the emitted carbonaceous aerosols and useful for similar dry areas.

81 1. Introduction

82 Atmospheric dust comprises solid particles, typically ranging in size from below 1 μm to 100
83 μm , which may become airborne, depending on their origin, physical characteristics and ambient
84 conditions (Xu, 2014). It is a key component of particulate matter (PM). Within this size spectrum,
85 larger particles (10-100 μm) that settle under gravity are defined as atmospheric dust deposition.
86 Notably, during long-distance transport, these coarse particles can undergo fragmentation into fine
87 particles ($\text{PM}_{2.5}$) and subsequently actively participate in atmospheric chemical and climatic
88 processes (Noll and Fang, 1989). As the dominant natural component of PM, atmospheric dust
89 deposition serves not only a crucial indicator of regional air quality but also a key biogeochemical
90 process linking the atmosphere, cryosphere, hydrosphere, and biosphere, with global-scale
91 influences that significantly shape environmental and climate systems (Feng et al., 2019).

92 Arid and semi-arid regions are the primary global sources of atmospheric dust (Griffin et al.,
93 2002; Schepanski, 2018). Long-distance transport of this dust via wind currents exerts multi-faceted
94 impacts on the environment and human society. A particularly critical effect is the alteration of the
95 cryosphere: dust deposition on snow and ice lowers surface albedo and modifies ice crystal structure,
96 thereby accelerating glacier and snowpack melt (Tuzet et al., 2017). This process disrupts regional
97 snow energy balance, which is directly linked to glacier retreat and water resource security. Dust
98 deposition also influences the atmospheric energy budget by attenuating solar radiation reaching the
99 surface and participates in the global carbon cycle through biogeochemical pathways, such as
100 delivering nutrients to oceans and affecting marine primary productivity (Mahowald et al., 2009;
101 Parajuli et al., 2022). For human health, harmful components associated with dust can induce
102 respiratory and cardiovascular diseases and even damage cellular DNA (Shahram et al., 2016). For
103 terrestrial ecosystems, the shading effect of dust on leaves can inhibit plant photosynthesis and
104 reduce biological productivity. Atmospheric dust, a critical component of particulate matter (PM),
105 serves as both an air quality indicator and environmental stressor, influencing hydrological cycles
106 and soil ecosystems (Feng et al., 2019).

107 Given the complexity and regional variability of atmospheric dust impacts, identifying dust
108 sources (source apportionment) is fundamental for understanding its environmental behavior and
109 effects. Recent advancements in understanding PM characteristics, particularly chemical

110 composition (e.g. water-soluble ions, carbonaceous components, and trace elements~~organic carbon,~~
111 ~~and elemental carbon~~) and source apportionment, have been driven by the integrated application of
112 methodological tools. These receptor models include~~achieved through~~ principal component
113 analysis (PCA), chemical mass balance (CMB), and positive matrix factorization (PMF) models,
114 are used to quantify source contributions. Specifically, the PMF model mathematically deconstructs
115 the chemical composition matrix of ambient samples to achieve this. Additionally, multivariate
116 statistical approaches like backward trajectory simulations (e.g., the HYSPLIT model) trace air mass
117 transport pathways to identify potential source regions (Lai et al., 2016; Yao et al., 2016; Zhang et
118 al., 2015a). This multi-method approach has greatly enhanced the precision of dust deposition
119 source analysis. For instance, PMF analysis of atmospheric dust in urban areas such as Lanzhou,
120 Taiyuan, and Jinan have identified diverse sources, including coal combustion, industrial emissions,
121 construction dust, windblown dust, vehicle emissions, and resuspended road dust. Seasonal
122 variations indicate that coal combustion during the domestic heating period and regional
123 meteorological conditions significantly influence dust deposition (Hu and Liu, 2022; Chen et al.,
124 2024; Yang et al., 2024; Zhang et al., 2022). These findings underscore the urgency of region-
125 specific pollution control strategies. When considering the global scale, arid and semi-arid regions
126 are unequivocally the dominant sources, contributing over 60% of the global atmospheric dust flux
127 (Zan et al., 2025). Therefore, a comprehensive investigation of atmospheric dust processes in these
128 key regions, encompassing emission intensity, physicochemical properties, transport pathways, and
129 environmental effects, is indispensable for elucidating global dust cycle mechanisms and assessing
130 their profound impacts on the cryosphere (e.g., glacial melting) and regional climate.

131 The Qinghai-Xizang Plateau (QXP) often referred to as the “Roof of the World” due to its
132 immense elevation, plays a crucial role in regulating the regional and global climate by altering
133 large-scale atmospheric circulation. Its vast glaciers and snow cover influence regional energy
134 balance through the albedo effect, and as the source of many major Asian rivers, it is known ~~is a key~~
135 ~~regulator of Northern Hemisphere climate variability and plays a vital role in global ecological and~~
136 ~~climatic stability, often referred to~~ as the “Asian Water Tower” (Liu et al., 2019; Liu et al., 2020b).
137 However, rapid glacier retreat on the plateau poses risks to the Asian hydrological cycle and the
138 monsoon system, with potential adverse impacts if unchecked (Luo et al., 2020). Beyond climate
139 warming and moistening~~increased humidity~~, black carbon (BC), a light-absorbing carbonaceous

140 aerosol component emitted from incomplete combustion processes of solid and liquid fuels during
141 household cooking, heating, and coke production (Bond et al., 2013), significantly accelerates
142 glacial melt. By depositing on ice, BC reduces surface albedo, enhances radiative absorption and
143 thus raises its temperatures, promoting glacial melt by inducing atmospheric warming and enhancing
144 radiative absorption at the glacier surface (Bond and Bergstrom, 2006; Chen et al., 2015). Notably,
145 biomass burning in South and Central Asia during winter serves as a major source of BC, further
146 exacerbating glacier decline on the plateau (Zhang et al., 2015b; Zheng et al., 2017; Xu et al., 2018b).
147 In addition to these external sources, local dust sources within the QXP itself remain significant.
148 Among these, the Qaidam Basin (QDB) in the northeastern plateau is a particularly important
149 contributor, identified as a key dust source for the plateau (Wei et al., 2017; Zheng et al., 2021) and
150 a critical, unique arid dust source area. However, local sources within the QTP, particularly the
151 Qaidam Basin (QDB) in the northeastern region, should not be underestimated, as QDB is a key
152 dust source for the plateau (Wei et al., 2017; Zheng et al., 2021).

153 The QDB, known as the “Treasure ~~Basin~~ Basin” of the QXP, is rich in minerals resources (e.g.,
154 copper, iron, and tin) as well as abundant oil and gas reserves. , coal, oil, and gas, positioning it
155 serves as a key economic development zone ~~hub~~ in northwest China, accounting for approximately
156 30% of the plateau's industrial and agricultural output despite comprising only about 8% of its
157 registered population (Fu, 2023). Extensive resource extraction has rendered its ecosystem fragile
158 (Li and Sha, 2022), exacerbating the impact of atmospheric pollution. The region is also highly
159 sensitive and vulnerable to climate change, with severe and extreme vulnerability zones covering
160 45.98% of its area (Xu et al., 2024). It has a high population density and intense human activity, yet
161 it is highly sensitive to climate change. Extensive resource extraction has rendered its ecosystem
162 fragile (Li and Sha, 2022), exacerbating atmospheric pollution. Unlike South Asia, Central Asia,
163 and Xizang, where biomass fuels dominate, the QDB relies primarily on distinct mix of coal (about
164 60%) and biomass fuels like yak dung, firewood (about 35%) for winter domestic heating, reflecting
165 a unique energy structure ~~QDB relies primarily on a mixture of coal, yak dung, and firewood for~~
166 winter domestic heating, reflecting a unique energy structure (Liu et al., 2008; Xiao et al., 2015;
167 Behera et al., 2015; Kerimray et al., 2018; Jiang et al., 2020; Shen et al., 2021). The combustion of
168 coal releases significant pollutants, including light-absorbing aerosols ~~organic compounds~~ like BC
169 and brown carbon (BrC), ~~and hazardous gases such as carbon dioxide (CO₂), nitrogen oxides (NO_x)~~

170 ~~and carbon monoxide (CO). These emissions impact human health and exacerbate climate warming,~~
171 ~~thereby influencing regional and global climate systems~~ (Munawer, 2018; Ye et al., 2020; Zhou et
172 al., 2025). ~~Brown carbon refers to organic compounds that can absorb light, particularly at shorter~~
173 ~~wavelengths, resulting in a reddish orange or brown appearance~~ (Donahue, 2018). ~~Both BC and BrC~~
174 ~~can influence solar radiation absorption and cloud properties, exerting a positive radiative forcing~~
175 ~~on climate~~ (Ramanathan and Carmichael, 2008; Bond et al., 2013). ~~When deposited on snow and~~
176 ~~ice, they further accelerate glacial melt~~ (Qian et al., 2015; Kang et al., 2020a). ~~Additionally, BC and~~
177 ~~BrC are significant contributors to global warming and can exacerbate adverse health effects by~~
178 ~~carrying toxic components~~ (Ramanathan and Carmichael, 2008; Shrivastava et al., 2017). ~~Notably,~~
179 ~~QDB's widespread use of yak dung as a fuel, a practice less common in other coal-intensive heating~~
180 ~~regions of northern China, releases pollutants like carbon monoxide (CO), volatile organic~~
181 ~~compounds (VOCs), and polycyclic aromatic hydrocarbons (PAHs), further affecting local air~~
182 ~~quality and health~~ (Zhang et al., 2022). Consequently, we posit that seasonal carbon emissions in
183 QDB, particularly during winter domestic heating, could exert a unique influence on the climate
184 and ecological stability of the QXP.

185 ~~The QDB, as a representative arid region with intensive human activity, exhibits climatic and~~
186 ~~environmental conditions comparable to other hyper-arid basins (e.g., the Tarim and Junggar Basins~~
187 ~~in Xinjiang, the Great Basin in the United States) and high-altitude salt lake regions (e.g., Uyuni in~~
188 ~~Bolivia, Atacama in Chile). Additionally, the QDB as a representative arid region with intensive~~
189 ~~human activity, exhibits climatic and environmental conditions comparable to the Tarim and~~
190 ~~Junggar Basins in Xinjiang, the Great Basin in the United States, and other hyper-arid areas.~~ These
191 regions are characterized by low precipitation, rich mineral resources subject to significant
192 anthropogenic impact, and abundant salt lakes. ~~Similarly, salt lakes such as the Uyuni in Bolivia,~~
193 ~~Atacama in Chile, and Ombre Muerto in Argentina are located on high plateaus averaging 3,000 m~~
194 ~~in elevation, with surrounding climates and environments comparable to those of the QDB.~~
195 Research in the Tarim and Junggar Basins has predominantly focused on dust events, their sources,
196 and associated gas emissions (Gao and Washington, 2010; Liu et al., 2016b; Filonchik et al., 2018;
197 Yu et al., 2019; Zhou et al., 2023). In the Great Basin, studies largely address ozone and dust sources
198 (Hahnenberger and Nicoll, 2012; Vancuren and Gustin, 2015; Miller et al., 2015). Research on salt
199 lake atmospheres has predominantly focused on high-salinity dust emissions resulting from lakebed

200 desiccation due to resource extraction (L w et al., 2013; Gholampour et al., 2015; Moravek et al.,
201 2019; Christie et al., 2025), with limited research on atmospheric carbon components, their sources,
202 and environmental impacts. Therefore, this research aims to investigate atmospheric carbonaceous
203 aerosols in arid basins with intensive human activity and climates comparable to the QDB, as well
204 as in salt lakes environments.

205 From January 2020 to March 2023, monthly dust deposition samples were collected at six
206 urban and rural monitoring sites in the southern QDB. Samples were categorized into two seasonal
207 periods: the domestic heating period (HP) and the non-domestic heating period (NHP). Measured
208 parameters included dust deposition flux, soluble ions, trace elements, and key carbonaceous
209 components. The objectives of this study were: (1) to clarify the variation trends of carbonaceous
210 components in atmospheric dust deposition under the unique energy structure of the QDB, and to
211 quantify the contribution of domestic heating; and (2) to identify the major sources of atmospheric
212 dust deposition in the basin and to evaluate their associated environmental impacts. To achieve these
213 aims, we applied OC/EC and char/soot ratios, the HYSPLIT trajectory, and PMF model for source
214 apportionment. This study, conducted from January 2020 to March 2023, involved monthly dust
215 deposition sampling at six urban and rural monitoring sites located in the southern QDB. Samples
216 were categorized into two seasonal periods: the domestic heating (HP) and the non-domestic heating
217 (NHP) periods. The HYSPLIT model, and PMF receptor modeling using analyses of dust flux,
218 soluble ions, trace elements, and carbonaceous components, alongside OC/EC and char/soot
219 ratios the primary sources of dust deposition were identified, with particular emphasis on
220 contributions from domestic heating. The study further evaluated the environmental impacts on the
221 QXP, considering its distinctive energy structure. Furthermore, these findings offer a scientific basis
222 and reference for examining atmospheric carbonaceous aerosols in arid basins with similar climates
223 and human activities to the QDB, as well as in salt lake regions.

224

225 **2. Materials and methods**

226 **2.1 Sampling**

227 The QDB, situated in the northeastern part of the QXP, is bordered by the Altyn-Tagh, Kunlun,
228 and Qilian mountains, making it one of China's largest intermontane basins (Zhang, 1987). With an

229 average elevation of 3,000 m, the basin features an extremely arid climate characterized by less than
230 20 mm of annual precipitation in the northwestern region, while evaporation rates exceed 2,000 mm
231 ([Feng et al., 2022](#)). The QDB is rich in salt lakes, non-ferrous metals, and hydrocarbon resources,
232 with significant coal deposits. It leads China in reserves of halite, potash, magnesium, lithium,
233 strontium, asbestos, earning it the nickname “Treasure Basin”. As a major salt lake resource area, it
234 hosts 33 lakes, including Qarhan, Dachaidan, and Caka Salt Lake, and faces notable conflicts
235 between resource extraction and ecological preservation. Agriculturally, it cultivates crops like goji
236 berries, quinoa, and forage grass, and hosts China’s largest resource-rich circular economy pilot
237 zone. The permanent population of the basin is approximately 400,000, primarily using coal, yak
238 dung, and firewood for domestic heating ([Jiang et al., 2020](#)). Additionally, annual tourism peaks
239 from May to September, attracting around 17 million visitors ([Qinghai Statistical Yearbook, 2023](#)),
240 which likely amplifies atmospheric pollutant emissions.

241 From January 2020 to March 2023, monthly dust deposition samples were collected from six
242 monitoring stations in the southern QDB. The stations included Xiao Zaohuo (XZH), Golmud
243 (GEM), Da Gele (LTC), Nuo Muhong (NMH), Balong (BLX), and Dulan station (DLX) ([Figure 1](#)).
244 Dry deposition collection employed the glass ball method using Marble dust collector (MDCO)
245 designed dust collection cylinders ([Sow et al., 2006](#)). [The MDCO sampler operates on the principle](#)
246 [of gravitational settling. It uses a collection vessel with a known opening to capture particulate](#)
247 [matter that settles naturally from the air. In field measurements, surrogate surfaces or deposition](#)
248 [traps are commonly employed to better quantify atmospheric deposition. These surfaces mimic the](#)
249 [original ground surface, are easy to deploy, and can be integrated without significantly disturbing](#)
250 [airflow. Examples include glass beads \(\[Ganor, 1975\]\(#\); \[Offer et al., 1992\]\(#\)\), moist filter paper \(\[Goossens\]\(#\)
251 \[and Offer, 1993\]\(#\)\), plastic surfaces \(\[Gregory, 1961\]\(#\)\), and water or antifreeze solutions \(\[Smith and\]\(#\)
252 \[Twiss, 1965\]\(#\)\). The MDCO deposition vessel is based on the original concept of \[Ganor \\(1975\\)\]\(#\), using
253 \[glass beads as a surrogate collection surface. Due to their very low microscopic roughness, the beads\]\(#\)
254 \[help prevent the resuspension of particles once they have been captured \\(\\[Goossens and Offer, 1993\\]\\(#\\)\\).\]\(#\)](#)

255 The stainless steel collection device (50×30×30 cm) contained a plastic sieve container of
256 identical dimensions, with the sieve base positioned 10 cm above the opening and perforated with
257 0.5 cm diameter holes (Figure S1). To minimize dust resuspension during high wind events ([Qian](#)
258 [and Dong, 2004](#)), two layers of 16 mm glass balls were placed within the sieve container. A high-

259 density polyethylene bag was attached to the base for sample collection. According to Sow et al
260 (2006), the collection efficiency of the MDCO decreases with increasing wind speed, dropping
261 below 20% when wind speed exceeds 3 m/s, and it preferentially collects the finer fraction of
262 atmospheric dust particles~~fine dust particles~~ ranging from 10 to 31 μm in size (Chow, 1995).
263 Furthermore, collection efficiency decreases significantly as the size of dust-fall increases. Based
264 on our findings, more than 50% of the collected dust particles are below 40 μm (Figure S2), whereas
265 the mean particle size of atmospheric dust deposition reported in other studies is approximately
266 80 μm (Lin et al., 2022a; Lin et al., 2022b). This confirms that the MDCO sampler preferentially
267 collects relatively finer particles. Consequently, this study may place greater emphasis on analyzing
268 the chemical activity of the finer fraction of atmospheric dust, thereby enhancing the detection
269 sensitivity for components such as secondary ions and carbonaceous species in deposited dust.
270 However, this particle-size selectivity introduces a sampling bias that can amplify inter-site
271 differences in deposition flux between sites, complicate local source apportionment, strengthen
272 signals from distant sources (e.g., combustion and vehicle emissions), and weaken the contribution
273 from local, coarse-particle-dominated sources (e.g., resuspended dust and construction dust). These
274 factors may affect the accuracy of both deposition flux estimates and source apportionment. Future
275 research should enhance data comparability and the reliability of ecological assessments through
276 efficiency correction and the combined application of multiple methods. The collection efficiency
277 at each site was calculated based on local dust grain-size distribution and wind speed; details are
278 provided in Supplementary Text S1. This type of collector has been widely used in many studies to
279 evaluate local dust conditions (Abdollahi et al., 2021; Barjoe et al., 2021; Alzahrani et al., 2024).
280 ~~Therefore, we consider this collector effective for capturing fine dust particles, and the actual dust~~
281 ~~deposition flux can be estimated by accounting for its approximately 20% collection efficiency.~~

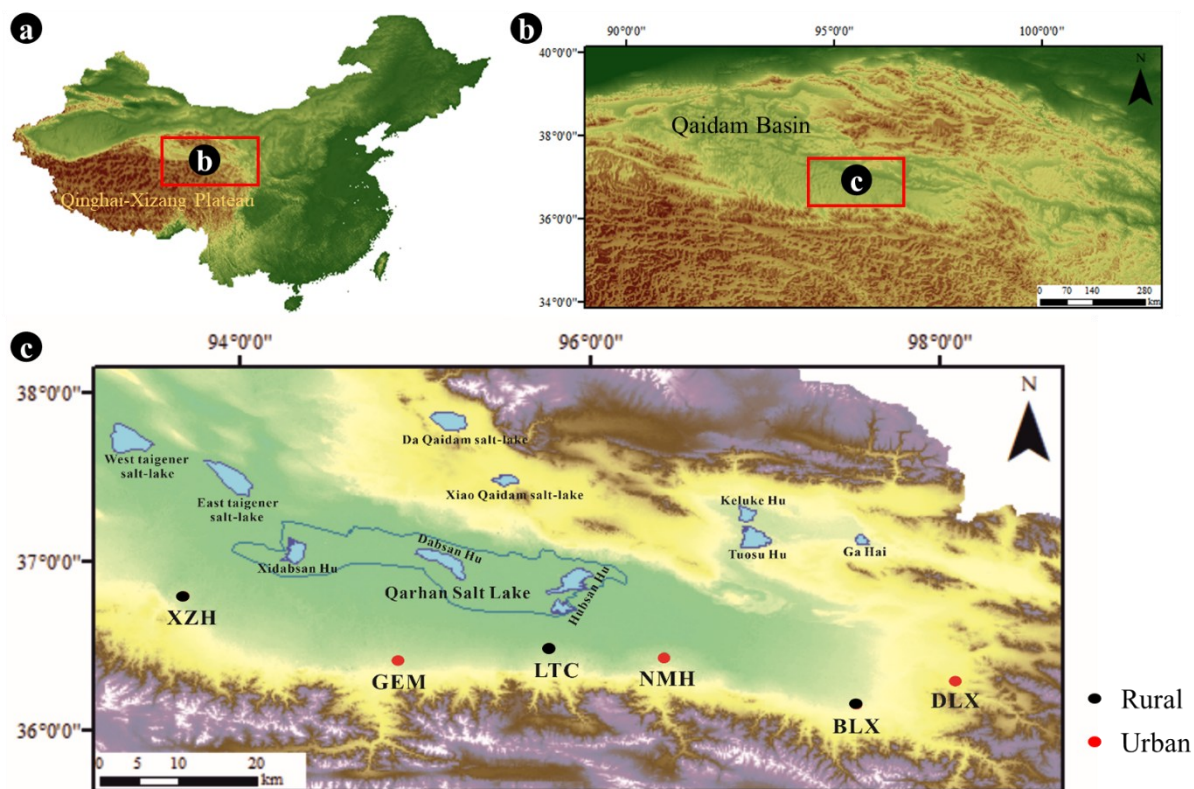
282 In this study, dust samples were collected monthly, with each sampling period lasting 30 or 31
283 days. The installation height and environment of the samplers are provided in Table S1. To ensure
284 only dry dust was collected, collection devices were manually-operated covered during rain or
285 snowfall. A total of 37, 39, 23, 30, 16, and 29 samples were obtained from XZH, GEM, LTC, NMH,
286 BLX, and DLX stations, respectively, and no duplicate samples were collected during the sampling
287 period. Laboratory protocols incorporated biannual analyses with negative controls and appropriate
288 control samples. As continuous dust monitoring commenced in 2020, site blanks were evaluated

289 during initial sampling. Stations were classified as Urban (GEM, NMH, DLX) and Rural (XZH,
 290 LTC, BLX) based on location characteristics. Consistent with the cold-arid climate in QDB, the HP
 291 was defined as October-April, while the NHP spanned May-September.

292 Materials such as plant remnants, microfauna, and bird droppings were removed from the
 293 sample bags with tweezers. The samples were then measured on a balance (0.0001 g) to determine
 294 the total dust deposition flux (DF) (Eq. 1) (Yu et al., 2016):

$$295 \quad M = \frac{m \times 30}{S \times K}, \quad (1)$$

296 where M is dust deposition [$\text{g}/(\text{m}^2 \cdot 30\text{d})$]; m is the sample mass (g); S is the area of the dust collection
 297 device (m^2); and K is the actual number of sampling days per month (d).



298
 299 **Figure 1.** Spatial distribution of monitoring stations in the southern Qaidam Basin. Urban stations
 300 (red) and rural stations (black) are labeled as follows: XZH (Xiao Zaohuo), GEM (Golmud), LTC
 301 (Da Gele), NMH (Nuo Muhong), BLX (Balong), DLX (Dulan).

302 303 2.2 Water-soluble inorganic ions

304 A 100 mg sample was weighed and transferred into a 250 mL bottle. The mixture underwent
 305 ultrasonic extraction for 20 minutes to ensure complete solubilization. The resulting supernatant

306 was then filtered through a 0.45 μm filter for analysis. Based on preliminary experimental results,
307 the concentrations of major ions (K^+ , Na^+ , Mg^{2+} , and Ca^{2+}) were measured using Inductively
308 Coupled Plasma Optical Emission Spectrometer (ICP-OES, NexIon 2000). Anions (Cl^- , SO_4^{2-} , and
309 NO_3^-) were quantified using ion chromatography (IC). To ensure measurement accuracy, samples
310 were organized in sets of twenty, with one randomly selected sample from each group serving as a
311 replicate, achieving an error margin of less than 10%. The detection limits for the various
312 components were as follows: K^+ (0.0560 mg/L), Na^+ (0.0100 mg/L), Ca^{2+} (0.0037 mg/L), Mg^{2+}
313 (0.0390 mg/L), SO_4^{2-} (0.0090 mg/L), NO_3^- (0.0125 mg/L), Cl^- (0.0100 mg/L). All standard solutions
314 employed in the analysis were sourced from the National Standard Material Center.

315

316 **2.3 Trace element analysis**

317 According to the Chinese State Standard “Ambient air and waste gas from stationary sources
318 emission-determination of metal elements in ambient particles” (HJ 777-2015), the concentrations
319 of elements such as iron (Fe), aluminum (Al), silicon (Si), titanium (Ti), copper (Cu), cadmium (Cd),
320 chromium (Cr), manganese (Mn), nickel (Ni), zinc (Zn), lead (Pb), and vanadium (V) were
321 quantified using Inductively Coupled Plasma Mass Spectrometry (ICP-MS) and ICP-OES. A dust
322 sample weighing 0.100 g was placed in a Teflon cup, to which 20.0 mL of a nitric acid-hydrochloric
323 acid digestion solution was added. The sample was heated to reflux at $100 \pm 5^\circ\text{C}$ for 2 h under a
324 watch glass, then cooled. Following this, the inner walls of the cup were rinsed with water, and
325 approximately 10 mL of water was added, allowing the mixture to stand for 30 minutes for
326 extraction. The extract was then filtered into a 100 mL volumetric flask and diluted to volume with
327 distilled water for analysis. In cases where organic matter content was high, an appropriate amount
328 of hydrogen peroxide was introduced during digestion to decompose the organic materials. Prior to
329 sample analysis, the system was flushed with a rinse solution until the blank intensity value reached
330 a minimum, and samples were analyzed only after the signal stabilized. If the concentration of any
331 element exceeded the calibration range, the sample was diluted and reanalyzed.

332

333 **2.4 Carbon analysis**

334 This study utilized a combination of wet chemical treatment and thermal/optical reflection

335 (TOR) to analyze carbon elements in dust deposition (Han et al., 2007b; Han et al., 2007a; Han et
336 al., 2016). Dust samples were digested stepwise to remove inorganic materials: first samples were
337 treated with 10 mL of 2 N hydrochloric acid (HCl) for 24 h at room temperature to dissolve
338 carbonates and partial metals, followed by centrifugation (4500 rpm, 12 min) to separate the
339 residue; then with 15 mL of a 1:2 (v/v) mixture of 6 N HCl and 48% hydrofluoric acid (HF) for 24
340 h at room temperature to dissolve silicates and residual metals; and finally with 15 mL of 4 N HCl
341 for 24 h at 60 °C to remove minerals such as fluorite formed during demineralization. After each
342 step, the mixture was centrifuged, and the supernatant was collected. ~~Dust samples were treated~~
343 ~~with hydrochloric and hydrofluoric acids to remove inorganic materials.~~ The solid residue was
344 diluted with 200 mL of deionized water and ~~The residual solution was then~~ filtered through a pre-
345 combusted quartz fiber filter (Whatman, 450°C for 4 h, diameter 47 mm) (Han et al., 2007a). This
346 method has been widely applied to measure OC and EC contents in lake sediments and urban soils
347 (Han et al., 2009; Khan et al., 2009; Han et al., 2011). Studies have shown that the EC collection
348 efficiency of this method is approximately 99.6% (Zhan et al., 2013); ~~however, its OC collection~~
349 ~~efficiency remains unclear.~~ However, because OC includes polar, basic, and mineral-bound
350 compounds that may dissolve in HCl/HF and be lost during filtration, the supernatant from all three
351 acid-digestion steps was collected and analyzed for water-soluble OC using a carbon-nitrogen
352 analyzer (Shimadzu, TOCN-4200, Japan). Total OC was obtained by summing the dissolved OC
353 and the particulate OC measured by TOR.

354 The filtered samples were air-dried and analyzed for carbon content using a DRI 2001
355 thermal/optical carbon analyzer (Atmoslytic Inc., Calabasas, CA) at the Institute of Earth
356 Environment, Chinese Academy of Sciences, adhering to the Interagency Monitoring of Protected
357 Visual Environments (IMPROVE) protocol.

358 A 0.544 cm² disc was extracted from the filter and placed in a quartz boat for analysis. During
359 the carbon analysis, the samples were initially heated in a 100% helium atmosphere, resulting in the
360 production of four organic carbon (OC) fractions (OC1, OC2, OC3, and OC4) at four different
361 temperature levels (140, 280, 480, and 580°C). The atmosphere was subsequently changed to 2%
362 O₂/98% He, generating three elemental carbon (EC) fractions (EC1, EC2, and EC3) at three
363 temperatures (580, 740, and 840°C). Volatile carbon underwent carbonization in an anaerobic
364 environment, indicated by a decrease in laser reflectance, and is referred to as pyrolyzed organic

365 carbon (OPC). In the oxidative atmosphere, OPC was emitted along with the original EC from the
366 filter. The amount of OPC is defined as the carbon evolved until the laser reflectance returned to its
367 baseline value (Han et al., 2007b). According to the IMPROVE protocol, EC is calculated as the
368 total of the three EC subfractions minus OPC (i.e., EC is defined as the sum of EC1, EC2, and EC3,
369 with OPC subtracted). The method enables differentiation between soot and char, as determined by
370 the gradual oxidation of these black carbon subtypes in standard reference materials during the EC1
371 and the EC2 plus EC3 –steps, where char is defined as EC1 minus OPC and soot as the sum of EC2
372 and EC3– (Han et al., 2007a; Han et al., 2016).

373 Please note that in this manuscript, we interchangeably use the terms "EC" and "BC." While
374 these terms do not strictly refer to the same component, they serve as an adequate approximation
375 within the scope of this study (Seinfeld et al., 1998; Bond et al., 2004). We use "EC" when discussing
376 emissions and modeling components, reserving "BC" for climate-related discussions. Throughout
377 this manuscript, the term “OC” refers to the total organic carbon (sum of the dissolved OC and the
378 particulate OC).

379

380 **2.5 The particle size analysis**

381 The grain size of dust-fall samples was measured using a laser particle analyzer (Malvern
382 Mastersizer 2000, UK). The particle size distribution was calculated for 100 grain size classes within
383 a range of 0.02-2000 μm. Sample preparation for grain size analysis included wet oxidation of
384 organic matter by adding 10 mL of 30% hydrogen peroxide (H₂O₂) per 1.5 g dry sample. Carbonates
385 were dissolved by boiling with 10 mL (10% HCl) over 10 min. The glass beakers were filled with
386 150 mL distilled water and suspended particles were left to deposit. After siphoning the supernatant
387 water, 10 mL of 0.05 N sodium hexametaphosphat [(NaPO₃)₆] were added, and the residue was
388 dispersed for 5 min in an ultrasonic bath before measurement (Lu and An, 1997). And the results
389 are expressed as volume percentages.

390

391 **2.6 Collection of Meteorological Factors**

392 Meteorological data used in this study were obtained from the Qinghai Meteorological Bureau
393 during the sampling period. Monthly meteorological parameters, including wind speed (WS), wind

394 direction (WD), temperature (Temp), relative humidity (RH), Precipitation (RF), sunshine duration
395 (SUN), and the frequency of visibility ≤10 km (VIS), were collected from four national-level
396 meteorological stations: XZH, GEM, DLX, and NMH. All of these stations are standard
397 meteorological observatories established by the state, equipped with standardized monitoring
398 capabilities, and provided continuous and reliable data for this study (https://data.cma.cn). In
399 addition, two atmospheric dust deposition sampling sites (LTC and BLX) were established
400 specifically for collecting dust samples. Due to field-monitoring constraints and research-budget
401 limitations, no meteorological instruments were deployed at these two sites.

403 **2.5.7 Statistical analysis**

404 **(+)2.7.1 Estimation of Secondary Organic Carbon**

405 ~~OC~~ Organic carbon consists of primary organic carbon (POC) and secondary organic carbon
406 (SOC). Due to the intricate physical and chemical processes involved, SOC in urban atmospheres
407 cannot be directly measured. Therefore, an indirect estimation method, known as the EC tracer
408 method, has been developed (Turpin and Huntzicker, 1991). If the concentrations of OC and EC are
409 available and primary OC from non-combustion sources (OC_{non-comb}) can be disregarded, EC can be
410 utilized as a tracer for POC from combustion sources, facilitating the estimation of SOC (Turpin
411 and Huntzicker, 1995):

$$412 \text{ POC} = \text{EC} \times (\text{OC}/\text{EC})_{\text{pri}}, \quad (2)$$

$$413 \text{ SOC} = \text{OC}_{\text{total}} - \text{POC}, \quad (3)$$

414 where OC_{total} represents total organic carbon.

415 Traditional methods for determining (OC/EC)_{pri} involve regressing OC and EC within a fixed
416 percentile range of the lowest (OC/EC) ratio data (typically 5-20%) or relying on sampling days
417 characterized by low photochemical activity and local emissions (Castro et al., 1999; Lim and
418 Turpin, 2002). However, these approaches are limited by their empirical nature, lacking clear
419 quantitative criteria for selecting the data subsets used to establish (OC/EC)_{pri}, defined as the
420 hypothetical primary OC/EC ratio. In this study, we employed the minimum R squared (MRS)
421 method (Millet et al., 2005; Wu and Yu, 2016; Wu et al., 2018a) to determine (OC/EC)_{pri}. This
422 method calculates a set of hypothetical (OC/EC)_{pri} and SOC values to identify the minimum

423 correlation coefficient (R^2) between SOC and EC, allowing for the accurate derivation of $(OC/EC)_{pri}$.
 424 The computational procedure followed the algorithm developed by Wu and Yu (2016) (available at:
 425 <https://sites.google.com/site/wuchengust>), implemented within the Igor Pro environment
 426 (WaveMetrics, Inc., Lake Oswego, OR, USA). Due to the limited dataset size and low temporal
 427 resolution, the MRS analysis was performed collectively across all sampling sites. In this approach,
 428 the R^2 between SOC and EC was calculated iteratively for a range of $(OC/EC)_{pri}$ values spanning 0
 429 to 10. The minimum R^2 value of 1.33 (Figure S32) identified the optimal $(OC/EC)_{pri}$ representative
 430 of the true primary ratio.

431

432 (2)2.7.2 Quantifying the contributions of Playa-playa salt (ps) and non-playa salt (nps) sources

433 To differentiate the contributions of salt lake sources to water-soluble ions in atmospheric
 434 deposition, we adopted a methodology similar to that used for marine aerosols. This approach relies
 435 on the ratio of water-soluble ions (SO_4^{2-} , Ca^{2+} , K^+ , Mg^{2+} , Cl^-) to Na^+ in the salt lakes of the QDB,
 436 enabling us to assess the contribution of ps- Na^+ components to nps (Zhang, 1987); details in Zhu
 437 (2025).

$$438 \quad nps-SO_4^{2-} = [SO_4^{2-}] - 0.333 \times ps-Na^+, \quad (4)$$

$$439 \quad nps-Ca^{2+} = [Ca^{2+}] - 0.062 \times ps-Na^+, \quad (5)$$

$$440 \quad nps-K^+ = [K^+] - 0.087 \times ps-Na^+, \quad (6)$$

$$441 \quad nps-Mg^{2+} = [Mg^{2+}] - 0.051 \times ps-Na^+, \quad (7)$$

$$442 \quad nps-Cl^- = [Cl^-] - 2.287 \times ps-Na^+, \quad (8)$$

443 This was accomplished using equations that incorporate total Na^+ , total Ca^{2+} , the average
 444 crustal ratio $(Na^+/Ca^{2+})_{crust} = 0.56$ w/w (Bowen, 1979), and the average (Ca^{2+}/Na^+) ratio for Qaidam
 445 salt lakes, $(Ca^{2+}/Na^+)_{salt\ lake} = 0.06$ w/w (Zhang, 1987). Among these, the mass concentration of
 446 $[SO_4^{2-}]$, $[Ca^{2+}]$, $[K^+]$, $[Mg^{2+}]$, $[Na^+]$ and $[Cl^-]$ were identified as constituents of dust-fall.

$$447 \quad ps-Na^+ = [Na^+] - nps-Na^+, \quad (9)$$

$$448 \quad nps-Na^+ = nps-Ca^{2+} \times (Na^+/Ca^{2+})_{crust}, \quad (10)$$

$$449 \quad nps-Ca^{2+} = [Ca^{2+}] - ps-Ca^{2+}, \quad (11)$$

$$450 \quad ps-Ca^{2+} = ps-Na^+ \times (Ca^{2+}/Na^+)_{salt\ lake}, \quad (12)$$

451

452 (3)2.7.3 HYSPLIT backward trajectory model

453 Backward trajectory clustering analysis was conducted on sampling points using the TrajStat
454 plugin within Meteoinfo software. Daily backward trajectories for 48 hours were calculated from
455 January 2020 to March 2023 and classified monthly based on differences in the horizontal
456 movement direction and velocity of air masses. The trajectories were initiated at Universal Time
457 (UTC) 00:00, with a 6-hour increment, originating from 500 m above sea level (Yang et al., 2014).
458 Meteorological data utilized in this research were obtained from the Global Data Assimilation
459 System (GDAS) provided by the U.S. National Centers for Environmental Prediction (NCEP),
460 covering the period from December 2019 to February 2023 (Meteoinfo software website:
461 <http://meteothink.org>).

462

463 ~~(4)~~2.7.4 PMF model

464 The PMF is a multivariate factor analysis tool that decomposes a matrix of speciated sample
465 data into two matrices: factor contributions (G) and factor profiles (F). The goal of the PMF model
466 is to solve the chemical mass balance between measured species concentrations and the respective
467 source profiles, with the purpose of minimizing the objective function Q (Eq. 13) based upon the
468 uncertainties (u_{ij}) of measured species (Paatero and Tapper, 1994).

$$469 \quad e_{ij} = x_{ij} - \sum_{h=1}^p g_{ih} f_{hj}; \quad Q = \sum_{i=1}^m \sum_{j=1}^n (e_{ij}/h_{ij} s_{ij})^2, \quad (13)$$

470 where x_{ij} is the measured concentration of the j_{th} species in the i_{th} sample at receptor sites. f_{kj} is the
471 source profile of the j_{th} species in the k_{th} factor and g_{ik} is the mass contribution of the k_{th} factor in
472 the i_{th} sample. e_{ij} is the difference between modeled concentrations and measured concentrations.

473 The uncertainty for individual species (u_{ij}) was defined as the sum of two components: the x_{ij}
474 multiplied by an error fraction, and one-third of the method detection limit (MDL).. For data below
475 the MDL, concentrations were replaced by 1/2 MDL and the corresponding uncertainty was set to
476 5/6 MDL (Reff et al., 2007). An extended description of the PMF parameters used in this study and
477 error estimate based on the model's Q value, displacement (DISP), and bootstrapping (BS) tests
478 (DISP-BS) are provided in the Supplementary Information. The error assessment and uncertainty
479 data for the PMF source apportionment can be found in Tables S2 and S3, respectively.

480

481 2.7.5 Statistical Analysis

482 A one-way analysis of variance (One-Way ANOVA) was performed to examine the differences
483 in dust deposition flux, soluble ions, carbonaceous components, and trace elements among various
484 monitoring sites and periods. All statistical analyses were conducted in SPSS (IBM SPSS Statistics
485 26.0.0), with the significance level (P) set at 0.05. Prior to ANOVA, the normality and homogeneity
486 of variance were tested for each dataset. The Shapiro-Wilk test was used to assess normality. If the
487 data met the normality assumption ($P > 0.05$), parametric ANOVA was applied directly. If not, the
488 data were log-transformed and retested; if the transformed data still violated this assumption, the
489 non-parametric Kruskal-Wallis H test was used instead. In this study, all datasets were confirmed to
490 follow a normal distribution. Homogeneity of variance was verified using Levene's test; meeting
491 this assumption ($P < 0.05$) is a prerequisite for conducting ANOVA. When the overall ANOVA
492 result was significant ($P < 0.05$), indicating that at least two group means differed statistically, a
493 post-hoc test was performed. Given the potentially unequal sample sizes among groups, Tukey's
494 Honestly Significant Difference test was used for pairwise comparisons to identify specific inter-
495 group differences. Data in this study are presented as mean \pm 1 standard deviation (Mean \pm 1 SD).

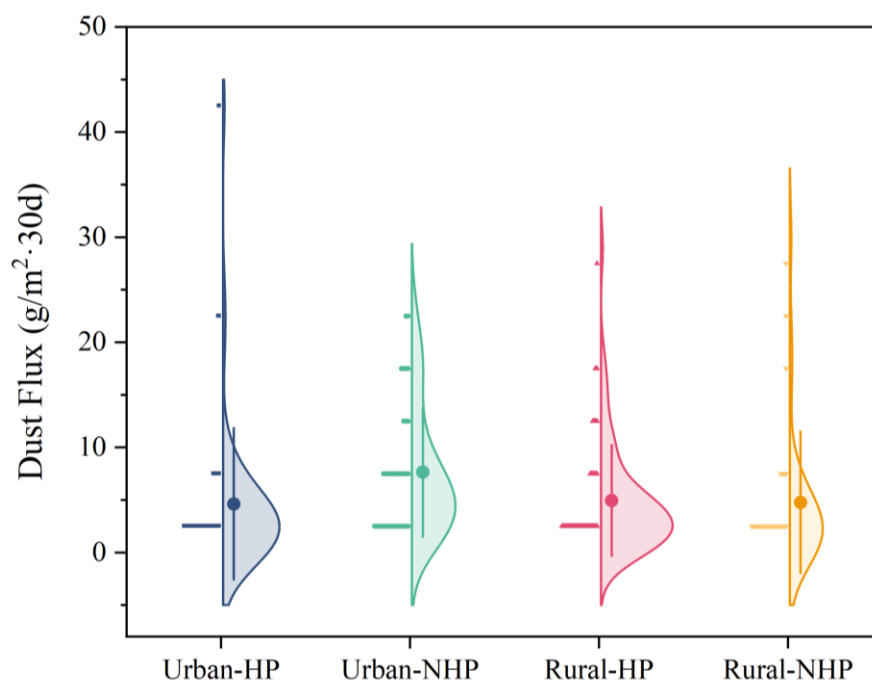
496 Furthermore, to investigate the influence of meteorological conditions on the chemical
497 composition of atmospheric dust, Pearson correlation analysis was applied to quantitatively assess
498 the linear relationships between meteorological factors (e.g., wind speed and direction, relative
499 humidity) and chemical components in dust (e.g., OC, EC, water-soluble ions). The underlying
500 assumptions of the Pearson correlation (continuous variables, bivariate normal distribution, and
501 linearity) were verified. All variables were tested for normality using the Shapiro-Wilk test and
502 screened for outliers. For data that did not meet the normality assumption, log transformation was
503 applied. The significance of correlation coefficients was tested using the t-test, with $P < 0.05$
504 considered statistically significant.

506 **3. Results and discussion**

507 **3.1 Atmospheric dust deposition flux and water soluble ions concentration**

508 The ~~total deposition flux~~ (DF) in the southern QDB is 5.41 ± 5.33 g/m²·30d, slightly lower
509 than that of the Lake Aibi Basin (10.77 g/m²·30d) (Li et al., 2022), but higher than the surrounding
510 areas of Akatama Salt Lake (2.93 g/m²·30d) (Wang et al., 2014). Specifically, DF was 4.67 ± 4.96

511 $\text{g/m}^2\cdot 30\text{d}$ in rural and $5.97 \pm 5.73 \text{ g/m}^2\cdot 30\text{d}$ in urban areas. During the HP, DF in rural and urban
 512 areas were $4.62 \pm 4.15 \text{ g/m}^2\cdot 30\text{d}$ and $4.95 \pm 5.25 \text{ g/m}^2\cdot 30\text{d}$, respectively. In contrast, NHP showed
 513 increased DF values of $4.77 \pm 4.42 \text{ g/m}^2\cdot 30\text{d}$ (rural) and $7.66 \pm 6.09 \text{ g/m}^2\cdot 30\text{d}$ (urban) (Figure 2).
 514 Notably, Urban DF during NHP demonstrated a 54.6% increase relative to HP, while rural DF rose
 515 by 7.1% (not statistically significant), contrasting previous findings that associated elevated DF with
 516 HP coal combustion (Cheng et al., 2009; Gao et al., 2013; Guo et al., 2010; Qi et al., 2018). We
 517 hypothesize that the increase in DF during the NHP is attributed to seasonal meteorological
 518 variations such as wind speed (Yang et al., 2024), and heightened anthropogenic emissions
 519 associated with tourism ~~eightened tourism activity (May to September peaks season) in the~~
 520 ~~QDB(Zhang et al., 2011), attracting approximately 17 million tourists annually, the number~~
 521 ~~continues to grow. This influx likely leads to increased urban emissions, particularly in densely~~
 522 ~~populated areas such as DLX and GEM (Figure S3), contributing to the elevated DF levels. The~~
 523 NHP coincides with the peak tourist season (May-September) in the QDB, which receives about 17
 524 million visitors annually, a number that continues to rise (Qinghai Statistical Yearbook, 2023). This
 525 elevated human activity likely enhances local emissions, contributing to increased dust deposition
 526 during this period. The influence of meteorological factors on dust deposition will be further
 527 examined in Section 3.5.



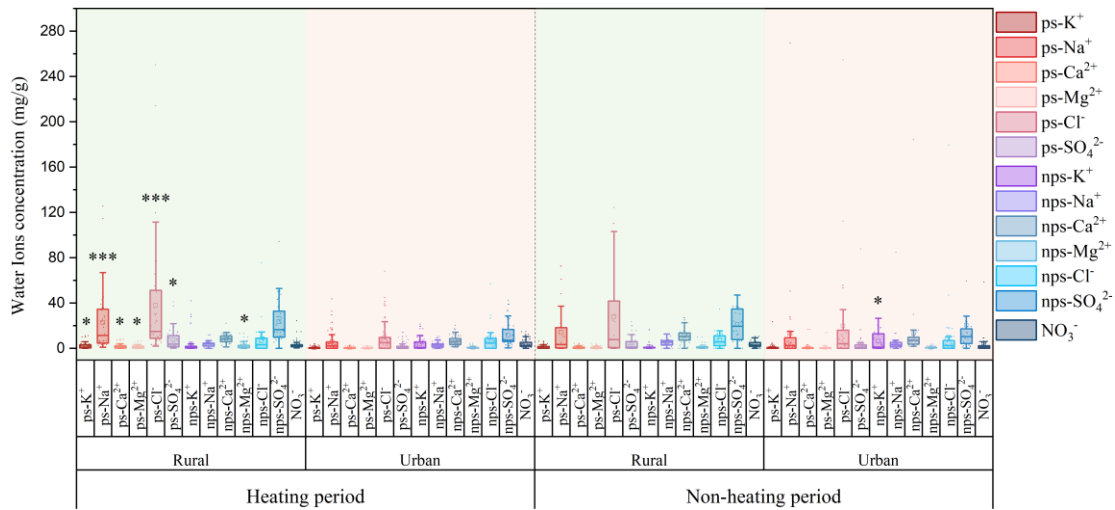
528
 529 **Figure 2** Dust flux distribution in urban and rural. The distribution of dust flux in four contexts:

530 Urban with domestic heating period (Urban-HP), Urban with non-HP (Urban-NHP), Rural with
531 domestic heating period (Rural-HP), and Rural with non-HP (Rural-NHP). Each violin plot
532 illustrates the density distribution of dust flux values, with the central dot representing the mean,
533 and the vertical lines indicating the interquartile range.

534

535 Water-soluble ion concentrations differed ~~significantly~~ between rural (115.31 mg/g) and urban
536 (72.81 mg/g) areas (not statistically significant). In rural, water-soluble ion content was greater
537 during the HP than in the NHP, while the opposite trend was observed in urban areas (not statistically
538 significant) (Figure 3 and [S4S5](#)). We categorized the water-soluble ions in dust deposits into ps and
539 nps based on their sources, following the model of marine aerosols (Zhu et al., 2025). Playa salt
540 content consistently surpassed nps in rural areas across both periods, while urban areas showed the
541 opposite trend (not statistically significant). Notably, during the NHP, ps content in urban and rural
542 increased by 54.46 and 36.86% respectively (not statistically significant). Backward trajectory
543 analysis indicated that airflow in both rural and urban areas primarily originated from the northwest
544 QDB and the eastern Tarim Basin during the HP, while during the NHP, it was influenced more
545 broadly by the salt lake of the QDB (Figure [S5-S6](#) and [S6S7](#)), aligning with the observed variations
546 in ps content. A similar increase in summer sea salt and non-sea salt ions has been reported in Rajkot,
547 India, attributed to ocean wind direction (Gupta and Dhir, 2022).

548 The ratio of $\text{nps-SO}_4^{2-}/\text{NO}_3^-$ in soluble ions is used to differentiate between coal combustion
549 (fixed sources) and vehicular emissions (mobile sources) (Arimoto et al., 1996; Shen et al., 2008).
550 The higher $\text{nps-SO}_4^{2-}/\text{NO}_3^-$ ratio in urban areas compared to rural areas (Figure [S7S8](#)) indicates that
551 during the study period, stationary sources (e.g., industrial emissions, coal, and biomass combustion)
552 contributed more significantly to the ionic composition of urban dust-fall (Pipal et al., 2019). In
553 contrast, the ratio was considerably lower during the NHP than during HP, suggesting that mobile
554 sources likely played a more important role in the dust ionic composition during the NHP. Generally,
555 emissions from coal combustion and biomass burning was intensified in northern China during the
556 HP (Liu et al., 2016), while vehicle emissions dominate during the NHP (Xu et al., 2012), supporting
557 the reliability of this analysis. Nevertheless, further investigation integrating atmospheric emission
558 inventories, source tracers, aerosol physicochemical processes, and meteorological conditions is
559 warranted.



561

562 **Figure 3** Concentrations of water ions in rural and urban across different seasonal periods (domestic
 563 heating and non-domestic heating periods). Asterisks indicate statistically significant differences
 564 between sites, with *, $P < 0.05$; **, $P < 0.01$; ***, $P < 0.001$.

565

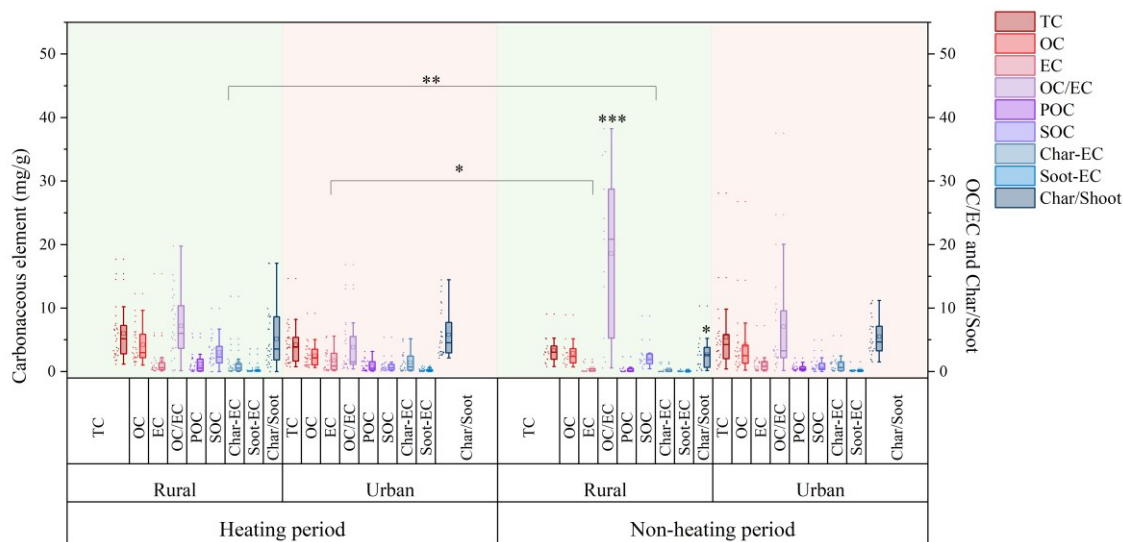
566 **3.2 Organic carbon and element carbon**Carbonaceous element –compositions

567 3.2.1 Organic carbon and elemental carbon

568 The average total carbon (TC) concentration in the southern QDB was $4.873.83 \pm 3.4.182$ mg/g,
 569 significantly lower than that of Huangshi, Hubei province (25.15 ± 11.79 mg/g) and Washington
 570 (157 ± 3.2 mg/g), Kumasi in West Africa (28 mg/g) and Xi'an (14.6 ± 5.8 mg/g) (Han et al., 2007a;
 571 Han et al., 2009b; Zhan et al., 2016; Bandowe et al., 2019), suggesting relatively low carbon
 572 emissions in the southern QDB. Average OC and EC levels in QDB (3.48 and 1.41 mg/g,
 573 respectively) are markedly lower than those in Xi'an (7.4 and 7.2 mg/g, respectively), Wuhu (33.26
 574 and 22.49mg/g, respectively), and Nanchang (25.15 and 11.46 mg/g, respectively) (Han et al., 2009a;
 575 Deng et al., 2014; Zhang, 2014), but significantly higher, particularly for EC, than in Nam Co (0.35
 576 mg/g) (Chen et al., 2015).

577 In urban, TC content ($3.054.75 \pm 2.464.47$ mg/g) was marginally lower than the rural level
 578 ($3.555.02 \pm 3.56-79$ mg/g), although this difference was not statistically significant. Contrasting
 579 spatial patterns emerged for carbon components: EC dominated urban areas (1.46 ± 1.60 mg/g),
 580 while OC prevailed in rural (2.25 ± 1.92 mg/g) (not statistically significant) (Figure 4 and S98).
 581 This disparity may be attributed to the long-term combustion of biomass, coal, and wood in rural

582 settings (Na et al., 2004). It may also be associated with meteorological conditions, particularly
 583 heightened solar radiation resulting from reduced primary emissions in rural areas, which facilitates
 584 the formation of SOC (Xu et al., 2018a; Wang et al., 2019). Overall, the contents of OC and EC
 585 showed small difference between rural (3.73 and 1.33 mg/g, respectively) and urban areas (3.28 and
 586 1.47 mg/g, respectively).
 587



588
 589 **Figure 4** Concentrations of organic carbon (OC), ~~elements~~ elemental carbon (EC), secondary
 590 organic carbon (SOC), primary organic carbon (POC), char-EC, soot-EC and OC/EC, char/soot
 591 ratios in different sites (Rural, Urban) and seasonal variations (domestic heating and non-domestic
 592 heating period). Significant differences are indicated by asterisks (*p < 0.05; **p < 0.01; ***p <
 593 0.001).

594
 595 Seasonal analysis revealed elevated carbonaceous compound concentrations, specifically OC
 596 and EC, during the HP (not statistically significant). This increase is primarily due to local domestic
 597 heating activities coupled with adverse meteorological conditions, such as low temperature, weak
 598 winds (Oliveira et al., 2007; Gong et al., 2017), weak atmospheric turbulence, and frequent
 599 atmospheric inversions (Guo et al., 2016). Rural emissions primarily stem from coal and biomass
 600 burning for heating and cooking (Zhang et al., 2000; He et al., 2004), contributing to reduced OC
 601 and EC content in the NHP, whereas elevated EC levels in urban areas are primarily linked to
 602 vehicular and industrial sources. Spatiotemporal transport dynamics show EC depletion during rural

603 ward pollutant migration due to atmospheric dispersion, particularly affecting coarse particulate
604 fractions.

605 Notably, rural carbon emissions exceed urban levels in the southern basin, potentially
606 attributable to extended HP duration (7 months) compelling low-grade fuel (crop residues, wood,
607 raw coal and yak dung) utilization (Na et al., 2004). In contrast, urban areas benefit from solar/wind
608 energy infrastructure and government-led clean heating initiatives (suitable electricity for electricity
609 policy), achieving 66.63% clean heating penetration (Statistical Yearbook of Haixi Xizang
610 Autonomous Prefecture of Qinghai Province, [2023](#)), leading to a comparatively lower TC content.

611 The OC/EC ratio is a valuable indicator of carbonaceous aerosol sources. In this study, Urban
612 areas exhibited stable OC/EC ratios ranging from 0.15 to ~~15.16~~[16.89](#) (mean = ~~2.16~~[3.97](#)), whereas
613 rural areas showed significantly higher ratios during NHP (~~7.27~~[18.58](#) \pm ~~4.66~~[12.80](#)) compared to HP
614 (~~4.57~~[7.20](#) \pm ~~3.02~~[4.99](#)) ($P < 0.001$) (Figure 4 and [S10S11](#)). Typically, the OC/EC ratio for vehicle
615 emissions ranges from 0.7 to 2.4, for coal combustion emissions from 0.3 to 7.6, and for biomass
616 burning from 3.8 to 14.5 (Schmidl et al., 2008; Gonçaves et al., 2010; Pio et al., 2011; Popovicheva
617 et al., 2016).

618 These findings suggest that urban OC/EC ratios (0.15-~~16.89~~[9.05](#)) are primarily associated with
619 vehicle and coal combustion, while rural ratios (0.14-~~15.16~~[38.25](#)) are predominantly linked to coal
620 and biomass burning. The rural OC/EC ratios are significantly higher than those in urban areas (P
621 < 0.001), which is consistent with the general distribution pattern of carbonaceous aerosols and
622 reflects a greater contribution of SOC (Zhang et al., 2008; Sandrini et al., 2014). ~~A~~The higher
623 OC/EC ratio typically indicates a greater contribution from biomass combustion; in this study, the
624 OC/EC ratio of rural was ~~5.56~~[10.99](#) \pm ~~3.93~~[10.00](#), which is significantly lower than values recorded
625 in ~~India (8.47) and~~ Nam Co in Xizang (16.3 ± 4.4) (~~Saud et al., 2013;~~ Chen et al., 2015), yet higher
626 than those observed in India (8.47) and Shanxi (0.7-1.6), Beijing (1.9-2.7), and Tianjin rural (2.66)
627 (Zhang et al., 2007; [Saud et al., 2013](#); Cheng et al., 2015; Wang et al., 2021). This finding indicates
628 that carbonaceous aerosols in rural QDB derive from both fossil fuel combustion and biomass
629 burning, with a pronounced influence from the burning of wood, yak dung, and similar biomass
630 fuels, suggesting source specificity.

631

632 [3.2.23](#) Char-EC and Soot-EC [compositions](#)

633 EC-Elemental carbon is classified into soot and char (Han et al., 2009b), with char-EC and
634 soot-EC defined as EC1 minus OPC and the sum of EC2 and EC3, respectively (Han et al., 2007).
635 Char-EC is typically produced from biomass burning at relatively low temperatures, whereas soot-
636 EC originates from high-temperature coal combustion and automotive emissions (Zhu et al., 2010;
637 Cao et al., 2013). The char-EC/soot-EC ratio, like the OC/EC ratio, serves as an indicator of carbon
638 aerosol sources. Since char and soot are mainly generated through combustion processes, their ratio
639 is typically influenced by two key factors: the primary emission source and the deposition removal
640 efficiency. For localized PM, such as in urban areas, the removal rate is generally negligible (Han
641 et al., 2009a).

642 Char-EC constitutes 75.88% of rural EC (74.71% HP; 78.84% NHP) and 85.00% of urban EC
643 (85.58% HP; 84.11% NHP) (Figure 4 and S109), demonstrating its dominance across spatial and
644 temporal scales (not statistically significant). Research suggests that char-EC constitutes a larger
645 proportion of coarse PM, while soot-EC is more predominant in fine particles, resulting in extended
646 atmospheric residence times for soot-EC due to reduced deposition velocities (Han et al., 2009b).
647 The increased levels of char-EC during the urban HP are linked to complex sources, including
648 biomass fuel usage and transportation emissions, resulting in elevated char concentrations in urban
649 areas and along busy roadways (Kim et al., 2011).

650 The char/soot ratios for automobile emissions, coal combustion, and biomass burning are 0.60,
651 1.9, and 11.6, respectively (Chow et al., 2004; Chuang et al., 2014). Generally, high-temperature
652 combustion (e.g., vehicle and industrial processes) yields lower char and soot concentrations, while
653 low-temperature combustion (e.g., household cooking and biomass burning) results in higher ratios
654 (Han et al., 2016; Han et al., 2012; Han et al., 2010; Han et al., 2009a). Differences in char/soot
655 ratios between urban and rural areas across seasons may be linked to wheat straw burning,
656 contrasting with minimal vegetation combustion impacts in cities like Xi'an (Cao et al., 2005). The
657 char/soot ratio for dust-fall observed in this study (4.97; Figure 4 and S110) is slightly higher than
658 those recorded in Jinchang (3.84) (Han et al., 2009a) and Daheihe, Inner Mongolia (3.2) (Han et al.,
659 2008). The relatively stable concentration of soot-EC in this study, along with the elevated char/soot
660 ratio, suggests a correlation with higher coal consumption among local residents and industries. This
661 indicates that, in comparison to other regions, carbon emissions in the remote QDB are
662 predominantly sourced from coal and biomass burning, supporting OC/EC ratio findings.

663 Furthermore, the char/soot ratio is elevated during HP (not statistically significant), highlighting the
664 predominant influence of coal and biomass burning in rural areas during HP, while fossil fuel
665 impacts are more pronounced in NHP.

667 3.2.34 ~~POC~~ Primary and secondary organic carbon ~~SOC~~ compositions

668 Aerosol samples with low OC/EC ratios typically exhibit low concentrations of POC, which
669 mainly comprises primary carbonaceous compounds. The MRS method enables discrimination of
670 OC into POC and SOC (Method 2.7.1) (Yoo et al., 2022; Liu et al., 2023). Secondary organic
671 carbon ~~OC~~ constitutes a dominant fraction of OC in atmospheric aerosols. Research on carbonaceous
672 aerosols in various Chinese cities indicates that SOC contributes 67% (53-83%) and 57% (48-62%)
673 to rural and urban OC, respectively (Zhang et al., 2008)—, marginally higher~~lower~~ than the
674 ~~62.62~~72.61% observed in this study (Figure 4 and S124). This is likely because~~Although~~ SOC
675 formation relies on solar radiation, the QDB experiences high levels of solar energy (Liu et al.,
676 2017), which may facilitate photochemical oxidation of VOCs into SOC (Hama et al., 2022).
677 ~~Nevertheless, the consistently low SOC concentrations indicate that VOCs emissions in QDB are~~
678 ~~significantly lower than the regional averages observed across China, reflecting relatively low~~
679 ~~pollution levels. This finding is consistent with the previously observed low concentrations of~~
680 ~~atmospheric carbon emission in the region.~~

681 During the NHP, rural areas exhibit the highest SOC/OC ratio of ~~86.70~~87.32% (Figure S132),
682 while urban areas record the lowest ratio of ~~44.32~~52.94% during the HP. This trend reflects elevated
683 potential for photochemical activity and reduced contributions from POC, likely due to local
684 emission sources, such as traffic and coal combustion (Mbengue et al., 2018). The high SOC/OC
685 ratio suggests that SOC largely displaces OC. Our findings indicate that SOC levels are greater in
686 rural areas (~~66.52~~78.44%) compared to urban regions (~~58.74~~67.78%) (not statistically significant),
687 which consistent with the observation of higher OC/EC ratios in rural areas, likely attributable to
688 significant coal consumption for domestic heating, which enhances emissions of semi-volatile
689 organic compounds and organic gases (Dan, 2004). As for seasonal variations, studies in California
690 show an increase in SOC levels during warmer months, which is consistent with our results (Na et
691 al., 2004). This contrasts with the broader observation that higher temperatures typically lead to
692 lower SOC concentrations (Strader et al., 1999; Sheehan and Bowman, 2001). This discrepancy

693 may stem from varying sources of SOC emissions throughout the seasons, necessitating further
694 investigation in conjunction with other carbonaceous indicators.

695 This study conducted a comparative analysis of carbonaceous element concentrations in
696 atmospheric dust-fall and road dust between the QDB and other global regions (Table S4). To ensure
697 data comparability, the selected road dust samples consisted of directly collected in-situ dust without
698 resuspension treatment. The results revealed that the concentrations of TC, OC, and EC in QDB
699 (~~3.274.87~~, ~~1.883.48~~, and 1.41 mg/g, respectively) were significantly lower than those in industrial
700 or urban areas such as Bolu, Turkey; New Delhi, India; and Ezhou, China, and were even lower
701 than many other Chinese cities (Table S4). The low concentrations of OC and EC in QDB indicate
702 minimal anthropogenic pollution influence in this region, and the data can represent the regional
703 background values of carbonaceous components in atmospheric dust-fall in the arid inland areas of
704 East Asia (Chen et al., 2019a). This is crucial for global models assessing the emission fluxes of
705 carbonaceous aerosols from dust source regions. In contrast, extremely high values of carbonaceous
706 elements were found primarily in urban road dust from locations like Bolu, Turkey (TC: 605.2 mg/g),
707 Gwangju, South Korea (TC: 31.97 mg/g), and Xi'an, China (TC: 36.53 mg/g), indicating strong
708 influences from traffic emissions (mainly non-exhaust emissions) (Wei et al., 2015; Lee et al., 2018;
709 Demir et al., 2022). For atmospheric dust-fall in major cities like New Delhi, India, and Wuhan,
710 China, the carbonaceous components are affected by the combination of traffic emissions (diesel
711 vehicle emissions being a major source of EC), industrial activities, and emissions from dense
712 populations (Deng et al., 2014; Zhang, 2014; Zhan et al., 2016; Mishra and Kulshrestha, 2017).

713 The OC/EC ratio in QDB (~~3.667.09~~) is ~~at~~ an intermediate level. It is much lower than that in
714 regions dominated by biomass burning, such as Kumasi, West Africa (17.07) and Huainan, China
715 (21.4), but is ~~relatively close~~ ~~higher~~ to ratios found in cities like Gwangju, South Korea (5.63) and
716 Ulaanbaatar, Mongolia (5.69), ~~albeit with significantly lower concentrations~~ (Lee et al., 2018;
717 Bandowe et al., 2019; Liu et al., 2020). We primarily analyzed the OC/EC ratios in cities across
718 different regions of China to reveal the influence of varying economic development levels.

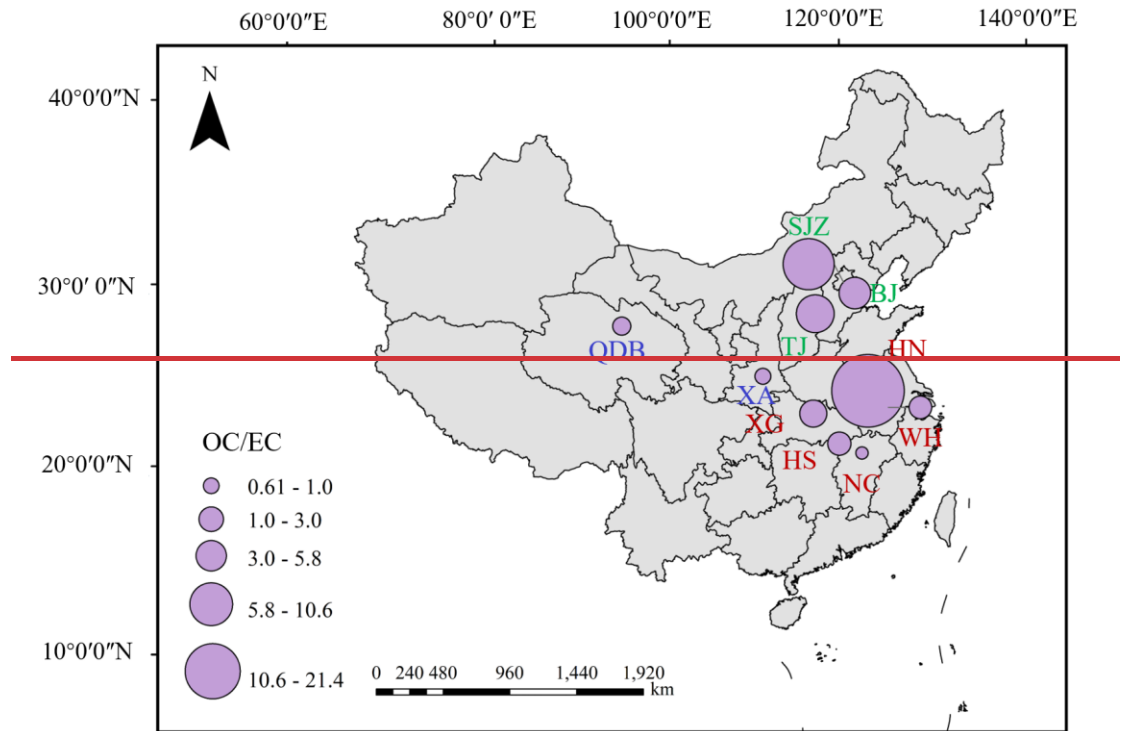
719 Figure 5 presents spatial variations in urban OC/EC ratios across China. The findings reveal
720 that the Northwest region, represented by QDB urban and Xi'an (XA) (Han et al., 2009b), exhibits
721 a significantly lower ratio (~~1.592.50~~ \pm ~~0.561.47~~) compared to central regions, including Nanchang
722 (NC) (Zhang, 2014), Huangshi (HS) (Zhan et al., 2016), Wuhu (WH) (Deng et al. 2014), Xiaogan

723 (XG) (Zhan et al., 2022), and Huainan (HN) (Liu et al., 2020), where the ratio is 5.86 ± 7.81 . This
724 ratio is also lower than that observed in eastern cities such as Beijing (BJ) (Tang et al., 2013), Tianjin
725 (TJ) (Ma et al., 2019), and Shijiazhuang (SJZ) (Guo et al., 2018), which have a ratio of 6.83 ± 2.77 .
726 This pattern is consistent with the trends in atmospheric PM OC/EC ratios (Xie et al., 2023),
727 suggesting that the carbon in the dust of the QDB urban primarily results from coal combustion and
728 industrial emissions, leading to elevated EC concentrations and lower OC/EC ratios (Liu et al.,
729 2022). Conversely, cities with higher economic development, such as Beijing and Tianjin,
730 characterized by greater population density and income levels, typically experience secondary
731 pollution, resulting in higher OC/EC ratios. ~~Furthermore, as the pretreatment used in this study~~
732 ~~removes impurities such as silicates from the carbonaceous components of dust, and the OC~~
733 ~~collection efficiency of this treatment is currently unknown, the lower OC/EC ratios observed may~~
734 ~~also be attributed to a lower OC collection efficiency.~~

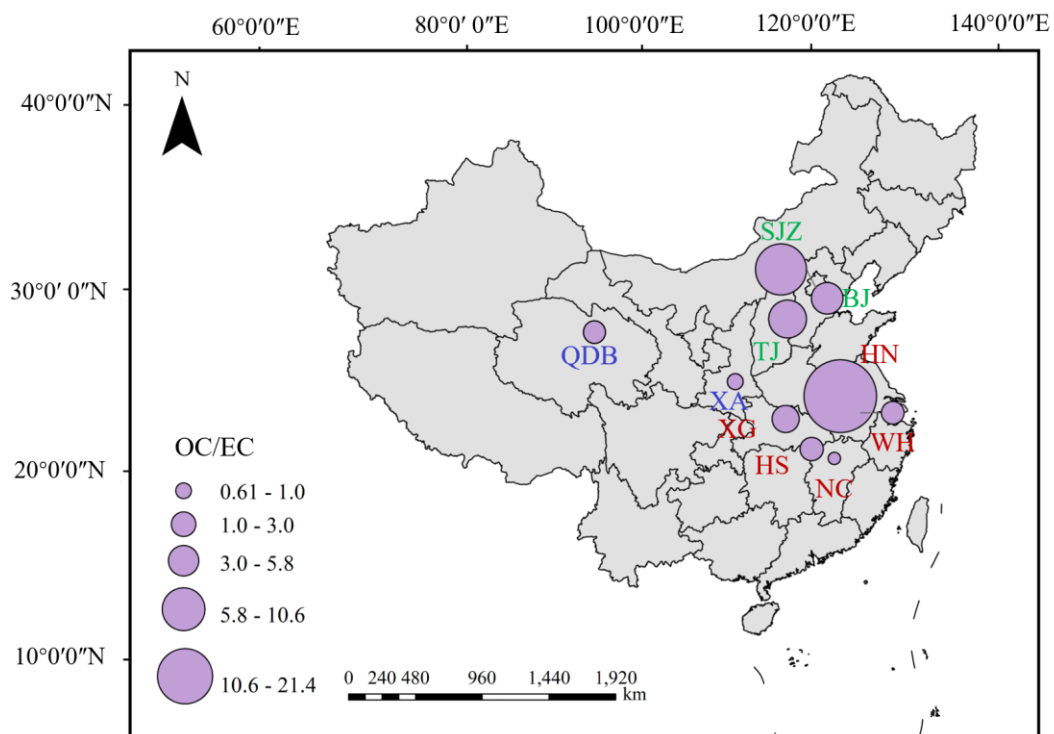
735 While the MDCO sampler effectively captures dry deposition flux, the reported OC and EC
736 values must be interpreted with specific limitations in mind. First, passive sampling is governed by
737 aerodynamic drag and gravitational settling; therefore, the collected OC is likely skewed toward the
738 coarse fraction (e.g., re-suspended soil, biological debris) while potentially under-representing fine-
739 mode anthropogenic combustion aerosols which have negligible settling velocities. This implies
740 that the OC fluxes reported here should be interpreted as fluxes of deposited particulate OC, not as
741 a direct surrogate for total atmospheric OC. Second, the extended exposure period inherent to
742 passive sampling may lead to negative artifacts due to volatilization. Semi-volatile organic
743 compounds may partition from the particulate to the gas phase, a process accelerated in
744 environments with high solar radiation and ambient temperatures (Turpin et al., 1994).
745 Consequently, the OC fluxes reported here likely represent a conservative lower limit. Finally,
746 environmental factors such as wind speed and humidity affect collection efficiency. High wind
747 speeds can induce turbulence leading to the resuspension of lighter organic particles from the
748 collector, while high humidity may facilitate chemical or biological degradation of the organic
749 fraction prior to laboratory analysis (Chow et al., 2011). Taken together, these processes imply that
750 the OC collection efficiency of the MDCO sampler is not a fixed quantity but varies with
751 temperature, relative humidity, precipitation, wind direction and other environmental factors. The
752 role of these meteorological factors in atmospheric dust deposition is examined in detail in Section

753

3.5.



754



755

756 **Figure 5** Distribution of OC/EC ratios across various regions of China. —Blue designations
757 represent the Northwest region, red indicates the Central region, and green denotes the Eastern
758 region. The circle size reflects the magnitude of the OC/EC ratios.

759

760 The Charchar/Sootsoot ratio in QDB is notably high at 5.04, significantly exceeding that of
761 other regions such as Xi'an (0.99) and Wuhan (0.09) (Wei et al., 2015; Liu et al., 2021). Char-EC
762 primarily originates from incomplete combustion processes like biomass burning and coal
763 combustion. Soot-EC mainly derives from high-temperature combustion sources such as fuel oil
764 and diesel vehicle exhaust (Han et al., 2009). The exceptionally high Charchar/Sootsoot ratio in
765 QDB strongly indicates that its limited carbonaceous components predominantly originated from
766 relatively inefficient combustion sources. These potentially included coal or small-scale biomass
767 burning for local residential/expedition activities (e.g., heating, cooking) and possibly long-range
768 transported biomass burning products (e.g., from forest/agricultural fires in South or Southeast Asia)
769 (Han et al., 2009; Han et al., 2006; Han et al., 2016). In contrast, the very low Charchar/Sootsoot
770 ratios observed in cities like Wuhan and Xi'an clearly point to traffic source emissions as their
771 primary contributor, a finding likely influenced by the specific focus of those studies on road dust.

772 However, we fully recognize the fundamental differences in sources and composition between
773 road dust and atmospheric dust-fall. Road dust is primarily secondary dust formed from traffic
774 activities, construction dust, soil particles, and resuspended deposited atmospheric particles, with
775 its carbonaceous composition strongly reflecting intense local anthropogenic emissions (Casotti
776 Rienda and Alves, 2021). In contrast, atmospheric dust-fall integrates contributions from local
777 sources, regional transport, and even long-range transport. Therefore, direct comparison between
778 these two may introduce bias when interpreting regional pollution characteristics and the degree of
779 anthropogenic influence, which cannot be overlooked. Building on this analysis, the next phase of
780 this research will focus on the sampling and analysis of fine atmospheric particulate matter (PM_{2.5}
781 and PM₁) to more accurately elucidate the emission levels and environmental and climatic impacts
782 of carbonaceous aerosols in the QDB.

783

784 **3.5.3 Trace elements concentration**

785 The total concentration of major (Fe, Si, Al) and trace elements (Ti, Cr, Cd, Cu, Mn, Ni, Pb, V,
786 Zn) was determined to be 8.74 ± 5.82 mg/g, while arsenic (As) remained below the detection limit
787 in all analyzed samples. Crustally derived elements—Fe, Al, Si, and Ti—dominated the elemental

788 profile, aligning with dust composition patterns reported in Ira, Singapore, and Beijing-Hebei
789 regions, China (Joshi et al., 2009; Qiao et al., 2013; Eivazzadeh et al., 2021). In comparison to cities
790 such as Beijing, Shanghai, Xi'an, and Lanzhou, and Junggar Basin the levels of heavy metals in dust
791 from the QDB are relatively low (Jiang et al., 2018) (Supplementary Table S5).

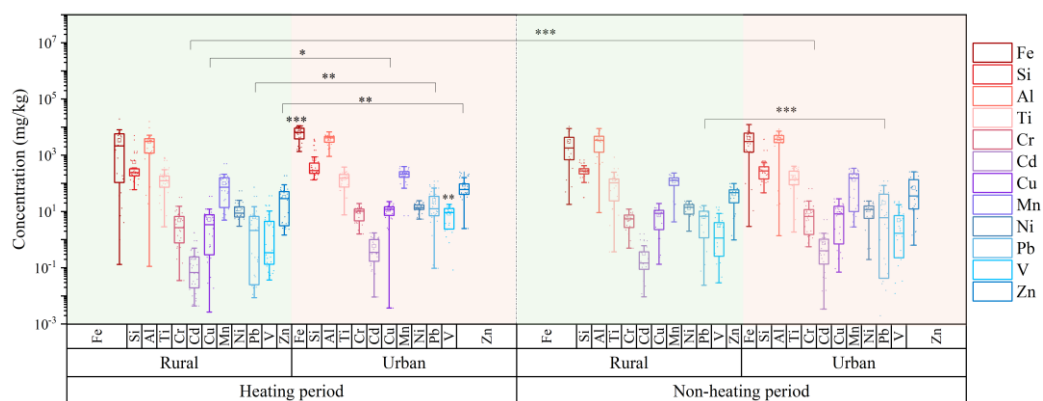
792 The low heavy metal content in dust deposition within the QDB can be attributed to the
793 following factors. The region has sparse human activity, lacks heavy industrial zones and dense
794 urban clusters, resulting in low total anthropogenic emissions of heavy metals. Furthermore, the
795 surface soil in the QDB itself has a low background level of heavy metals, primarily derived from
796 natural sources with relatively weak influence from human activities (Nuralykyzy et al., 2021; Chen
797 et al., 2021). From the meteorological perspectives, the basin's high altitude, strong winds, and arid
798 conditions with minimal precipitation favor the dispersion of atmospheric pollutants. This makes
799 the formation of prolonged stagnant weather conditions unlikely, thereby preventing the
800 accumulation of pollutants and the occurrence of high concentrations near the ground. A particularly
801 unique aspect of the QDB is its role as a significant source of salt dust. The recent study indicates
802 that salt dust emitted from the playa lakes within the basin contributes substantially to atmospheric
803 dust deposition (Zhu et al., 2025). These salt dust particles, composed mainly of soluble salts like
804 NaCl and gypsum, may dilute the relative concentration of non-salt components, such as heavy
805 metals, when released into the atmosphere in large quantities. The combined effect of these factors
806 leads to the observed low heavy metal content in dust deposition in this region.

807 Throughout both the HP and NHP, trace elements concentrations in urban areas were
808 consistently higher than in rural areas (not statistically significant), with the exception of Ti (Figure
809 6 and S143). During the HP, urban levels of Zn, Pb, and Cu were significantly elevated compared
810 to rural areas ($P < 0.05$), and Pb also demonstrated a significant increase in urban during the NHP
811 ($P < 0.01$). In rural, the differences in metal concentrations between HP and NHP were minimal. In
812 contrast, urban areas exhibited higher concentrations of all elements except for Ti, Cd, and Cr during
813 the HP, with Fe and V showing notably elevated levels compared to other regions (not statistically
814 significant). These variations in average concentrations indicate that coal combustion for domestic
815 heating in urban areas contributes to increased atmospheric heavy metal levels (Duan and Tan, 2013;
816 Meng et al., 2017). In contrast, Cd and Cr exhibited mixed anthropogenic sources with limited coal
817 combustion contributions, while Ti concentrations remained stable across seasons, reflecting

818 minimal anthropogenic influence.

819 Analysis of the carbonaceous components in QDB dust deposition reveals more intensive coal
820 combustion in rural areas, yet the heavy metal concentrations in atmospheric deposition are lower
821 than in urban area (not statistically significant). This observation can be explained by the following
822 factors. First, pollution sources in rural areas are relatively singular, whereas urban areas are
823 influenced by more complex heavy metal sources. During the heating period, heavy metals in the
824 rural atmosphere of the QDB mainly originate from coal and biomass combustion. In contrast, urban
825 areas are affected by a wider range of sources, including industrial activities, traffic emissions, and
826 others (Liu et al., 2021; Huang et al., 2021a). Additionally, the dense building layout in urban areas
827 hinders pollutant dispersion, leading to accumulation, while the open terrain in rural areas facilitates
828 dilution and diffusion. This pattern, where rural heavy metal concentrations (particularly Pb, Cr, Cd,
829 As, and other elements associated with coal combustion) are lower than those in urban areas during
830 the heating season, has also been observed in studies conducted in Northeast China, Shanghai,
831 Taiyuan, the Yangtze River Delta, and Southern Nigeria (Shi et al., 2012; Liu et al., 2021; Huang et
832 al., 2021a; Liu et al., 2023b; Hilary et al., 2025).

833



834

835 **Figure 6** Concentration of heavy metals by rural and urban settings during domestic heating and
836 non-domestic heating periods. Significant differences are indicated by asterisks (* $p < 0.05$; ** $p <$
837 0.01 ; *** $p < 0.001$).

838

839 **3.6.4** Source apportionment

840 We conducted a PMF source apportionment analysis on soluble ions, trace and carbonaceous
841 elements present in dust, specifically focusing on ps-SO_4^{2-} , ps-Ca^{2+} , ps-K^+ , ps-Mg^{2+} , ps-Cl^- , ps-Na^+ ,

842 nps-SO₄²⁻, nps-Ca²⁺, nps-K⁺, nps-Mg²⁺, nps-Cl⁻, nps-Na⁺, Fe, Si, Al, Ti, Cr, Cd, Cu, Mn, Ni, Pb, V,
843 Zn, SOC, POC and ~~Char~~char-EC, ~~Soot~~soot-EC. Seven source factors were identified based on prior
844 research and an understanding of potential local sources: salt lakes, soil, ~~vehicular~~traffic emissions,
845 secondary ~~sources~~inorganics, biomass and coal burning, and industrial activities (Figure 7 and
846 S154). A plot of the time series is provided in Figure S165. The generation of Figure 7a involved
847 extracting factors identified as the same source from the PMF factor profiles of each site (Urban
848 and Rural) and each heating season (HP and NHP) shown in Figure S154. The arithmetic mean of
849 the contributions from characteristic species (elements and ions) corresponding to each factor was
850 calculated. Species with average contributions exceeding 20% were defined as characteristic species
851 of that source in atmospheric dust over the QDB.

852 The factor profiles for each element in these source categories represent the arithmetic mean
853 of profiles from six stations, with detailed operational methods provided in Supplementary Text S1.
854 The uncertainty of the source contributions was calculated directly from the standard error of the
855 multiple regression coefficients between the deposition flux (independent variable) and the source
856 contribution (dependent variable) at different monitoring sites (Belis et al., 2015; Manousakas et al.,
857 2017). The regression method assumes that all factors explaining the mass have been identified;
858 however, if a significant portion of the mass not directly related to the species in the PMF analysis
859 is omitted, the source contributions may be overestimated, which could be an important additional
860 source of uncertainty. The results are shown in Table S6. It must be noted that this method captures
861 only a portion of the total uncertainty, as it does not include errors from profile uncertainty or
862 rotational ambiguity. The low errors calculated by this method indicate a good model fit. In this
863 study, the sample numbers used for PMF source apportionment were 690, 780, 480, and 750 for the
864 Urban-NHP, Urban-HP, Rural-NHP, and Rural-HP groups, respectively. Limited sample number can
865 increase the risk of model overfitting, reduce the representativeness of source profiles, and
866 potentially lead to the merging of multiple sources into a mixed factor (Norris et al., 2014). Future
867 research will extend the observation period and increase the sample number to further enhance the
868 reliability of the source apportionment results.

869 The ions ss-Na⁺, ss-Cl⁻, ss-SO₄²⁻, ss-Ca²⁺, ss-K⁺, and ss-Mg²⁺ are widely acknowledged as
870 indicators of sea salt (Ambade et al., 2022; Aswini et al., 2022; Gluscic et al., 2023). In this study,
871 we identified ps-Cl⁻ (~~82.71~~83.96%), ps-Ca²⁺ (83.71%), and ps-SO₄²⁻ (83.71%), ps-Na⁺ (83.70%),

872 ps-Mg²⁺ (~~79.03~~83.66%), ps-K⁺ (~~79.02~~82.35%), ~~ps-Na⁺ (78.69%), ps-Ca²⁺ (78.70%), and ps-SO₄²⁻~~
873 (~~78.69%~~) as key markers of salt lake sources. ~~Furthermore, Cd (29.70%) was detected at multiple~~
874 ~~sampling sites, indicating contributions from both salt lakes and industrial emissions. Salt lake~~
875 ~~emissions were most pronounced in rural areas during the HP of 2023 at site LTC and during the~~
876 ~~NHP of 2020 at site XZH. In urban areas, elevated contributions occurred during the NHP and HP~~
877 ~~of 2022 at site GEM, and during the HP of 2023 at site DLX.~~ The contribution of salt lake sources
878 in rural (~~12.93~~29%) was ~~significantly~~ higher than in urban (~~10.33~~6.87%). During the HP, the
879 proportion of salt lake sources in rural areas was ~~5.49~~4.97%, compared to ~~20.37~~19.61% in the NHP;
880 urban showed contributions of ~~18.24~~2.16% during the HP and ~~2.42~~11.58% in the NHP, showing
881 opposite seasonal trends. Backward trajectory simulations indicated that during the HP, air mass in
882 both urban and rural areas mainly originated from the northwestern part of the basin and the eastern
883 Tarim Basin, whereas during the NHP, they were broadly influenced by the salt lake regions within
884 the basin (Figure S6). The minor wind direction differences and the inter-distributed sampling points
885 (Figure 1), suggests no substantial geographical disparity between urban and rural sites. Additionally,
886 the ion content derived from playa salts in dust deposits increased during the NHP in both areas.
887 Therefore, we propose that the anomalous increase in salt lake contribution during the urban HP
888 may be closely related to human activities. The enhanced Urban Heat Island (UHI) effect and
889 temperature inversion structures during the HP can alter boundary layer height, turbulence, and
890 deposition conditions, thereby increasing the residence time of externally transported particles
891 within the urban boundary layer and elevating their measured contribution (Cichowicz and
892 Bochenek, 2024). Urban heat sources and heating emissions may also modify local transport
893 pathways, leading to more concentrated deposition of dust originating from playa regions over urban
894 areas. Furthermore, dry road surfaces, increased traffic, and construction activities during the HP
895 can promote the resuspension of previously deposited playa dust. The use and subsequent
896 resuspension of road de-icing salts (e.g., NaCl, CaCl₂) may further amplify the contribution of tracer
897 ions indicative of playa salts (Gertler et al., 2006; Casotti Rienda and Alves, 2021).

898 The second factor pertains to soil dust, characterized by trace element such as ~~Fe (47.03%)~~Si
899 (~~37.17%~~) and Si (36.22%)~~Al (29.18%)~~, along with ions such as ~~nps-Cl~~Na⁺ (34.90
900 54.21%), ~~nps-~~Ca²⁺ (44.05%), ~~nps-Mg²⁺ (28.21~~32.30%), and ~~Fe (24.43%)~~ (Pervez et al., 2018; Tian et al., 2021).
901 Additionally, the proportions of elements such as SOC (~~28.20~~32.58%) and POC (~~47.70~~20.84%)

902 suggest that the dust is likely mixed with fossil fuel emissions. ~~Furthermore, Cd~~V (29.7024.62%)
903 was detected at multiple sampling sites, indicating contributions from both salt lakes soil dust and
904 industrial traffic emissions. Mg, ~~Ca²⁺~~, Al, Si, and Fe are typical tracers for soil dust (Liu et al., 2003;
905 Heo et al., 2009). ~~The temporal variation of soil dust was largely consistent with that of the salt lake~~
906 ~~source, indicating the fact that they may be influenced by similar factors.~~ Notably, the contribution
907 of soil dust in rural areas (~~22.44~~21.14%) exceeded that in urban areas (~~43.33~~12.97%), indicating
908 that soil dust is a major source of atmospheric deposition. In urban areas, the contribution during
909 the NHP was relatively low (~~7.36~~6.84%), likely due to higher wind speeds and the effectiveness of
910 frequent summer precipitation (Zhang et al., 2015a).

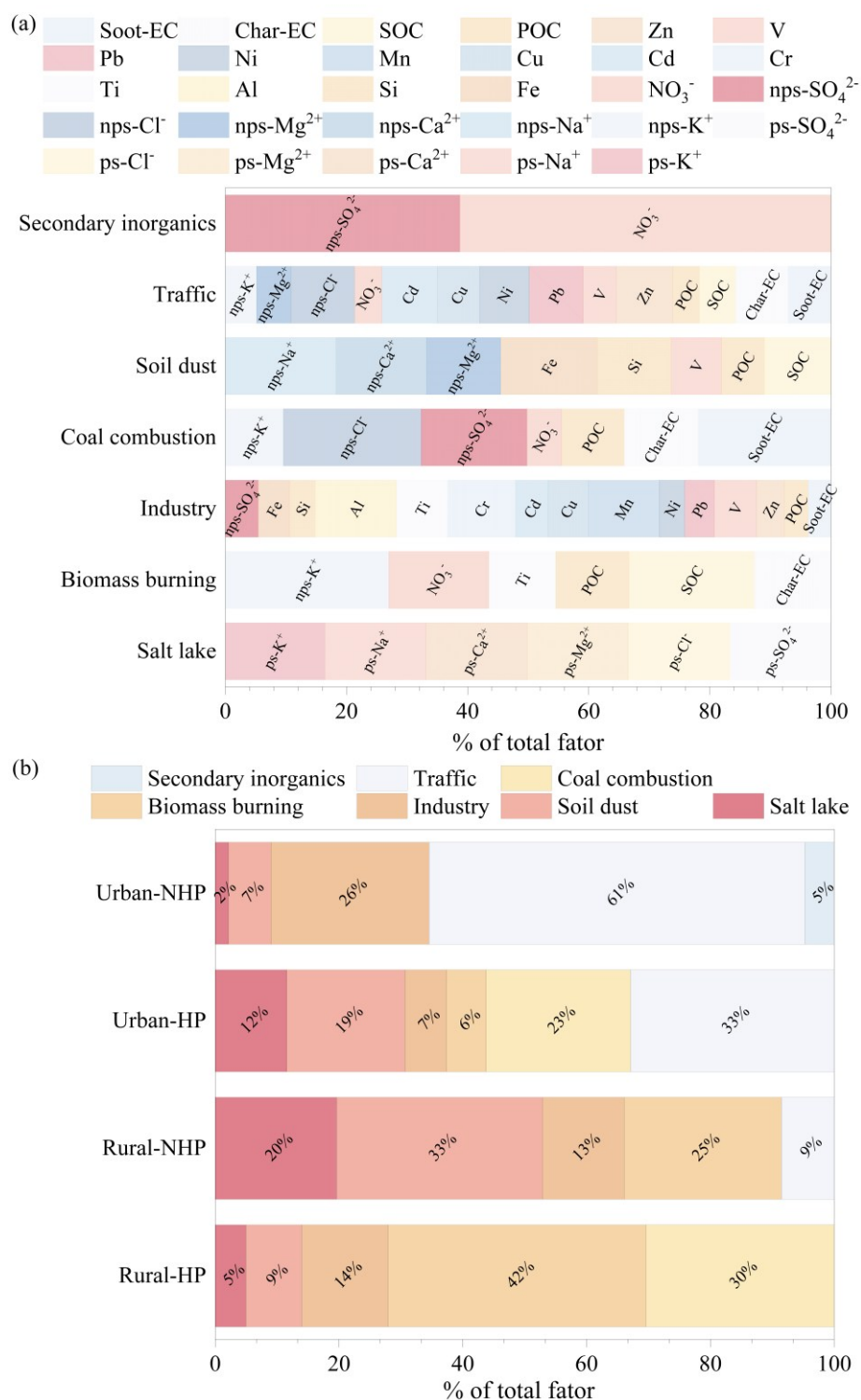
911 The third factor is traffic emissions, which are particularly pronounced in urban areas. Key
912 characteristic elements and ions include nps-Cl(56.71%), Zn (50.13%), Cd (49.41%), Pb
913 (59.5247.84%), Ni(44.22%), Cu(37.61%), V(48.73%), nps-Mg²⁺ (40.7830.54%), V (29.63%), Zn
914 (37.47%), ~~nps-Cl(33.83%), Cd (32.43%), nps-K⁺ (29.647.74%), Ni (27.01%), NO₃⁻~~
915 (20.9924.35%)and char-EC (46.71%), soot-EC (38.12%), SOC (32.25%), POC (23.72%) ~~SOE~~
916 (51.71%), Soot-EC (37.56%), Char-EC (24.94%) (Adeniran et al., 2017). In rural areas, ~~vehicular~~
917 traffic emissions contributed ~~8.17~~8.52% to atmospheric deposition during the NHP, whereas in
918 urban areas, the contribution was significantly higher at ~~45.13~~46.83%, with ~~30.07~~32.91% during the
919 HP and ~~58.78~~60.75% in the NHP. These findings correlate with previous studies on OC/EC and
920 char/soot ratios, suggesting that carbonaceous elements in the NHP primarily derive from
921 ~~traffic~~vehicular emissions. The traffic emission factor in the QDB represents a mixture of vehicle
922 exhaust and non-exhaust sources (e.g., tire and brake wear, and resuspended road dust). Elements
923 and ions including V, NO₃⁻, Ni, and carbonaceous components primarily associated with vehicle
924 exhaust (Cong et al., 2011; Zhang et al., 2012). For instance, Ni can be emitted from fuel combustion
925 and vehicle exhaust (Pacyna and Pacyna, 2001). In contrast, elements such as Cu, Zn, nps-Mg²⁺,
926 and nps-K⁺ originate from non-exhaust vehicle emissions, including brake and tire wear, as well as
927 the resuspension of road dust (Amato et al., 2014). For example, Zn may derive from the wear of
928 rubber tires on roads (Rogge et al., 1993), Pb emissions may be related to wear (tires/brakes)
929 (Smichowski et al., 2007), and Cu is associated with brake wear (Lin et al., 2015). Furthermore, the
930 presence of crustal elements and ions such as Fe, Si, and nps-Mg²⁺ in the traffic emission factor for
931 Urban-NHP, Urban-HP, and Rural-NHP suggests an additional contribution from resuspended road

932 dust (Chen et al., 2019). ~~For traffic emissions during the NHP, peaks were observed in both rural~~
933 ~~and urban areas in 2022, generally concentrated in July, August, and September, coinciding with the~~
934 ~~tourism high season. During the HP, traffic emissions primarily occurred in 2021 at GEM and in~~
935 ~~2023 at DLX. Due to the impact of the COVID-19 pandemic, tourist numbers in the QDB sharply~~
936 ~~declined in 2020 and 2021. The peak in tourism activity in 2022 (Qinghai Statistical Yearbook, 2022)~~
937 ~~corresponded with the highest level of traffic emissions during the three-year period, indicating a~~
938 ~~direct impact of tourism flux on emission levels. However, given the relatively short sampling~~
939 ~~duration of this study (three years), longer term data and further research are needed to substantiate~~
940 ~~this hypothesis.~~

941 The fourth factor is coal combustion, characterized by high concentrations of nps-Cl⁻
942 (~~50.9375.40%~~), nps-SO₄²⁻ (~~26.6157.87%~~), nps-K⁺ (31.75%), NO₃⁻ (22.8219.10%), and soot-EC
943 (72.54%). ~~Char-EC (73.0140.63%)~~, ~~Soot-EC (65.98%)~~, POC (46.0434.10%), ~~SOC~~
944 ~~(21.12%)~~ (Kundu and Stone, 2014; Contini et al., 2016). Zhang et al (2023) found that coal
945 combustion emits particles rich in Cl⁻. Coal combustion was more intense at site LTC in rural areas
946 and at site DLX in urban areas. Coal combustion occurs exclusively during the HP, contributing
947 34.5730.38% in rural areas and 20.6323.31% in urban areas. These results align with earlier studies
948 on carbonaceous aerosols, indicating that the carbon content from coal combustion emissions is
949 higher in rural ~~regions~~ than in urban ~~environments~~ aeras. Consistent with northern China, air
950 pollution in QDB urban has declined due to the adoption of clean heating technologies (Zhang et
951 al., 2021; Xue et al., 2023). However, rural coal combustion remains a major source of carbonaceous
952 aerosols during the HP.

953

954



955

956 **Figure 7** Factor profile and contributions in urban and rural area. (a) presents the factor profiles,
 957 represented as the arithmetic mean of individual elements across various locations, highlighting
 958 only those elements that constitute more than 20% of each profile. (b) illustrates the contributions
 959 of different sources at each location. [HP, domestic heating period; NHP, non-domestic heating
 960 period].

961 The fifth factor, biomass burning, is characterized by significant concentrations of non-
962 precipitating species, including nps-K⁺ (~~42.76~~56.99%), ~~nps-Na⁺ (35.49%), nps-Ca²⁺ (29.23%), nps-~~
963 ~~SO₄²⁻ (26.56%), NO₃⁻ (24.46~~34.97%), Ti (~~23.41~~23.26%) and SOC(43.68%), char-EC (26.78%),
964 POC (46.48~~25.60~~%), ~~Soot-EC (28.33%)~~ (Simoneit, 2002; Sulong et al., 2019). K⁺ serves as an
965 important tracer for biomass burning (Cachier and Ducret, 1991). Biomass burning contributes
966 ~~32.82~~33.55% to rural atmospheric dust deposition, with a higher proportion during the HP
967 (~~39.21~~41.67%) compared to NHP (~~26.44~~5.43%). ~~Biomass burning made significant contributions~~
968 ~~in urban areas in 2021 and 2022. In rural areas, biomass burning emissions were particularly strong,~~
969 ~~especially during the HP at LTC and the NHP at XZH.~~ In urban, biomass burning is primarily
970 observed during the HP, contributing only ~~2.19~~6.41%. These findings underscore biomass burning
971 as a major source of carbon emissions in rural settings, aligning with the prevalent use of biomass
972 fuels for cooking and domestic heating in Northern China's rural areas (Meng et al., 2019), where
973 70% to 80% of energy demand are fulfilled by materials such as dung cakes, firewood, charcoal,
974 and crop residues (Tao et al., 2018; Shi et al., 2019). Furthermore, increased biomass burning is also
975 associated with the autumn harvest period (Chen et al., 2017; Li et al., 2021).

976 The sixth factor pertains to industrial emissions, which are characterized by high
977 concentrations of Mn (61.98%), Cr (59.22%), Ti (44.90%), V (37.17%), Cu (34.95%), Cd (28.63%),
978 Fe (27.47%) Pb (55.18~~25.75~~%), ~~Fe (48.91%), Cr (37.05%), Zn (36.42%), Ti (35.10%), Cu (34.91%),~~
979 ~~V (34.44%), Ni (29.69%), Mn (29.59%)~~ and Zn (24.03%) Cd (21.29%) (Almeida et al., 2015; Yao
980 et al., 2016). These elements were consistently detected across all sampling sites, alongside Al
981 (~~38.84~~71.17%), nps-SO₄²⁻ (~~34.15~~28.84%), Si (~~23.39~~22.24%) and ~~nps-Ca²⁺ (20.48%), nps-Na⁺~~
982 ~~POC (20.02~~20.95%), soot-EC (19.97%), which indicate potential contributions from soil dust. Zn,
983 Cu, Fe, and Mn are major chemical components in industrial emission profiles; Cd is a trace element
984 found in metallurgical industries (Xu et al., 2022), while Zn and Mn emitte from oil combustion,
985 metallurgy, and steel manufacturing processes (You et al., 2017). Pb and Cd are associated with
986 metal smelting and processing (Fang et al., 2021). Industrial emissions showed greater contributions
987 during the HP at XZH and at DLX. In rural areas, industrial emissions constitute ~~11.10~~13.57% of
988 carbon output, with contributions of ~~10.86~~13.95% during the HP and ~~11.33~~23.20% during the NHP.
989 In urban areas, industrial emissions account for 16.~~41~~12% overall, with ~~7.37~~6.69% during the HP
990 and 25.~~44~~55% in the NHP. ~~Due to the abundance of non-ferrous metal resources (e.g., lead-zinc~~

991 ores), oil, natural gas, and saline minerals (e.g., potassium, lithium) in the QDB, the primary
992 industrial activities are mining and associated chemical industries. Particularly around the GEM and
993 DLX sites, the presence of numerous ~~lead-zinc~~Pb-Zn, ~~iron~~Fe, and ~~copper~~Cu mining enterprises
994 leads to significant contributions from industrial emissions to urban dust fallout, making it one of
995 the major sources of air pollution in the basin.

996 The seventh factor is secondary inorganic aerosols, primarily composed of NO_3^- (~~68.54~~72.46%),
997 ~~nps-~~ $\text{SO}_4^{2-}\text{Mg}^{2+}$ (~~41.04~~45.79%), ~~nps-~~ Na^+ (~~39.01~~39.01%) and ~~nps-~~ Ca^{2+} (~~30.79~~30.79%) (Liu et al., 2015; Liu et
998 al., 2016a). High mass loadings of NO_3^- and SO_4^{2-} are characteristic of typical secondary inorganic
999 aerosols (Huang et al., 2021). Research indicates that NO_3^- and SO_4^{2-} primarily result from the
1000 conversion of gaseous precursors, such as SO_2 and NO_x , through photochemical reactions,
1001 predominantly sourced from local and regional emission (Liu et al., 2015; Tao et al., 2013).
1002 Secondary inorganic aerosols are predominantly observed in urban areas during the NHP, where
1003 they contribute ~~6.00~~4.70% to total aerosol sources. This increase is likely due to elevated
1004 temperatures and enhanced solar radiation during this period, which promote photochemical activity
1005 (Pandolfi et al., 2010). ~~The secondary inorganic aerosol source was identified only in Urban NHP,~~
1006 ~~peaking in August 2022 at GEM and in June, July, and August 2022 at NMH. This trend closely~~
1007 ~~followed the distribution of traffic emissions, suggesting that the formation of secondary aerosols is~~
1008 ~~linked to increased traffic activity. Traffic emissions, particularly vehicle exhaust, are a significant~~
1009 ~~source of secondary inorganic aerosols (especially NO_3^-) in urban atmospheres (Ma et al., 2017).~~
1010 ~~Source apportionment studies in Beijing have similarly found that the contribution of secondary~~
1011 ~~inorganic aerosols increases in summer, closely associated with traffic emissions (Zhang et al.,~~
1012 ~~2013).~~

1013 Dust deposition sources exhibit significant seasonal and spatial variations. In the QDB, coal
1014 combustion (~~27.60~~26.85%) and biomass burning (~~22.21~~24.04%) dominate during HP, transitioning
1015 to traffic emissions (~~33.48~~34.64%), soil dust (~~21.27~~20.04%) and industry emission (~~18.39~~19.37%)
1016 as the primary contributor in NHP. Rural areas predominantly contribute to dust through biomass
1017 burning and coal combustion, as well as natural sources like windblown dust and salt lake emissions.
1018 This pattern aligns with increased coal usage for winter domestic heating and heightened biomass
1019 burning for cooking and heating in rural areas. In urban, dust deposition is briefly influenced by
1020 anthropogenic activities, including traffic and industrial emissions, with minimal contributions from

1021 domestic heating. Such differences can be attributed to varying economic development models,
1022 industrial and energy structures, and levels of human activity (Kataki et al., 2016).

1023 Time series analysis (Figure S16) indicates that atmospheric dust deposition in rural areas
1024 primarily originates from natural processes and dispersed anthropogenic combustion due to sparse
1025 human activities. During the NHP, the contribution of salt-lake emissions increases in May and June.
1026 Strong winds in spring and summer in southern QDB transport saline soil particles, making them a
1027 key source of dust deposition (Zhu et al., 2025). Soil-derived dust shows variations highly
1028 synchronized with the salt-lake source, with elevated contributions also occurring in May and June,
1029 reflecting the natural erosion of exposed surfaces under high wind conditions (Zhang, 2010). Traffic
1030 contributions rise noticeably in July and August, likely linked to increased summer tourism and
1031 transportation. During the HP, contributions from biomass and coal combustion increase, peaking
1032 from November to January. This peak is attributed to the widespread use of biomass fuels such as
1033 livestock dung for decentralized heating in rural areas, leading to increased particulate matter
1034 emissions (Chen et al., 2023). In contrast, contributions from salt lakes and wind-blown dust
1035 decrease significantly, likely due to lower wind speeds and reduced natural source emissions in
1036 winter (Jiménez et al., 2018; Li et al., 2019a; Yang et al., 2024).

1037 In urban areas, where human activities are more concentrated, pollution sources are dominated
1038 by centralized anthropogenic emissions (industry, traffic, and centralized heating), with temporal
1039 trends driven by both industrial activity and the heating cycle. During the NHP, industrial
1040 contributions increase, especially in towns such as GEM and DLX, where surrounding mining
1041 operations constitute a major anthropogenic source (Zhu et al., 2016). Traffic-related contributions
1042 follow a trend similar to that in rural NHP, also peaking in July and August, reflecting the common
1043 influence of increased vehicle flow during the tourism season. Meanwhile, precursors such as SO₂
1044 and NO_x from industrial and traffic emissions undergo photochemical and gas-to-particle conversion
1045 under summer sunlight, enhancing the formation of secondary inorganic aerosols (e.g., SO₄²⁻, NO₃⁻)
1046 (Zhang et al., 2013; Ma et al., 2017). During the HP, trends in salt-lake emissions, soil dust, and
1047 coal/biomass combustion are generally similar to those in rural areas. However, unlike in rural
1048 regions, traffic contributions in urban areas continue to increase during the HP, highlighting the
1049 higher intensity and less seasonally-variable nature of human activities in towns (Peng et al., 2021).

1050 This study observed that the contribution of biomass burning to atmospheric dust deposition in

1051 rural areas of the QDB during the HP was higher than that of soil dust. Given that the collected dust
1052 samples had particle sizes $>10\ \mu\text{m}$, while biomass burning typically emits aerosols in the submicron
1053 range, we propose several potential explanations. Firstly, during the HP, factors such as increased
1054 soil moisture and snow cover significantly suppress soil dust emission, resulting in a lower intensity
1055 than in other seasons (An et al., 2018; Yang et al., 2019). Simultaneously, biomass and coal burning
1056 for heating increases substantially, leading to intense, short-term emissions of fine particles.
1057 Although it was fine initially, these high-concentration ultrafine particles can undergo coagulation
1058 or coalescence, aggregating with each other or onto pre-existing coarse particles, thereby increasing
1059 their size (Butler and Mulholland, 2004; Kulmala et al., 2004; Li et al., 2020). Furthermore, fine
1060 particles from biomass burning (e.g., carbonaceous materials) may mix internally with coarse
1061 particles like soil dust or salt dust from the QDB, forming internally mixed particles (Li et al., 2003;
1062 Hand et al., 2010). During source apportionment, such coarse particles are more likely to be
1063 attributed to the biomass burning source. Additionally, the QDB is a significant source of salt dust
1064 (Zhu et al., 2025). Salt dust particles (e.g., halite, gypsum) provide excellent condensation nuclei
1065 for soluble substances emitted from biomass burning, greatly promoting hygroscopic growth (Li et
1066 al., 2003; Kumar, 2010; Wang, 2013). The basin's topography also favors stable inversion layers,
1067 inhibiting pollutant dispersion and allowing particles more time to grow, mix, and age in the
1068 atmosphere. Prevailing wintertime winds may also transport pollutants from surrounding regions
1069 into the basin.

1070 Moreover, the dust in this study was collected using a passive sampler. Over 90% of the
1071 collected dust particles were smaller than $100\ \mu\text{m}$, with approximately 25% less than $10\ \mu\text{m}$ (Figure
1072 S2+6), indicating the presence of fine particles ($<10\ \mu\text{m}$), albeit in a relatively small proportion. The
1073 particle size distribution of atmospheric dust deposition is similar to that of TSP, with both primarily
1074 consisting of particles smaller than $100\ \mu\text{m}$. Using PMF source apportionment, this study identified
1075 a notably high contribution from biomass burning in rural areas, particularly during the heating
1076 period. Similarly, studies on atmospheric TSP in Iran (Ashrafi et al., 2018), the Qinghai-Xizang
1077 Plateau (Lulang) (Zhao et al., 2013), Northeast China (Jia et al., 2024), and Qingdao (Liu et al.,
1078 2022) have also reported significant contributions from biomass and coal combustion. This suggests
1079 that contributions from biomass and coal combustion can indeed be observed in particles larger than
1080 $10\ \mu\text{m}$. Finally, the PMF model may have uncertainties in resolving sources with similar chemical

1081 profiles. If the chemical compositions of local soil dust and biomass burning particles overlap after
1082 long-range transport and complex atmospheric reactions, the model might not fully separate them
1083 (Cesari et al., 2016).

1084 1085 **3.5 Influence of meteorological factors**

1086 Meteorological parameters critically influence the accumulation and dispersion of airborne
1087 pollutants. To examine their impact on the chemical composition of dust deposition in this study,
1088 monthly data for temperature, humidity, precipitation, wind speed and direction, sunshine duration,
1089 frequency of visibility ≤ 10 km were obtained from four monitoring stations (XZH, GEM, NMH,
1090 DLX) during the study period (Table 1 and Figure S17). Data from the LTC and BLX sites were
1091 excluded from this analysis due to a lack of on-site meteorological instrumentation.

1092 Based on ANOVA results, wind speed and temperature were significantly higher during the
1093 NHP ($P < 0.05$), promoting dust emission and consequently increasing atmospheric dust flux
1094 (Jiménez et al., 2018; Li et al., 2019b; Yang et al., 2024). However, at DLX, wind speed showed no
1095 significant seasonal difference, while precipitation and relative humidity were significantly higher
1096 in the NHP ($P < 0.05$). Since precipitation is a known suppressor of dust deposition (Li et al., 2019b),
1097 meteorological factors were not the primary driver of the elevated dust flux at DLX during the NHP
1098 (Figure S18); other factors, such as increased tourism, likely played a more important role.
1099 Additionally, correlation analysis revealed that dust and salt dust flux were positively correlated
1100 with the frequency of visibility ≤ 10 km and wind speed ($P < 0.05$) and negatively correlated with
1101 relative humidity ($P < 0.05$), consistent with previous findings (Wei et al., 2023).

1102 Pearson correlation analysis further elucidated the relationships between dust chemical
1103 components and meteorological parameters. Ions derived from salt lake (ps ions) and crustal
1104 elements (e.g., Al) showed significant correlations with wind direction and speed ($P < 0.05$, Figure
1105 S19), indicating the dominant control of wind on the emission and transport of both playa salt and
1106 soil dust. During the HP in both rural and urban areas, relative humidity was negatively correlated
1107 with ps ions and crustal elements ($P < 0.05$), suggesting that higher humidity promotes the removal
1108 of airborne particles (Deshmukh et al., 2011). Playa salt ions are hygroscopic, so higher relative
1109 humidity facilitates their deliquescence (Rörig-Dalgaard, 2021). The mean annual relative humidity

in the QDB (about 34 %RH) is notably lower than Wuhan (75.4 %RH) (Zang et al., 2021), Handan (63.35 %RH) (Meng et al., 2016), Pearl River Delta region (67.05 %RH) (Yue et al., 2015), Jorhat, India (80.29 %RH) (Rabha et al., 2021) and other regions, providing favorable conditions for the long-range transport of salt-lake-derived particles.

Table 1 Meteorological conditions at the monitoring stations during the sampling periods.

Site	Period	Temperature (°C)	Relative humidity (%)	Precipitation (mm·d ⁻¹)	Wind speed (m·s ⁻¹)	Wind direction	Sunshine duration (h·m ⁻¹)	Frequency of visibility ≤10 km
Whole		4.27 ± 10.58	33.56 ± 5.74	2.63 ± 3.64	3.29 ± 0.63	WNW	237.73 ± 26.86	36.52 ± 15.27
XZH	HP	-3.16 ± 6.30	33.57 ± 6.36	1.47 ± 2.95	2.93 ± 0.49	WNW	240.58 ± 25.04	41.19 ± 16.61
	NHP	15.65 ± 2.86	33.54 ± 4.63	4.41 ± 3.97	3.83 ± 0.40	W	233.55 ± 28.82	29.36 ± 9.10
Whole		5.76 ± 9.80	31.22 ± 5.39	3.07 ± 4.03	1.94 ± 0.43	W	237.44 ± 30.10	65.89 ± 26.78
GEM	HP	-0.91 ± 5.94	30.38 ± 5.58	1.78 ± 1.69	1.75 ± 0.35	W	233.03 ± 30.95	83.54 ± 14.18
	NHP	16.45 ± 2.83	32.57 ± 4.38	6.1 ± 4.77	2.24 ± 0.36	W	244.21 ± 27.40	37.65 ± 15.71
Whole		5.42 ± 10.01	33.03 ± 6.99	2.93 ± 4.05	1.53 ± 0.39	WNW	221.93 ± 23.79	78.58 ± 16.21
NMH	HP	-1.57 ± 6.08	30.23 ± 6.09	0.54 ± 1.14	1.70 ± 0.37	W	218.58 ± 20.84	88.75 ± 8.04
	NHP	16.13 ± 2.77	37.32 ± 6.04	6.59 ± 4.17	1.29 ± 0.30	WNW	226.84 ± 26.79	62.99 ± 12.84
Whole		3.32 ± 9.07	38.24 ± 8.48	18.45 ± 23.90	2.40 ± 0.35	WNW	254.63 ± 56.83	33.69 ± 12.3
DLX	HP	-3.08 ± 5.39	34.04 ± 6.26	7.12 ± 8.89	2.42 ± 0.33	WNW	260.09 ± 49.28	34.5 ± 11.45
	NHP	13.12 ± 2.78	44.68 ± 5.95	35.83 ± 29.34	2.38 ± 0.35	W	230.33 ± 32.44	32.45 ± 11.98

Note: HP = heating period; NHP = non-heating period.

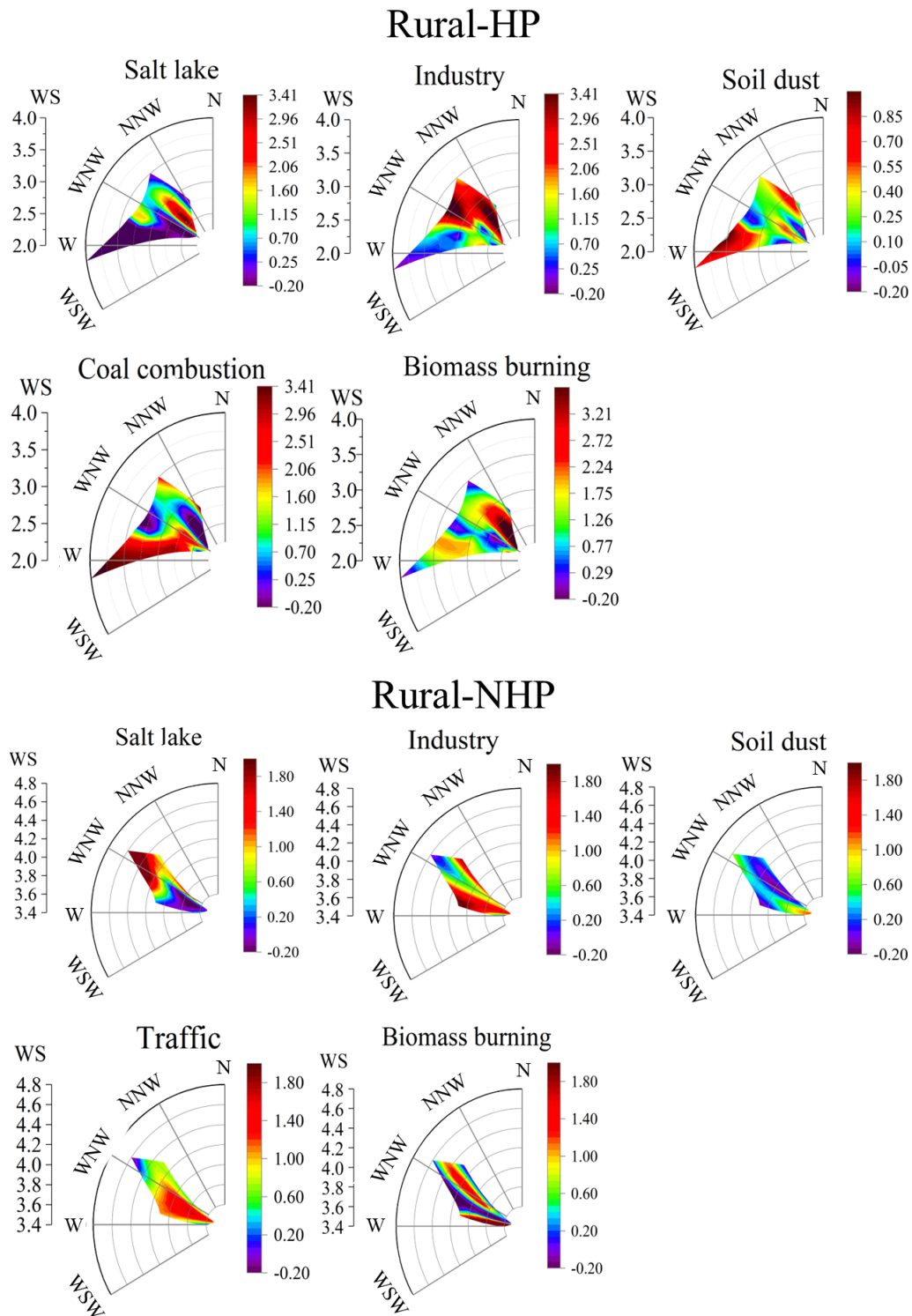
For nps ions, nps-Cl⁻ (a tracer of coal combustion) during the HP was positively correlated with wind direction ($P < 0.05$, Figure S19), indicating downwind transport. In contrast, nps-K⁺ (a tracer of biomass burning) was negatively correlated with wind speed and solar radiation ($P < 0.05$), consistent with the observed peak in combustion contributions during winter when solar radiation is the lowest. Increased wind speed may suppress biomass-burning intensity (Zhang, 2024), while higher solar radiation can reduce smoldering-phase nps-K⁺ emissions and enhance photochemical removal of aerosols (Kuang et al., 2020; Huang and Gao, 2021).

1125 For carbonaceous components (Figure S20), in the rural NHP, soot-EC, OC, and the char/soot
1126 ratio were positively correlated with precipitation and negatively with the frequency of visibility
1127 ≤10 km ($P < 0.05$). In the rural HP, the char/soot ratio was positively correlated with precipitation.
1128 In the urban NHP, char-EC, soot-EC, and their ratios showed positive correlations with humidity
1129 and precipitation ($P < 0.01$), while POC was positively correlated with the frequency of visibility
1130 ≤10 km ($P < 0.01$). Total carbon, OC, and SOC were negatively correlated with wind speed ($P <$
1131 0.05). In the urban HP, EC and char-EC were negatively correlated with the frequency of visibility
1132 ≤10 km; POC was positively correlated with wind speed and solar radiation but negatively with the
1133 frequency of visibility ≤10 km ($P < 0.05$); and the char/soot ratio was positively correlated with
1134 wind speed and negatively with the frequency of visibility ≤10 km ($P < 0.01$).

1135 Overall, wind speed was negatively correlated with TC, OC, SOC, POC, and the char/soot ratio
1136 ($P < 0.05$). This pattern aligns with findings from Xi'an (Cao et al., 2009), New Delhi (Tiwari et al.,
1137 2015), and Karachi (Bibi et al., 2017), although it was not observed in rural areas (Sharma et al.,
1138 2002). Increased wind speed enhances ventilation, promoting aerosol dispersion and reducing
1139 carbonaceous aerosol concentrations (Saha and Despiiau, 2009). The low mean wind speed (about
1140 2.30 m/s) may also indicate that carbon emissions are predominantly local rather than distant sources
1141 (Shen et al., 2021). Positive correlations of precipitation and relative humidity with soot-EC,
1142 char-EC, OC, and the char/soot ratio likely reflect the hygroscopic nature of carbonaceous aerosols:
1143 under humid conditions, particles absorb water, increase in mass, and undergo accelerated dry
1144 deposition. For instance, PM_{2.5} deposition rates can increase 2-3 fold as relative humidity rises from
1145 30% to 70%, thereby shortening their atmospheric residence time (Wu et al., 2016). The negative
1146 correlations of EC, char-EC, and POC with the frequency of visibility ≤10 km align with findings
1147 in cities such as Suzhou (Zhang et al., 2010) and Beijing (Kong et al., 2021), attributable to the
1148 strong light-absorbing (EC) and light-scattering (OC) properties of these components, which jointly
1149 enhance atmospheric extinction and reduce visibility (Zhang et al., 2010; Kong et al., 2021). Weaker
1150 correlations in rural areas indicate that carbonaceous components are less influenced by local
1151 meteorological dilution and removal processes, pointing to more complex source influences.

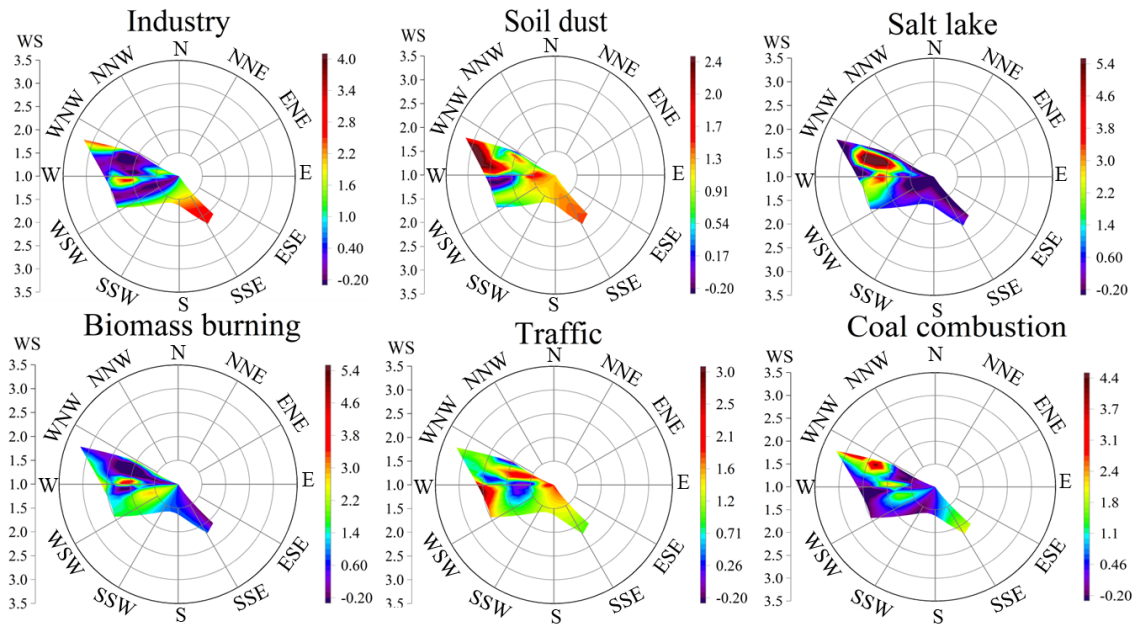
1152 In summary, seasonal variations in atmospheric dust deposition result from the combined
1153 effects of meteorological conditions and anthropogenic emissions. In urban areas, meteorological
1154 factors, especially wind speed and relative humidity, play a dominant role in the dispersion and

1155 removal of local anthropogenic pollutants. In rural areas, dust composition is more strongly
1156 influenced by large-scale wind-driven dust transport and regional combustion activities.

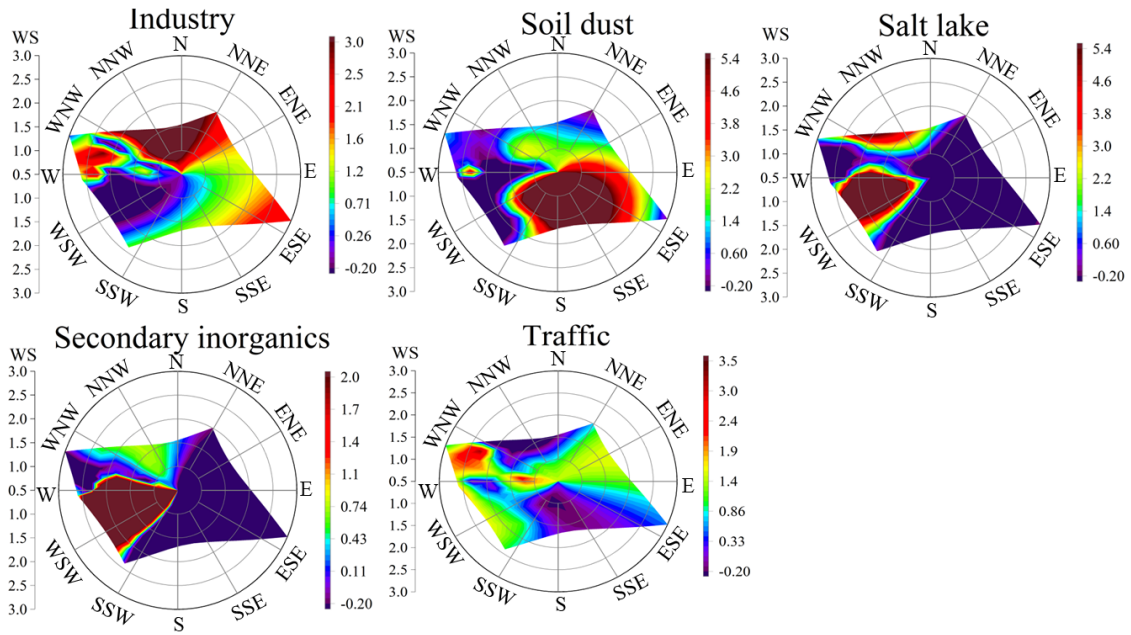


1157
1158 Figure 8 Relationship between wind speed, wind direction, and atmospheric dust deposition
1159 sources in rural of the Qaidam Basin during domestic heating (HP) and non-heating (NHP)
1160 periods.

Urban-HP



Urban-NHP



1162

1163 Figure 9 Relationship between wind speed, wind direction, and atmospheric dust deposition
 1164 sources in urban of the Qaidam Basin during domestic heating (HP) and non-heating (NHP)
 1165 periods.

1166

1167 Wind direction analysis provides a valuable supplement to the PMF model (Watson et al., 2008).

1168 Studies have shown that emissions from sources such as traffic, biomass burning, coal combustion,
1169 and salt lakes exhibit significant directional patterns, which can be effectively visualized using polar
1170 plots (Saraga et al., 2021). In this study, bivariate polar plots were generated for the concentrations
1171 of POC, SOC, char-EC, soot-EC, and selected ions/elements (Figure S21-S24), as well as for the
1172 source contributions resolved by the PMF model (Figure 8 and 9), to illustrate their directional
1173 provenance. Notably, the directional patterns of the various aerosol components exhibited distinct
1174 differences and did not fully align with the local prevailing wind directions.

1175 The polar plots of key tracer ions and elements (Figure S21-S24) showed patterns consistent
1176 with the corresponding PMF-resolved source factors (Figure 8 and 9), supporting the validity of the
1177 source apportionment. Specifically, the following pairs showed similar directional distributions:
1178 Total-ps and the salt-lake source; nps-K⁺, POC, and char-EC with biomass burning; nps-Ca²⁺ and
1179 Si with soil dust; nps-SO₄²⁻, nps-Cl⁻, and SOC with coal combustion; Fe and Cd with industry; Ni
1180 and Zn with vehicle combustion; Fe and Al with industry; and nps-SO₄²⁻ together with NO₃⁻ with
1181 secondary formation. These spatial consistencies reinforce that the selected chemical tracers are
1182 associated with their respective PMF-identified sources.

1183 Wind speeds in rural areas are generally higher than those in urban environments, with
1184 predominant wind directions between west (W) and north (N), indicating the potential long-distance
1185 transport of pollutants. Specifically, emissions from saline lakes primarily originate from the west-
1186 northwest (WNW) direction. Back trajectory modeling suggests that HP levels are mainly attributed
1187 to salt lake emissions from the northwestern QDB, while in NHP, sources include long-distance
1188 transport from salt lakes in the Tarim Basin (Figure S6, S7). For industrial emissions during the HP,
1189 sources primarily originate from medium- to short-distance transport in the W direction, with NHP
1190 periods showing contributions from both the west (W) and northwest-northwest (NNW) directions.
1191 In contrast, soil dust in HP is predominantly sourced from long-distance transport from the W
1192 direction, whereas in NHP, it is largely of local origin. Biomass burning during HP mainly arises
1193 from local sources, while its contribution during NHP is minimal and comes from both local and
1194 long-distance transport, consistent with PMF results.

1195 In urban areas, lower wind speeds and varying dominant wind directions between the HP and
1196 NHP lead to different sources of pollutants. During HP, emissions from saline lakes and coal
1197 combustion primarily originate from short-distance transport in the WNW direction, while biomass

1198 burning is sourced from the W. In contrast, industrial emissions, soil dust, and vehicle combustion
1199 are predominantly attributed to local sources. In NHP, pollutants demonstrate a dispersion trend
1200 from their sources to urban areas. Industrial emissions primarily come from the WNW to north-
1201 northeast (NNE) directions, soil dust from the southwest (SW), and vehicle emissions from the W
1202 direction. Notably, both salt lake and secondary formation sources exhibit similar directional
1203 patterns, indicating a common origin from the SW direction. The presence of processing enterprises
1204 near salt lakes suggests that secondary aerosols may form from emitted SO₂ and NO₂ (Hewitt, 2001).
1205 These findings align with previous analyses showing that urban industrial and traffic emissions
1206 mainly derive from local sources, while coal and biomass burning predominantly originate from
1207 surrounding rural areas, corroborating the role of nearby soil sources in salt lake and soil emissions.

1209 **3.67 Environmental implication**

1210 The source apportionment analysis using the PMF model indicates that in the QDB, rural dust-
1211 fall predominantly originates from the combustion of solid fuels, including firewood, yak dung, and
1212 coal, accounting for approximately ~~74.64~~72.05% of the total contribution. This proportion
1213 significantly exceeds contributions reported for rural areas in Beijing (41%) (Hua et al., 2018), Agra
1214 (54.3%) (Agarwal et al., 2020), and Beihai, Guangxi Province (66.7%) (Zhang et al., 2019).

1215 The higher contribution in this study likely reflects the local energy profile, as the sampling
1216 site in Haixi Mongol and Xizang Autonomous Prefecture, Qinghai Province, primarily relies on coal,
1217 yak dung, and firewood, constituting 58%, 23.5%, and 13% of rural energy consumption,
1218 respectively (Jiang et al., 2020; Shen et al., 2021). In contrast, solid biomass fuels, including wood
1219 and yak dung, account for over 70% of rural household energy consumption in Xizang, with yak
1220 dung alone representing 53% (Liu et al., 2008; Xiao et al., 2015). Similar patterns emerge in South
1221 and Central Asia, where biomass fuels dominate residential heating (firewood: 39%; dung: 29%)
1222 (Amacher et al., 1999; Heltberg et al., 2000; Hoeck et al., 2007; Foysal et al., 2012; Behera et al.,
1223 2015; Kerimray et al., 2018). In northern China, rural domestic heating primarily relies on coal
1224 (46%), firewood (23.8%), and electricity (15.1%) (Tao et al., 2018), further highlighting the unique
1225 energy composition of QDB.

1226 Recent studies have shown that South Asia, Central Asia, and Xizang contribute significantly

1227 to high concentrations of atmospheric PM, particularly BC, which accelerates glacier melting in the
1228 QXP (Ming et al., 2010; Xia et al., 2011; Chen et al., 2015). The QDB is recognized as a significant
1229 dust source affecting the glacier surfaces on the QXP, although it is often overlooked (Dong et al.,
1230 2014; Wei et al., 2017; Zheng et al., 2021). Compared to other dust sources, the QDB exhibits higher
1231 emissions from coal combustion, giving it a unique influence on the QXP. The organic matter and
1232 pollutants, such as ~~polycyclic aromatic hydrocarbons (PAHs)~~, released from household solid fuel
1233 combustion, particularly coal (98%) and dung (94%), are substantially higher than those from
1234 firewood (Leavey et al., 2017; Secrest et al., 2017; Ye et al., 2020). Consequently, the impact of PM
1235 from coal combustion in the QDB on the QXP is significant. Specifically, the presence of BC in PM
1236 increases glacier albedo, accelerating the melting of glaciers and snow in the region (Kang et al.,
1237 2020) and impacting global freshwater resources (Huss and Hock, 2018). Additionally, BC enhances
1238 cloud condensation nuclei ~~(CCN)~~, ice number concentration, and cloud cover (Zhou et al., 2025),
1239 thereby influencing global climate change. Furthermore, coal combustion releases harmful
1240 emissions, including CO₂, NO_x, CO, SO₂ and sulfur trioxide ~~(SO₂)~~ (Munawer, 2018), adversely
1241 affecting local human health and exacerbating climate warming on the QXP (Liu et al., 2006; Li et
1242 al., 2023), with broader implications for global climate. Therefore, the atmospheric pollutants
1243 emission of the QDB deserves considerable attention. However, this study focuses primarily on
1244 larger particles, indicating a need for further research on the environmental impacts of carbonaceous
1245 aerosols in atmospheric PM within the QDB.

1246 In addition to the distinctive energy consumption structure in the rural QDB, which leads to
1247 significant contributions from coal and biomass burning during HP, atmospheric dust deposition in
1248 the QDB during the NHP primarily originates from traffic and industrial emissions. The contribution
1249 from traffic emissions during the NHP was twice that during the HP. Considering the larger particle
1250 size of the dust samples collected in this study, the traffic-related dust is likely derived mainly from
1251 vehicle non-exhaust emissions, such as road dust (Gondwal and Mandal, 2021). This indicates that
1252 NHP atmospheric conditions are significantly influenced by resource development and tourism.
1253 Sampling sites, such as Qarhan Salt Lake, along with GEM and LTC stations within approximately
1254 100 km (Figure 1), suggest that salt lake resource extraction has a lower impact on regional aerosols
1255 than traffic emissions, despite salt lakes being the primary resource. This is likely because salt lake
1256 development mainly involves solar evaporation and chemical processes like extraction and

1257 adsorption, which emit fewer pollutants compared to other mining methods (Zhen, 2010).
1258 Consequently, salt lake resource exploitation exerts a relatively minor effect on local atmospheric
1259 carbonaceous aerosol.

1260 Similar salt lakes with comparable environments to QDB, such as Salar de Uyuni in Bolivia,
1261 the Atacama Salt Lake in Chile, and Ombre Muerto in Argentina, are rich in lithium resources (Li
1262 et al., 2014), making them focal points for resource development. Additionally, Salar de Uyuni, the
1263 Atacama Salt Lake, Junggar Basin, and the Great Salt Lake are renowned tourist destinations. This
1264 suggests that, in arid basin salt lakes with similar climates and intensive human activity, atmospheric
1265 carbonaceous aerosols are likely influenced by resource exploitation and tourism, especially tourism.
1266 The study's findings can inform policy decisions regarding unexploited salt lakes in South America,
1267 such as Ombre Muerto and Salar de Uyuni. However, while QDB also hosts mineral resources such
1268 as copper, iron, and tin, this research focused on larger particles ($>100\ \mu\text{m}$), which are more
1269 indicative of local sources. Given that sampling was conducted around the salt lakes, potential
1270 impacts from other mineral resource developments may have been underestimated. Further research
1271 is necessary to fully assess the environmental effects of carbonaceous aerosols in QDB atmospheric
1272 particles.

1273 In conclusion, the localized source profiles developed in this study, such as OC/EC ratios for
1274 heating-period emissions and key heavy-metal tracers, provide critical input parameters for regional
1275 climate and air quality models. This enables more accurate simulation of the emission, transport,
1276 and deposition of carbonaceous aerosols in the QDB and supports quantitative assessment of their
1277 contribution to glacier retreat on the QXP. Based on that rural areas in arid and semi-arid basins
1278 such as QDB rely heavily on solid fuels for heating, with associated environmental impacts, we
1279 recommend that local governments implement targeted clean-energy transition policies. These
1280 should prioritize promoting clean heating alternatives (e.g., solar and electric heating) in rural
1281 regions, supported by financial subsidies and technical assistance. Simultaneously, the adoption of
1282 clean stoves and upgraded biomass fuels should be encouraged to reduce emissions from traditional
1283 biomass and coal combustion (Dickinson et al., 2015; Li et al., 2011; Shen et al., 2017). Given the
1284 close climatic and environmental linkage between QDB and QXP, we further propose integrating
1285 air pollution control in QDB into the broader environmental protection framework of QXP.
1286 Establishing a joint regional air pollution prevention and control mechanism for the “QDB–QXP”

1287 system would help align emission reduction in the basin with glacier protection goals on the plateau.
1288 To strengthen the scientific foundation of such a mechanism, future studies should focus on
1289 clarifying the key transport pathways, transformation processes, and quantitative impacts of air
1290 pollutants from QDB to QXP glaciers.

1292 **4. Conclusion**

1293 This study analyzed the composition of dust deposition at six sampling sites in the southern
1294 Qaidam BasinQDB from January 2020 to March 2023 and examined DF, soluble ions, trace and
1295 carbonaceous element content in urban and rural samples during both domestic heating and non-
1296 domestic heating periods. Through integrated application of backward trajectory modeling, PMF,
1297 and carbon speciation indices, we identified dominant dust sources and evaluated domestic heating
1298 impacts on atmospheric processes in remote regions.

1299 The findings revealed that DF and carbon emissions were significantly higher in rural than in
1300 urban areas. Among carbon indicators, urban areas exhibited elevated EC levels (1.46 ± 1.60 mg/g),
1301 while OC levels were higher in rural ($2.253.73 \pm 1.922.61$ mg/g). Economic development increase
1302 OC/EC ratios, but they are driven by different intrinsic factors. Char-EC was the dominant
1303 contributor to EC (80.44%), with urban ~~Char~~char-EC levels (85.00%) showing a notable increase
1304 compared to rural levels (75.88%). ~~SO~~Secondary organic carbon was the principal contributor to
1305 OC (~~68.1772.61~~%), with rural SOC levels surpassing (~~6778.44~~%) those in urban areas (~~5767.78~~%).
1306 The OC/EC and char-EC/soot-EC ratios, along with PMF results, indicated that during HP, dust
1307 deposition in the QDB was primarily derived from coal combustion (~~28.4426.85~~%) and biomass
1308 burning (~~22.1424.04~~%), while traffic emissions accounted for ~~34.1934.64~~% of dust during NHP.
1309 Coal and biomass burning were the main contributors to rural dust, strongly influenced by domestic
1310 heating, whereas urban dust predominantly originated from traffic (~~45.1346.83~~%) and industrial
1311 emissions (~~16.4116.12~~%). Compared to other dust sources in the Qinghai-Xizang PlateauQXP, coal
1312 consumption in the QDB is higher during the domestic heating period. The resulting emissions of
1313 ~~black carbon~~BC and greenhouse gases may exacerbate glacier melting in the region, warranting
1314 increased attention. Given the distinctive carbonaceous aerosol signatures identified in the
1315 QDBQaidam Basin, we recommend prioritizing their radiative forcing effects in regional

1316 environmental policymaking and climate modeling frameworks. Furthermore, findings of this study
1317 offer a valuable scientific basis for understanding atmospheric carbonaceous aerosols in arid basins
1318 and salt lake regions with climates similar to QDB. They can particularly inform policy decisions
1319 regarding unexploited salt lakes in South America, such as Ombre Muerto and Salar de Uyuni.

1320 However, this study primarily focused on larger-scale PM and examined the effects of heating
1321 on carbonaceous aerosols in the QDB. It lacks an investigation of aerosols with smaller particle
1322 sizes (e.g., PM₁₀, PM_{2.5}, PM₁), which is essential for a comprehensive understanding of
1323 carbonaceous aerosol characteristics in this unique region. Furthermore, in addition to offline
1324 observations, future research should incorporate online observations with high spatiotemporal
1325 resolution and utilize numerical air quality models such as CMAQ, CAMx, WRF-CHEM, and
1326 NAQPMS to analyze the spatiotemporal distribution and future trends of carbon aerosols in the
1327 QDB.

1328

1329 **Author contribution**

1330 HZ: Conceptualization, data curation, formal analysis, funding acquisition, investigation,
1331 methodology, project administration, validation, writing – original draft.

1332 LZ: Data curation, formal analysis, methodology.

1333 SZ: funding acquisition, validation, writing – review & edited.

1334 XZ: Supervision, conceptualization, funding acquisition, writing – review & edited.

1335

1336 **Acknowledgements**

1337 This research was funded by [Major Science and Technology Project of Gansu Province](#)
1338 [\(24ZD13FA003\)](#) ~~Youth Joint Fund of Lanzhou Branch of Chinese Academy of Sciences (E4400304)~~,
1339 and by Qinghai Provincial Innovation Platform Construction Special Program (Project No. 2024-
1340 ZJ-J03), and supported by Qinghai Provincial Key Laboratory of Geology and Environment of Salt
1341 Lakes (No. The Science and Technology Plan Project of Qinghai Province Incentive Fund 2024).

1342

1343 **Declaration of competing interest**

1344 The authors declare that there is no conflict of interest.

1345

1346 **Data availability**

1347 Datasets for this research has been uploaded in Zenodo and is available at

1348 <https://doi.org/10.5281/zenodo.14382853> (Zhu, 2024).

1349 **Reference**

- 1350 Abdollahi, S., Karimi, A., Madadi, M., Eslamian, S., Ostad-Ali-Askari, K., and Singh, V. P.: Lead
1351 concentration in dust fall in Zahedan, Sistan and Baluchistan Province, Iran, *Journal of Geography
1352 and Cartography*, 4, 6, <https://doi.org/10.24294/jgc.v4i2.601>, 2021.
- 1353 Adeniran, J. A., Yusuf, R. O., and Olajire, A. A.: Exposure to coarse and fine particulate matter at and
1354 around major intra-urban traffic intersections of Ilorin metropolis, Nigeria, *Atmospheric
1355 Environment*, 166, 383-392, <https://doi.org/10.1016/j.atmosenv.2017.07.041>, 2017.
- 1356 Agarwal, A., Satsangi, A., Lakhani, A., and Kumari, K. M.: Seasonal and spatial variability of secondary
1357 inorganic aerosols in PM_{2.5} at Agra: Source apportionment through receptor models, *Chemosphere*,
1358 242, 125132, <https://doi.org/10.1016/j.chemosphere.2019.125132>, 2020.
- 1359 Aiken, A. C., DeCarlo, P. F., Kroll, J. H., Worsnop, D. R., Huffman, J. A., Docherty, K. S., Ulbrich, I. M.,
1360 Mohr, C., Kimmel, J. R., Sueper, D., Sun, Y., Zhang, Q., Trimborn, A., Northway, M., Ziemann, P.
1361 J., Canagaratna, M. R., Onasch, T. B., Alfarra, M. R., Prevot, A. S. H., Dommen, J., Duplissy, J.,
1362 Metzger, A., Baltensperger, U., and Jimenez, J. L.: O/C and OM/OC ratios of primary, secondary,
1363 and ambient organic aerosols with High-Resolution Time-of-Flight Aerosol Mass Spectrometry,
1364 *Environmental Science & Technology*, 42, 4478-4485, <https://doi.org/10.1021/es703009q>, 2008.
- 1365 Almeida, S. M., Lage, J., Fernández, B., Garcia, S., Reis, M. A., and Chaves, P. C.: Chemical
1366 characterization of atmospheric particles and source apportionment in the vicinity of a steelmaking
1367 industry, *Science of The Total Environment*, 521-522, 411-420,
1368 <https://doi.org/10.1016/j.scitotenv.2015.03.112>, 2015.
- 1369 Alzahrani, A. J., Alghamdi, A. G., and Ibrahim, H. M.: Assessment of soil loss due to wind erosion and
1370 dust deposition: Implications for sustainable management in arid regions, *Applied Sciences*, 14(23),
1371 10822, <https://doi.org/10.3390/app142310822>, 2024.
- 1372 Amacher, G. S., Hyde, W. F., and Kanel, K. R.: Nepali fuelwood production and consumption: Regional
1373 and household distinctions, substitution and successful intervention, *The Journal of Development
1374 Studies*, 35, 138-163, <https://doi.org/10.1080/00220389908422584>, 1999.
- 1375 Ambade, B., Sankar, T. K., Sahu, L. K., and Dumka, U. C.: Understanding sources and composition of
1376 black carbon and PM_{2.5} in urban environments in East India, *Urban Science*, 6(3), 60,
1377 <https://doi.org/10.3390/urbansci6030060>, 2022.
- 1378 Amato, F., Alastuey, A., de la Rosa, J., Gonzalez Castanedo, Y., Sánchez de la Campa, A. M., Pandolfi,

1379 M., Lozano, A., Contreras González, J., and Querol, X.: Trends of road dust emissions contributions
1380 on ambient air particulate levels at rural, urban and industrial sites in southern Spain, Atmospheric
1381 Chemistry and Physics, 14, 3533-3544, <https://doi.org/10.5194/acp-14-3533-2014>, 2014.

~~1382 Arimoto, R., Duce, R. A., Savoie, D. L., Prospero, J. M., Talbot, R., Cullen, J. D., Tomza, U., Lewis, N.~~
~~1383 F., and Ray, B. J.: Relationships among aerosol constituents from Asia and the North Pacific during~~
~~1384 PEM West A, Journal of Geophysical Research: Atmospheres, 101, 2011-2023,~~
~~1385 <https://doi.org/10.1029/95JD01071>, 1996.~~

1386 Arimoto, R., Duce, R. A., Savoie, D. L., Prospero, J. M., Talbot, R., Cullen, J. D., Tomza, U., Lewis, N.
1387 F., and Ray, B. J.: Relationships among aerosol constituents from Asia and the North Pacific during
1388 PEM-West A, Journal of Geophysical Research: Atmospheres, 101, 2011-2023,
1389 <https://doi.org/10.1029/95JD01071>, 1996.

1390 Ashrafi, K., Fallah, R., Hadei, M., Yarahmadi, M., and Shahsavani, A.: Source apportionment of Total
1391 Suspended Particles (TSP) by Positive Matrix Factorization (PMF) and Chemical Mass Balance
1392 (CMB) modeling in Ahvaz, Iran, Archives of Environmental Contamination and Toxicology, 75,
1393 278-294, <https://doi.org/10.1007/s00244-017-0500-z>, 2018.

1394 Bandowe, B. A. M., Nkansah, M. A., Leimer, S., Fischer, D., Lammel, G., and Han, Y.: Chemical (C, N,
1395 S, black carbon, soot and char) and stable carbon isotope composition of street dusts from a major
1396 West African metropolis: Implications for source apportionment and exposure, Science of The Total
1397 Environment, 655, 1468-1478, <https://doi.org/10.1016/j.scitotenv.2018.11.089>, 2019.

1398 Barjoe, S. S., Abadi, S. Z. M., Elmi, M. R., Varoon, V. T., and Nikbakht, M.: Evaluation of trace
1399 elements pollution in deposited dust on residential areas and agricultural lands around Pb/Zn
1400 mineral areas using modified pollution indices, Journal of Environmental Health Science and
1401 Engineering, 19, 753-769, <https://doi.org/10.1007/s40201-021-00643-8>, 2021.

1402 Behera, B., Rahut, D. B., Jeetendra, A., and Ali, A.: Household collection and use of biomass energy
1403 sources in South Asia, Energy, 85, 468-480, <https://doi.org/10.1016/j.energy.2015.03.059>, 2015.

1404 Belis, C. A., Pernigotti, D., Karagulian, F., Pirovano, G., Larsen, B. R., Gerboles, M., and Hopke, P. K.:
1405 A new methodology to assess the performance and uncertainty of source apportionment models in
1406 intercomparison exercises, Atmospheric Environment, 119, 35-44,
1407 <https://doi.org/10.1016/j.atmosenv.2015.08.002>, 2015.

1408 [Bibi, S., Alam, K., Chishtie, F., Bibi, H., and Rahman, S.: Temporal variation of Black Carbon](#)

1409 [concentration using Aethalometer observations and its relationships with meteorological variables](#)
1410 [in Karachi, Pakistan, Journal of Atmospheric and Solar-Terrestrial Physics, 157-158, 67-77,](#)
1411 <https://doi.org/10.1016/j.jastp.2017.03.017>, 2017.

1412 Bond, T. C. and Bergstrom, R. W.: Light absorption by carbonaceous particles: An investigative review,
1413 Aerosol Science and Technology, 40, 27-67, <https://doi.org/10.1080/02786820500421521>, 2006.

1414 Bond, T. C., Streets, D. G., Yarber, K. F., Nelson, S. M., Woo, J. -H., and Klimont, Z.: A technology-
1415 based global inventory of black and organic carbon emissions from combustion, Journal of
1416 Geophysical Research: Atmospheres, 109, <https://doi.org/10.1029/2003JD003697>, 2004.

1417 [Bond, T. C., Doherty, S. J., Fahey, D. W., Forster, P. M., Berntsen, T., DeAngelo, B. J., Flanner, M. G.,](#)
1418 [Ghan, S., Kärcher, B., Koch, D., Kinne, S., Kondo, Y., Quinn, P. K., Sarofim, M. C., Schultz, M. G.,](#)
1419 [Schulz, M., Venkataraman, C., Zhang, H., Zhang, S., Bellouin, N., Guttikunda, S. K., Hopke, P. K.,](#)
1420 [Jacobson, M. Z., Kaiser, J. W., Klimont, Z., Lohmann, U., Schwarz, J. P., Shindell, D., Storelvmo,](#)
1421 [T., Warren, S. G., and Zender, C. S.: Bounding the role of black carbon in the climate system: A](#)
1422 [scientific assessment, Journal of Geophysical Research: Atmospheres, 118, 5380-5552,](#)
1423 <https://doi.org/10.1002/jgrd.50171>, 2013.

1424 Boreddy, S. K. R., Kawamura, K., Okuzawa, K., Kanaya, Y., and Wang, Z.: Temporal and diurnal
1425 variations of carbonaceous aerosols and major ions in biomass burning influenced aerosols over Mt.
1426 Tai in the North China Plain during MTX2006, Atmospheric Environment, 154, 106-117,
1427 <https://doi.org/10.1016/j.atmosenv.2017.01.042>, 2017.

1428 Bowen, H. -J. -M.: Environmental chemistry of the elements. Academic Press,
1429 <https://doi.org/10.1002/9780470140451>, 1979.

1430 Brooks, J., Liu, D., Allan, J. D., Williams, P. I., Haywood, J., Highwood, E. J., Kompalli, S. K., Babu, S.
1431 S., Satheesh, S. K., Turner, A. G., and Coe, H.: Black carbon physical and optical properties across
1432 northern India during pre-monsoon and monsoon seasons, Atmospheric Chemistry and Physics, 19,
1433 13079-13096, <https://doi.org/10.5194/acp-19-13079-2019>, 2019.

1434 Butler, K. M. and Mulholland, G. W.: Generation and transport of smoke components, Fire Technology,
1435 40, 149-176, <https://doi.org/10.1023/B:FIRE.0000016841.07530.64>, 2004.

1436 Cachier, H. and Ducret, J.: Influence of biomass burning on equatorial African rains, Nature, 352, 228-
1437 230, <https://doi.org/10.1038/352228a0>, 1991.

1438 Cao, J. -J., Wang, Q. -Y., Chow, J. C., Watson, J. G., Tie, X. -X., Shen, Z. -X., Wang, P., and An, Z. -S.:

1439 Impacts of aerosol compositions on visibility impairment in Xi'an, China, Atmospheric
1440 Environment, 59, 559-566, <https://doi.org/10.1016/j.atmosenv.2012.05.036>, 2012a.

1441 [Cao, J. J., Zhu, C. S., Chow, J. C., Watson, J. G., Han, Y. M., Wang, G. H., Shen, Z. X., and An, Z. S.:](#)
1442 [Black carbon relationships with emissions and meteorology in Xi'an, China, Atmospheric Research,](#)
1443 [94, 194-202, <https://doi.org/10.1016/j.atmosres.2009.05.009>, 2009.](#)

1444 Cao, J.: Characteristics of carbonaceous aerosol in Pearl River Delta Region, China during 2001 winter
1445 period, Atmospheric Environment, 37, 1451-1460, [https://doi.org/10.1016/s1352-2310\(02\)01002-6](https://doi.org/10.1016/s1352-2310(02)01002-6),
1446 2003.

1447 Cao, J. J., Shen, Z. X., Chow, J. C., Watson, J. G., Lee, S. C., Tie, X. X., Ho, K. F., Wang, G. H., and
1448 Han, Y. M.: Winter and summer PM_{2.5} chemical compositions in fourteen Chinese cities, Journal of
1449 Air Waste Manage Association, 62, 1214-1226, <https://doi.org/10.1080/10962247.2012.701193>,
1450 2012b.

1451 Cao, J. J., Zhu, C. S., Tie, X. X., Geng, F. H., Xu, H. M., Ho, S. S. H., Wang, G. H., Han, Y. M., and Ho,
1452 K. F.: Characteristics and sources of carbonaceous aerosols from Shanghai, China, Atmospheric
1453 Chemistry and Physics, 13, 803-817, <https://doi.org/10.5194/acp-13-803-2013>, 2013.

1454 Casotti Rienda, I. and Alves, C. A.: Road dust resuspension: A review, Atmospheric Research, 261,
1455 105740, <https://doi.org/10.1016/j.atmosres.2021.105740>, 2021.

1456 Cesari, D., Amato, F., Pandolfi, M., Alastuey, A., Querol, X., and Contini, D.: An inter-comparison of
1457 PM₁₀ source apportionment using PCA and PMF receptor models in three European sites,
1458 Environmental Science and Pollution Research, 23, 15133-15148, [https://doi.org/10.1007/s11356-](https://doi.org/10.1007/s11356-016-6599-z)
1459 [016-6599-z](#), 2016.

1460 Chen, L., Zhang, X. Y., Tang, Q. L., Geng, Y., Wang, E. L., and Li, J. Y.: Heavy metal pollution and
1461 source analysis of surface soil in the Qaidam Basin (in Chinese), Environmental Science, 42, 4880–
1462 4888, <https://doi.org/10.13227/j.hjcx.202101052>, 2021.

1463 Chen, M., Li, M.-Y., Zhou, J.-Y., Fu, R.-B., Wang, X.-F., and Shen Z.: Characteristics and source
1464 analysis of heavy metal pollution in dust in a heavy industrial area of Northwest China (in Chinese),
1465 Environmental Science and Technology, 47(02), 155-164, [https://doi.org/10.19672/j.cnki.1003-](https://doi.org/10.19672/j.cnki.1003-6504.1004.23.338)
1466 [6504.1004.23.338](#), 2024.

1467 Chen, P., Kang, S., Bai, J., Sillanpää, M., and Li, C.: Yak dung combustion aerosols in the Tibetan Plateau:
1468 Chemical characteristics and influence on the local atmospheric environment, Atmospheric

1469 Research, 156, 58-66, <https://doi.org/10.1016/j.atmosres.2015.01.001>, 2015.

1470 Chen, W., Tong, D. Q., Dan, M., Zhang, S., Zhang, X., and Pan, Y.: Typical atmospheric haze during crop
1471 harvest season in northeastern China: A case in the Changchun region, *Journal of Environmental*
1472 *Sciences*, 54, 101-113, <https://doi.org/10.1016/j.jes.2016.03.031>, 2017.

1473 Cheng, X. and Lin, X.: Temporal and spatial distribution characteristics of dust in Shenyang and analysis
1474 of influencing factors (in Chinese). *Environmental Protection Science* 35(06), 1-3 + 58,
1475 <https://doi.org/10.16803/j.cnki.issn.1004-6216.2009.06.001>, 2009.

1476 Chow, J. C.: Measurement methods to determine compliance with ambient air quality standards for
1477 suspended particles, *Journal of the Air & Waste Management Association*, 45, 320-382,
1478 <https://doi.org/10.1080/10473289.1995.10467369>, 1995.

1479 Chow, J. C., Lowenthal, D. H., Chen, L. W. A., Wang, X., and Watson, J. G.: Mass reconstruction methods
1480 for PM_{2.5}: A review, *Air Quality, Atmosphere & Health*, 8, 243-263, <https://doi.org/10.1007/s11869-015-0338-3>, 2015.

1482 Chow, J. C., Watson, J. G., Kuhns, H., Etyemezian, V., Lowenthal, D. H., Crow, D., Kohl, S. D.,
1483 Engelbrecht, J. P., and Green, M. C.: Source profiles for industrial, mobile, and area sources in the
1484 Big Bend Regional Aerosol Visibility and Observational study, *Chemosphere*, 54, 185-208,
1485 <https://doi.org/10.1016/j.chemosphere.2003.07.004>, 2004.

1486 Christie, J. A., Elliott, H. E., O'Connell-Lopez, S. M. O., Perry, K., Pratt, K. A., Hallar, A. G., Hrdina,
1487 A., Murphy, J. G., Riedel, T. P., Long, R. W., Mitroo, D., Haskins, J. D., and Gaston, C. J.: Halogen
1488 production from playa dust emitted from the Great Salt Lake: Implications of the shrinking Great
1489 Salt Lake on regional air quality, *ACS Earth and Space Chemistry*, 9, 480-493,
1490 <https://doi.org/10.1021/acsearthspacechem.4c00258>, 2025.

1491 Chuang, M.-T., Lee, C.-T., Chou, C. C. K., Lin, N.-H., Sheu, G.-R., Wang, J.-L., Chang, S.-C., Wang,
1492 S.M.-H., Chi, K. H., Young, C.-Y., Huang, H., Chen, H.-W., Weng, G.-H., Lai, S.-Y., Hsu, S.-P.,
1493 Chang, Y.-J., Chang, J.-H., and Wu, X.-C.: Carbonaceous aerosols in the air masses transported
1494 from Indochina to Taiwan: Long-term observation at Mt. Lulin, *Atmospheric Environment*, 89, 507-
1495 516, <https://doi.org/10.1016/j.atmosenv.2013.11.066>, 2014.

1496 Cichowicz, R. and Bochenek, A. D.: Assessing the effects of urban heat islands and air pollution on
1497 human quality of life, *Anthropocene*, 46, 100433, <https://doi.org/10.1016/j.ancene.2024.100433>,
1498 2024.

1499 Cong, Z., Kang, S., Luo, C., Li, Q., Huang, J., Gao, S., and Li, X.: Trace elements and lead isotopic
1500 composition of PM₁₀ in Lhasa, Tibet, Atmospheric Environment, 45, 6210-6215,
1501 <https://doi.org/10.1016/j.atmosenv.2011.07.060>, 2011.

1502 Dang, X., Chang, L., and Lu, N.: The impact of climatic warm-wet situation of the Tibetan Plateau on
1503 the water resources and environment in Qaidam Basin, Geology of China, 46, 359-368, 2019.

1504 Demir, T., Karakaş, D., and Yeniso-y-Karakaş, S.: Source identification of exhaust and non-exhaust traffic
1505 emissions through the elemental carbon fractions and Positive Matrix Factorization method,
1506 Environmental Research, 204, 112399, <https://doi.org/10.1016/j.envres.2021.112399>, 2022.

1507 Deng Z.-W., Fang, F.-M., Jiang, P.-L., Zhang J.-Q. and Lin Y.-S.: Distribution characteristics of black
1508 carbon content in surface dust in Wuhu city (in Chinese), Journal of Anqing Normal University
1509 (Natural Science Edition), 37(01), 58-62, [https://doi.org/10.14182/j.cnki.1001-](https://doi.org/10.14182/j.cnki.1001-2443.2014.01.009)
1510 [2443.2014.01.009](https://doi.org/10.14182/j.cnki.1001-2443.2014.01.009), 2014.

1511 [Deshmukh, D. K., Deb, M. K., Tsai, Y. I., and Mkoma, S. L.: Water soluble ions in PM_{2.5} and PM₁
1512 aerosols in Durg City, Chhattisgarh, India, Aerosol and Air Quality Research, 11, 696-708,
1513 <https://doi.org/10.4209/aaqr.2011.03.0023>, 2011.](https://doi.org/10.4209/aaqr.2011.03.0023)

1514 [Dickinson, K. L., Kanyomse, E., Piedrahita, R., Coffey, E., Rivera, I. J., Adoctor, J., Alirigia, R.,
1515 Muvandimwe, D., Dove, M., Dukic, V., Hayden, M. H., Diaz-Sanchez, D., Abisiba, A. V., Anaseba,
1516 D., Hagar, Y., Masson, N., Monaghan, A., Titiati, A., Steinhoff, D. F., Hsu, Y. Y., Kaspar, R., Brooks,
1517 B. A., Hodgson, A., Hannigan, M., Oduro, A. R., and Wiedinmyer, C.: Research on emissions, air
1518 quality, climate, and cooking technologies in Northern Ghana \(Reaccting\): study rationale and
1519 protocol, BMC Public Health, 15, 126, <https://doi.org/10.1186/s12889-015-1414-1>, 2015.](https://doi.org/10.1186/s12889-015-1414-1)

1520 [Donahue, N. M.: Chapter 3.2 - Air pollution and air quality, in: Green chemistry, Elsevier, 151-176,
1521 <https://doi.org/10.1016/B978-0-12-809270-5.00007-8>, 2018.](https://doi.org/10.1016/B978-0-12-809270-5.00007-8)

1522 Dong, Z., Qin, D., Kang, S., Ren, J., Chen, J., Cui, X., Du, Z., and Qin, X.: Physicochemical
1523 characteristics and sources of atmospheric dust deposition in snow packs on the glaciers of western
1524 Qilian Mountains, China, Tellus B: Chemical and Physical Meteorology, 66, 20956,
1525 <https://doi.org/10.3402/tellusb.v66.20956>, 2014.

1526 Duan, J. and Tan, J.: Atmospheric heavy metals and Arsenic in China: Situation, sources and control
1527 policies, Atmospheric Environment, 74, 93-101, <https://doi.org/10.1016/j.atmosenv.2013.03.031>,
1528 2013.

1529 Eivazzadeh, M., Hassanvand, M. S., Faridi, S., and Gholampour, A.: Source apportionment and
1530 deposition of dustfall-bound trace elements around Tabriz, Iran, *Environmental Science and*
1531 *Pollution Research International*, 28, 59403-59415, <https://doi.org/10.1007/s11356-020-12173-1>,
1532 2021.

1533 Fan, Q., Cheng, Y., Chen, T., and Xu, N.: Influence of water replenishment of lakes in the Northern
1534 Qaidam Basin on salt lake resources and ecological environment, *Journal of Salt Lake Research*, 30,
1535 11-18, <https://doi.org/10.18307/2024.0344> 2022.

1536 Fang, B., Zeng, H., Zhang, L., Wang, H., Liu, J., Hao, K., Zheng, G., Wang, M., Wang, Q., and Yang, W.:
1537 Toxic metals in outdoor/indoor airborne PM_{2.5} in port city of Northern, China: Characteristics,
1538 sources, and personal exposure risk assessment, *Environmental Pollution*, 279, 116937,
1539 <https://doi.org/10.1016/j.envpol.2021.116937>, 2021.

1540 Fang, H., Lowther, S. D., Zhu, M., Pei, C., Li, S., Fang, Z., Yu, X., Yu, Q., Wang, Y., Zhang, Y., Jones,
1541 K. C., and Wang, X.: PM_{2.5}-bound unresolved complex mixtures (UCM) in the Pearl River Delta
1542 region: Abundance, atmospheric processes and sources, *Atmospheric Environment*, 226,
1543 <https://doi.org/10.1016/j.atmosenv.2020.117407>, 2020.

1544 Feng, W., Guo, Z., Xiao, X., Peng, C., Shi, L., Ran, H., and Xu, W.: Atmospheric deposition as a source
1545 of cadmium and lead to soil-rice system and associated risk assessment, *Ecotoxicology and*
1546 *Environmental Safety*, 180, 160-167, <https://doi.org/10.1016/j.ecoenv.2019.04.090>, 2019.

1547 Filonchik, M., Yan, H., Yang, S., and Lu, X.: Detection of aerosol pollution sources during sandstorms
1548 in Northwestern China using remote sensed and model simulated data, *Advances in Space Research*,
1549 61, 1035-1046, <https://doi.org/10.1016/j.asr.2017.11.037>, 2018.

1550 Foysal, M., Hossain, M., Rubaiyat, A., Sultana, S., Uddin, M. K., Sayem, M., and Akhter, J.: Household
1551 energy consumption pattern in rural areas of Bangladesh, *Indian Journal of Energy*, 1, 72-85, 2012.

1552 [Fu, B.: Socio-economic data set of Qinghai-Tibet Plateau \(1982-2018\). National Tibetan Plateau / Third](http://data.tpcd.ac.cn)
1553 [Pole Environment Data Center, http://data.tpcd.ac.cn, 2023.](http://data.tpcd.ac.cn)

1554 Gao, G.-S., Song, L.-M., and Ma, Z.-T.: Temporal and spatial distribution of dust-fall in Qinghai
1555 Province and analysis of its influencing factors (in Chinese), *Chinese Journal of Desert Research*,
1556 33(04), 1124-1130, <https://doi.org/10.7522/j.issn.1000-694X.2013.00153>, 2013.

1557 Gao, H. and Washington, R.: Arctic oscillation and the interannual variability of dust emissions from the
1558 Tarim Basin: a TOMS AI based study, *Climate Dynamics*, 35, 511-522,

1559 <https://doi.org/10.1007/s00382-009-0687-4>, 2010.

1560 Gao, Y., Wang, H., Yuan, L., Jing, S., Yuan, B., Shen, G., Zhu, L., Koss, A., Li, Y., Wang, Q., Huang, D.
1561 D., Zhu, S., Tao, S., Lou, S., and Huang, C.: Measurement report: Underestimated reactive organic
1562 gases from residential combustion – insights from a near-complete speciation, *Atmospheric
1563 Chemistry and Physics*, 23, 6633-6646, <https://doi.org/10.5194/acp-23-6633-2023>, 2023.

1564 Garaga, R., Gokhale, S., and Kota, S. H.: Source apportionment of size-segregated atmospheric particles
1565 and the influence of particles deposition in the human respiratory tract in rural and urban locations
1566 of north-east India, *Chemosphere*, 255, <https://doi.org/10.1016/j.chemosphere.2020.126980>, 2020.

1567 Gertler, A., Kuhns, H., Abu-Allaban, M., Damm, C., Gillies, J., Etyemezian, V., Clayton, R., and Proffitt,
1568 D.: A case study of the impact of Winter road sand/salt and street sweeping on road dust re-
1569 entrainment, *Atmospheric Environment*, 40, 5976-5985,
1570 <https://doi.org/10.1016/j.atmosenv.2005.12.047>, 2006.

1571 Gholampour, A., Nabizadeh, R., Hassanvand, M. S., Taghipour, H., Nazmara, S., and Mahvi, A. H.:
1572 Characterization of saline dust emission resulted from Urmia Lake drying, *Journal of Environmental
1573 Health Science & Engineering*, 13, 82, <https://doi.org/10.1186/s40201-015-0238-3>, 2015.

1574 Gonçalves, C., Alves, C., Evtugina, M., Mirante, F., Pio, C., Caseiro, A., Schmidl, C., Bauer, H., and
1575 Carvalho, F.: Characterisation of PM₁₀ emissions from woodstove combustion of common woods
1576 grown in Portugal, *Atmospheric Environment*, 44, 4474-4480, <https://doi.org/10.1016/j.atmosenv>,
1577 2010.

1578 Gondwal, T. K. and Mandal, P.: Review on classification, sources and management of road dust and
1579 determination of uncertainty associated with measurement of particle size of road dust, *Mapan*, 36,
1580 909-924, <https://doi.org/10.1007/s12647-021-00501-w>, 2021.

1581 Gong, M., Yin, S., Gu, X., Xu, Y., Jiang, N., and Zhang, R.: Refined 2013-based vehicle emission
1582 inventory and its spatial and temporal characteristics in Zhengzhou, China, *Science of The Total
1583 Environment*, 599-600, 1149-1159, <https://doi.org/10.1016/j.scitotenv.2017.03.299>, 2017.

1584 [Goossens, D. and Offer, Z. Y. J. Z. F. G.: Eolian deposition of dust over symmetrical hills: an evaluation
1585 of wind-tunnel data by means of terrain measurement, *Zeitschrift für Geomorphologie*, 37, 103-111,
1586 <https://doi.org/10.1127/zfg/37/1993/103>, 1993.](https://doi.org/10.1127/zfg/37/1993/103)

1587 Gray, H. A., Cass, G. R., Huntzicker, J. J., Heyerdahl, E. K., and Rau, J. A.: Characteristics of atmospheric
1588 organic and elemental carbon particle concentrations in Los Angeles, *Environmental Science &*

1589 Technology, 20, 580-589, <https://doi.org/10.1021/es00148a006>, 1986.

1590 Griffin, D. W., Kellogg, C. A., Garrison, V. H., and Shinn, E. A.: The global transport of dust: An
1591 Intercontinental river of dust, microorganisms and toxic chemicals flows through the Earth's
1592 atmosphere, American Scientist, 90, 228-235, <https://www.jstor.org/stable/27857658>, 2002.

1593 Guo, J., Miao, Y., Zhang, Y., Liu, H., Li, Z., Zhang, W., He, J., Lou, M., Yan, Y., Bian, L., and Zhai, P.:
1594 The climatology of planetary boundary layer height in China derived from radiosonde and
1595 reanalysis data, Atmospheric Chemistry and Physics, 16, 13309-13319, [https://doi.org/10.5194/acp-](https://doi.org/10.5194/acp-16-13309-2016)
1596 16-13309-2016, 2016.

1597 Guo, S., Wang, L., Zhou, P., Guo, S., Qin, W., An, S., Xiao, J.-Y., Liu, J., and Ji, Y.: Characteristics and
1598 sources of organic carbon and elemental carbon in summer road dust in Shijiazhuang (in Chinese),
1599 Environmental Engineering, 36(04), 122-126, <https://doi.org/10.13205/j.hjgc.201804025>, 2018.

1600 Guo, W.-T., Zhao, F.-Q., and Chang, H.-L.: Analysis of the trend of environmental air quality changes
1601 in the main urban area of Changzhi City (in Chinese), Proceedings of Shanghai, China 3, 2010.

1602 Gupta, A. and Dhir, A.: Assessment of air quality and chemical fingerprints for atmospheric fine aerosols
1603 in an Indian smart city, Environmental Pollutants and Bioavailability, 34, 21-33,
1604 <https://doi.org/10.1080/26395940.2021.2024091>, 2022.

1605 Hahnenberger, M. and Nicoll, K.: Meteorological characteristics of dust storm events in the eastern Great
1606 Basin of Utah, U.S.A, Atmospheric Environment, 60, 601-612, [https://doi.org/10.1016/j.atmosenv,](https://doi.org/10.1016/j.atmosenv.2012.02.012)
1607 2012.

1608 ~~Hakanson, L.: An ecological risk index for aquatic pollution control: a sedimentological approach, Water~~
1609 ~~Research, 14, 975-1001, [https://doi.org/10.1016/0043-1354\(80\)90143-8](https://doi.org/10.1016/0043-1354(80)90143-8), 1980.~~

1610 Hama, S., Ouchen, I., Wyche, K. P., Cordell, R. L., and Monks, P. S.: Carbonaceous aerosols in five
1611 European cities: Insights into primary emissions and secondary particle formation, Atmospheric
1612 Research, 274, [https://doi.org/10.1016/j.atmosres](https://doi.org/10.1016/j.atmosres.2022.101612), 2022.

1613 Han, Y., Cao, J., An, Z., Chow, J. C., Watson, J. G., Jin, Z., Fung, K., and Liu, S.: Evaluation of the
1614 thermal/optical reflectance method for quantification of elemental carbon in sediments,
1615 Chemosphere, 69, 526-533, [https://doi.org/10.1016/j.chemosphere](https://doi.org/10.1016/j.chemosphere.2007a), 2007a.

1616 Han, Y., Cao, J., Chow, J. C., Watson, J. G., An, Z., Jin, Z., Fung, K., and Liu, S.: Evaluation of the
1617 thermal/optical reflectance method for discrimination between char- and soot-EC, Chemosphere,
1618 69, 569-574, [https://doi.org/10.1016/j.chemosphere](https://doi.org/10.1016/j.chemosphere.2007b), 2007b.

- 1619 Han, Y. M., Lee, S. C., Cao, J. J., Ho, K. F., and An, Z. S.: Spatial distribution and seasonal variation of
1620 char-EC and soot-EC in the atmosphere over China, *Atmospheric Environment*, 43, 6066-6073,
1621 <https://doi.org/10.1016/j.atmosenv, 2009a>.
- 1622 Han, Y. M., Cao, J. J., Chow, J. C., Watson, J. G., An, Z. S., and Liu, S. X.: Elemental carbon in urban
1623 soils and road dusts in Xi'an, China and its implication for air pollution, *Atmospheric Environment*,
1624 43, 2464-2470, <https://doi.org/10.1016/j.atmosenv, 2009b>.
- 1625 Han, Y. M., Han, Z. W., Cao, J. J., Chow, J. C., Watson, J. G., An, Z. S., Liu, S. X., and Zhang, R. J.:
1626 Distribution and origin of carbonaceous aerosol over a rural high-mountain lake area, Northern
1627 China and its transport significance, *Atmospheric Environment*, 42, 2405-2414,
1628 <https://doi.org/10.1016/j.atmosenv, 2008>.
- 1629 Han, Y. M., Cao, J. J., Yan, B. Z., Kenna, T. C., Jin, Z. D., Cheng, Y., Chow, J. C., and An, Z. S.:
1630 Comparison of elemental carbon in lake sediments measured by three different methods and 150-
1631 year pollution history in Eastern China, *Environmental Science & Technology*, 45, 5287-5293,
1632 <https://doi.org/10.1021/es103518c, 2011>.
- 1633 Han, Y. M., Chen, L. W. A., Huang, R. J., Chow, J. C., Watson, J. G., Ni, H. Y., Liu, S. X., Fung, K. K.,
1634 Shen, Z. X., Wei, C., Wang, Q. Y., Tian, J., Zhao, Z. Z., Prévôt, A. S. H., and Cao, J. J.: Carbonaceous
1635 aerosols in megacity Xi'an, China: Implications of thermal/optical protocols comparison,
1636 *Atmospheric Environment*, 132, 58-68, <https://doi.org/10.1016/j.atmosenv, 2016>.
- 1637 Hand, V. L., Capes, G., Vaughan, D. J., Formenti, P., Haywood, J. M., and Coe, H.: Evidence of internal
1638 mixing of African dust and biomass burning particles by individual particle analysis using electron
1639 beam techniques, *Journal of Geophysical Research: Atmospheres*, 115,
1640 <https://doi.org/10.1029/2009JD012938, 2010>.
- 1641 ~~He, B., Wang, J., Kong, F., Yu, D., Chen, L., Ling, Z., and Hu, J.: Analysis of environmental pollution~~
1642 ~~dissipation capacity of salt lake area in the Qaidam Basin, *Journal of Salt Lake Research*, 30, 52-60,~~
1643 ~~2022.~~
- 1644 He, L.-Y., Hu, M., Huang, X.-F., Yu, B.-D., Zhang, Y.-H., and Liu, D.-Q.: Measurement of emissions
1645 of fine particulate organic matter from Chinese cooking, *Atmospheric Environment*, 38, 6557-6564,
1646 <https://doi.org/10.1016/j.atmosenv, 2004>.
- 1647 Heltberg, R., Arndt, T. C., and Sekhar, N. U.: Fuelwood consumption and forest degradation: A household
1648 model for domestic energy substitution in rural India, *Land Economics*, 76, 213-232,

1649 <https://doi.org/10.2307/3147225>, 2000.

1650 [Heo, J. B., Hopke, P., Yi, S. M. J. A. C., Source apportionment of PM_{2.5} in Seoul, Korea, Atmospheric](#)

1651 [Chemistry and Physics: 9, 4957-4971, https://doi.org/10.5194/acp-9-4957-2009, 2009.](#)

1652 [Hewitt, C. N.: The atmospheric chemistry of sulphur and nitrogen in power station plumes, Atmospheric](#)

1653 [Environment, 35, 1155-1170, https://doi.org/10.1016/S1352-2310\(00\)00463-5, 2001.](#)

1654 Hilary, U., Efeoghene, E. A., Issac, A. O., Sami, R., Baakdah, F., and Pareek, S.: Exposure to airborne

1655 pollutants in urban and rural areas: levels of metals and microorganisms in PM₁₀ and gaseous

1656 pollutants in ambient air, Air Quality, Atmosphere & Health, 18, 317-332,

1657 <https://doi.org/10.1007/s11869-024-01644-w>, 2025.

1658 [Hoang, H. G., Chiang, C. F., Lin, C., Wu, C. Y., Lee, C. W., Cheruiyot, N. K., Tran, H. T., and Bui, X. T.:](#)

1659 [Human health risk simulation and assessment of heavy metal contamination in a river affected by](#)

1660 [industrial activities, Environment Pollution, 285, 117414, 10.1016/j.envpol.2021.117414, 2021.](#)

1661 Hoeck, T., Droux, R., Breu, T., Hurni, H., and Maselli, D.: Rural energy consumption and land

1662 degradation in a post-Soviet setting – an example from the west Pamir mountains in Tajikistan,

1663 Energy for Sustainable Development, 11, 48-57, [https://doi.org/10.1016/S0973-0826\(08\)60563-3](https://doi.org/10.1016/S0973-0826(08)60563-3),

1664 2007.

1665 Hu, Y.-N. and Liu, Y.-L.: Characteristics and source analysis of heavy metal pollution in indoor dust in

1666 Jinan (in Chinese). Environmental Science and Technology 45(06), 179-184,

1667 <https://doi.org/10.19672/j.cnki.1003-6504.0043.22.338>, 2022.

1668 Hua, Y., Wang, S., Jiang, J., Zhou, W., Xu, Q., Li, X., Liu, B., Zhang, D., and Zheng, M.: Characteristics

1669 and sources of aerosol pollution at a polluted rural site southwest in Beijing, China, Science of The

1670 Total Environment, 626, 519-527, <https://doi.org/10.1016/j.scitotenv>, 2018.

1671 Huang, H., Xu, Z.-Q., Yan, J.-X., Zhao, X.-G., and Wang, D.-L.: Characteristics of heavy metal

1672 pollution and ecological risk evaluation of indoor dust from urban and rural areas in Taiyuan City

1673 during the heating season (in Chinese), Journal of Environmental Science, 42, 2143-2152,

1674 <https://doi.org/10.13227/j.hjhx.202008045>, 2021a.

1675 [Huang, X. and Gao, J.: A review of near-limit opposed fire spread, Fire Safety Journal, 120, 103141,](#)

1676 <https://doi.org/10.1016/j.firesaf.2020.103141>, 2021a.

1677 Huang, X., Tang, G., Zhang, J., Liu, B., Liu, C., Zhang, J., Cong, L., Cheng, M., Yan, G., Gao, W., Wang,

1678 Y., and Wang, Y.: Characteristics of PM_{2.5} pollution in Beijing after the improvement of air quality,

1679 Journal of Environmental Sciences, 100, 1-10, <https://doi.org/10.1016/j.jes.2020.06.004>, 2021b.

1680 ~~Huo, J., Ren, L., Pan, Y., Zhao, J., Xiang, X., Yu, C., Meng, D., Wang, Y., Lu, R., and Huang, Y.:~~
1681 ~~Functional traits of desert plants and their responses to environmental factors in Qaidam Basin,~~
1682 ~~China, *Acta Ecologica Sinica*, 42, 4494-4503, 2022.~~

1683 Ji, X., Xu, K., Liao, D., Chen, G., Liu, T., Hong, Y., Dong, S., Choi, S.-D., and Chen, J.: Spatial-temporal
1684 characteristics and source apportionment of ambient VOCs in Southeast Mountain Area of China,
1685 *Aerosol And Air Quality Research*, 22, 220016, <https://doi.org/10.4209/aaqr.220016>, 2022.

1686 Jia, H., Yan, C., and Xing, X.: Evaluation of eco-environmental quality in Qaidam Basin based on the
1687 Ecological Index (MRSEI) and GEE, *Remote Sensing*, 13, <https://doi.org/10.3390/rs13224543>,
1688 2021.

1689 Jia, S.-M., Chen, M.-H., Yang, P.-F., Wang, L., Wang, G.-Y., Liu, L.-Y., and Ma, W.-L.: Seasonal
1690 variations and sources of atmospheric EPFRs in a megacity in severe cold region: Implications for
1691 the influence of strong coal and biomass combustion, *Environmental Research*, 252,
1692 <https://doi.org/10.1016/j.envres.2024.119067>, 2024.

1693 Jian, X., Guan, P., Fu, S.-T., Zhang, D.-W., Zhang, W., and Zhang, Y.-S.: Miocene sedimentary
1694 environment and climate change in the northwestern Qaidam basin, northeastern Tibetan Plateau:
1695 Facies, biomarker and stable isotopic evidences, *Palaeogeography Palaeoclimatology*
1696 *Palaeoecology*, 414, 320-331, <https://doi.org/10.1016/j.palaeo.2014.09.011>, 2014.

1697 Jiang, L., Xue, B., Xing, R., Chen, X., Song, L., Wang, Y., Coffman, D. M., and Mi, Z.: Rural household
1698 energy consumption of farmers and herders in the Qinghai-Tibet Plateau, *Energy*, 192,
1699 <https://doi.org/10.1016/j.energy.2019.116649>, 2020.

1700 Jiang, Y., Shi, L., Guang, A. L., Mu, Z., Zhan, H., and Wu, Y.: Contamination levels and human health
1701 risk assessment of toxic heavy metals in street dust in an industrial city in Northwest China,
1702 *Environmental Geochemistry and Health*, 40, 2007-2020, [https://doi.org/10.1007/s10653-017-](https://doi.org/10.1007/s10653-017-0028-1)
1703 [0028-1](https://doi.org/10.1007/s10653-017-0028-1), 2018.

1704 ~~Jiménez, L., Rühland, K. M., Jeziorski, A., Smol, J. P., and Pérez-Martínez, C.: Climate change and~~
1705 ~~Saharan dust drive recent cladoceran and primary production changes in remote alpine lakes of~~
1706 ~~Sierra Nevada, Spain, *Global Change Biology*, 24, e139-e158, <https://doi.org/10.1111/gcb.13878>,~~
1707 ~~2018.~~

1708 Joshi, U. M., Vijayaraghavan, K., and Balasubramanian, R.: Elemental composition of urban street dusts

1709 and their dissolution characteristics in various aqueous media, *Chemosphere*, 77, 526-533,
1710 <https://doi.org/10.1016/j.chemosphere>, 2009.

1711 Kang, S., Zhang, Y., Qian, Y., and Wang, H.: A review of black carbon in snow and ice and its impact on
1712 the cryosphere, *Earth-Science Reviews*, 210, <https://doi.org/10.1016/j.earscirev.2020.103346>, 2020.

1713 ~~Karimian Torghabeh, A., Jahandari, A., and Jamasb, R.: Concentration, contamination level, source~~
1714 ~~identification of selective trace elements in Shiraz atmospheric dust sediments (Fars Province, SW~~
1715 ~~Iran), *Environmental Science and Pollution Research (International)*, 26, 6424-6435,~~
1716 ~~[10.1007/s11356-018-04100-2](https://doi.org/10.1007/s11356-018-04100-2), 2019.~~

1717 Kataki, R., Goswami, K., Bordoloi, N. J., Narzari, R., Saikia, R., Sut, D., and Gogoi, L.: Biomass
1718 resources for biofuel production in Northeast India, in: *Bioprospecting of indigenous bioresources*
1719 *of North-East India*, edited by: ~~Purkayastha, J.~~, Springer Singapore, Singapore, 127-151,
1720 https://doi.org/10.1007/978-981-10-0620-3_8, 2016.

1721 Kerimray, A., Suleimenov, B., De Miglio, R., Rojas-Solórzano, L., Amouei Torkmahalleh, M., and Ó
1722 Gallachóir, B. P.: Investigating the energy transition to a coal free residential sector in Kazakhstan
1723 using a regionally disaggregated energy systems model, *Journal of Cleaner Production*, 196, 1532-
1724 1548, <https://doi.org/10.1016/j.jclepro>, 2018.

1725 Khan, A. J., Swami, K., Ahmed, T., Bari, A., Shareef, A., and Husain, L.: Determination of elemental
1726 carbon in lake sediments using a thermal-optical transmittance (TOT) method, *Atmospheric*
1727 *Environment*, 43, 5989-5995, <https://doi.org/10.1016/j.atmosenv.2009.08.030>, 2009.

1728 Kim, K. H., Sekiguchi, K., Kudo, S., and Sakamoto, K.: Characteristics of atmospheric elemental carbon
1729 (Char and Soot) in ultrafine and fine particles in a roadside environment, Japan, *Aerosol and Air*
1730 *Quality Research*, 11, 1-12, <https://doi.org/10.4209/aaqr.2010.07.0061>, 2011.

1731 ~~Kong, L., Xin, J., Gao, W., Tang, G., Wang, X., Wang, Y., Zhang, W., Chen, W., and Jia, S.: A~~
1732 ~~comprehensive evaluation of aerosol extinction apportionment in Beijing using a high-resolution~~
1733 ~~time-of-flight aerosol mass spectrometer, *Science of The Total Environment*, 783, 146976,~~
1734 ~~<https://doi.org/10.1016/j.scitotenv.2021.146976>, 2021.~~

1735 ~~Kuang, Y., He, Y., Xu, W., Yuan, B., Zhang, G., Ma, Z., Wu, C., Wang, C., Wang, S., Zhang, S., Tao, J.,~~
1736 ~~Ma, N., Su, H., Cheng, Y., Shao, M., and Sun, Y.: Photochemical aqueous-phase reactions induce~~
1737 ~~rapid daytime formation of oxygenated organic aerosol on the North China Plain, *Environmental*~~
1738 ~~*Science & Technology*, 54, 3849-3860, <https://doi.org/10.1021/acs.est.9b06836>, 2020.~~

1739 Kulmala, M., Vehkamäki, H., Petäjä, T., Dal Maso, M., Lauri, A., Kerminen, V. M., Birmili, W., and
1740 McMurry, P. H.: Formation and growth rates of ultrafine atmospheric particles: a review of
1741 observations, *Journal of Aerosol Science*, 35, 143-176,
1742 <https://doi.org/10.1016/j.jaerosci.2003.10.003>, 2004.

1743 Kumar, A.: Chemical characterization of mineral aerosols: Sources, transport and atmospheric
1744 transformations, Mohanlal Sukhadia University Udaipur, 2010.

1745 Kumar, N., Johnson, J., Yarwood, G., Woo, J.-H., Kim, Y., Park, R. J., Jeong, J. I., Kang, S., Chun, S.,
1746 and Knipping, E.: Contributions of domestic sources to PM_{2.5} in South Korea, *Atmospheric
1747 Environment*, 287, 119273, <https://doi.org/10.1016/j.atmosenv.2022.119273>, 2022.

1748 Lai, S., Zhao, Y., Ding, A., Zhang, Y., Song, T., Zheng, J., Ho, K. F., Lee, S.-e C., and Zhong, L.:
1749 Characterization of PM_{2.5} and the major chemical components during a 1-year campaign in rural
1750 Guangzhou, Southern China, *Atmospheric Research*, 167, 208-215,
1751 <https://doi.org/10.1016/j.atmosres>, 2016.

1752 Leavey, A., Patel, S., Martinez, R., Mitroo, D., Fortenberry, C., Walker, M., Williams, B., and Biswas, P.:
1753 Organic and inorganic speciation of particulate matter formed during different combustion phases
1754 in an improved cookstove, *Environmental Research*, 158, 33-42, <https://doi.org/10.1016/j.envres>,
1755 2017.

1756 Lee, K. Y., Batmunkh, T., Joo, H. S., and Park, K.: Comparison of the physical and chemical
1757 characteristics of fine road dust at different urban sites, *Journal of the Air & Waste Management
1758 Association*, 68, 812-823, <https://doi.org/10.1080/10962247.2018.1443855>, 2018.

1759 Li, J.-K., Liu, X.-F. and Wang, D.-H.: Overview of mineralization laws of lithium deposits in China (in
1760 Chinese). *Acta Geologica Sinica*, 88: 2269-2283. <https://doi.org/DOI:10.19762/j.cnki.dizhixuebao>,
1761 2014.

1762 Li, L., Ni, W., Cheng, Y., Wang, H., Yuan, K., and Zhou, B.: Evaluation of the eco-geo-environment in
1763 the Qaidam Basin, China, *Environmental Earth Sciences*, 80, <https://doi.org/10.1007/s12665-020-09312-9>, 2021a.

1764
1765 Li, M., Liu, Z., Chen, J., Huang, X., Liu, J., Xie, Y., Hu, B., Xu, Z., Zhang, Y., and Wang, Y.:
1766 Characteristics and source apportionment of metallic elements in PM_{2.5} at urban and suburban sites
1767 in Beijing: Implication of emission reduction, *Atmosphere*, 10,
1768 <https://doi.org/10.3390/atmos10030105>, 2019a.

- 1769 Li, P.-~~H~~H., Wang, Y., Li, T., Sun, L., Yi, X., Guo, L.-~~Q~~Q., and Su, R.-~~H~~H.: Characterization of
1770 carbonaceous aerosols at Mount Lu in South China: implication for secondary organic carbon
1771 formation and long-range transport, *Environmental Science and Pollution Research*, 22, 14189-
1772 14199, <https://doi.org/10.1007/s11356-015-4654-9>, 2015b.
- 1773 Li, Q.-L and Sha, Z.-J.: Remote sensing monitoring of ecological environment quality in the Qaidam
1774 Basin under climate warming (in Chinese), *Ecological Science*, 41(06), 92-99,
1775 <https://doi.org/10.14108/j.cnki.1008-8873>, 2022.
- 1776 Li, R., Li, C., Zhuang, J., Zhu, H., Fang, L., and Sun, D.: Mechanistic influence of chemical
1777 agglomeration agents on removal of inhalable particles from coal combustion, *ACS Omega*, 5,
1778 25906-25912, <https://doi.org/10.1021/acsomega.0c03263>, 2020.
- 1779 Li, Y., Ma, L., Ge, Y., and Abuduwaili, J.: Health risk of heavy metal exposure from dustfall and source
1780 apportionment with the PCA-MLR model: A case study in the Ebinur Lake Basin, China,
1781 *Atmospheric Environment*, 272, 118950, <https://doi.org/10.1016/j.atmosenv>, 2022.
- 1782 [Li, Y., Song, Y., Kaskaoutis, D. G., Chen, X., Mamadjanov, Y., and Tan, L.: Atmospheric dust dynamics](#)
1783 [in southern Central Asia: Implications for buildup of Tajikistan loess sediments, *Atmospheric*](#)
1784 [*Research*, 229, 74-85, <https://doi.org/10.1016/j.atmosres.2019.06.013>, 2019b.](#)
- 1785 [Li, Z., Sjödin, A., Romanoff, L. C., Horton, K., Fitzgerald, C. L., Eppler, A., Aguilar-Villalobos, M., and](#)
1786 [Naecher, L. P.: Evaluation of exposure reduction to indoor air pollution in stove intervention projects](#)
1787 [in Peru by urinary biomonitoring of polycyclic aromatic hydrocarbon metabolites, *Environment*](#)
1788 [*International*, 37, 1157-1163, <https://doi.org/10.1016/j.envint.2011.03.024>, 2011.](#)
- 1789 Li, Z., Liu, J., Zhai, Z., Liu, C., Ren, Z., Yue, Z., Yang, D., Hu, Y., Zheng, H., and Kong, S.:
1790 Heterogeneous changes of chemical compositions, sources and health risks of PM_{2.5} with the "Clean
1791 Heating" policy at urban/suburban/industrial sites, *Science of The Total Environment*, 854, 158871,
1792 <https://doi.org/10.1016/j.scitotenv.2022.158871>, 2023.
- 1793 Li, Z., Yue, Z., Yang, D., Wang, L., Wang, X., Li, Z., Wang, Y., Chen, L., Guo, S., Yao, J., Lou, X., Xu,
1794 X., and Wei, J.: Levels, chemical compositions, and sources of PM_{2.5} of rural and urban area under
1795 the impact of wheat harvest, *Aerosol and Air Quality Research*, 21,
1796 <https://doi.org/10.4209/aaqr.210026>, 2021.
- 1797 [Lin, Y., Mu, G., Chen, L., Wu, C., and Xu, L.: Sorting characteristics and implications indicated by the](#)
1798 [grain size of near-surface atmospheric dust fall in the Qira Oasis \(in Chinese\), *Journal of Desert*](#)

1799 [Research, 42, 139-146, https://doi.org/10.7522/j.issn.1000-694X, 2022a.](https://doi.org/10.7522/j.issn.1000-694X, 2022a)

1800 [Lin, Y., Mu, G., and Xu, L.: Grain size and sedimentary sorting characteristics of atmospheric dust in the](https://doi.org/10.3390/su14138093, 2022b)

1801 [Cele Oasis, Southern Margin of Taklimakan Desert, 14\(13\), 8093,](https://doi.org/10.3390/su14138093, 2022b)

1802 [https://doi.org/10.3390/su14138093, 2022b.](https://doi.org/10.3390/su14138093, 2022b)

1803 Lin, Y. C., Tsai, C. J., Wu, Y. C., Zhang, R., Chi, K. H., Huang, Y. T., Lin, S. H., and Hsu, S. C.:

1804 Characteristics of trace metals in traffic-derived particles in Hsuehshan Tunnel, Taiwan: size

1805 distribution, potential source, and fingerprinting metal ratio, Atmospheric Chemistry and Physics,

1806 15, 4117-4130, [https://doi.org/10.5194/acp-15-4117-2015, 2015.](https://doi.org/10.5194/acp-15-4117-2015, 2015)

1807 Liu, B., Song, N., Dai, Q., Mei, R., Sui, B., Bi, X., and Feng, Y.: Chemical composition and source

1808 apportionment of ambient PM_{2.5} during the non-heating period in Taian, China, Atmospheric

1809 Research, 170, 23-33, [https://doi.org/10.1016/j.atmosres, 2016a.](https://doi.org/10.1016/j.atmosres, 2016a)

1810 Liu, G., Lucas, M., and Shen, L.: Rural household energy consumption and its impacts on eco-

1811 environment in Tibet: Taking Taktse county as an example, Renewable and Sustainable Energy

1812 Reviews, 12, 1890-1908, [https://doi.org/10.1016/j.rser, 2008.](https://doi.org/10.1016/j.rser, 2008)

1813 Liu, G., Li, J., Wu, D., and Xu, H.: Chemical composition and source apportionment of the ambient PM_{2.5}

1814 in Hangzhou, China, Particuology, 18, 135-143, [https://doi.org/10.1016/j.partic, 2015.](https://doi.org/10.1016/j.partic, 2015)

1815 Liu, G., Yin, G., Kurban, A., Aishan, T., and You, H.: Spatiotemporal dynamics of land cover and their

1816 impacts on potential dust source regions in the Tarim Basin, NW China, Environmental Earth

1817 Sciences, 75, 1477, [https://doi.org/10.1007/s12665-016-6269-y, 2016b.](https://doi.org/10.1007/s12665-016-6269-y, 2016b)

1818 Liu, H., Hu, B., Zhang, L., Zhao, X. J., Shang, K. Z., Wang, Y. S., and Wang, J.: Ultraviolet radiation

1819 over China: Spatial distribution and trends, Renewable and Sustainable Energy Reviews, 76, 1371-

1820 1383, [https://doi.org/10.1016/j.rser, 2017.](https://doi.org/10.1016/j.rser, 2017)

1821 [Liu, H., Jia, M., Tao, J., Yao, D., Li, J., Zhang, R., Li, L., Xu, M., Fan, Y., Liu, Y., and Cheng, K.:](https://doi.org/10.1016/j.atmosenv.2023.119626, 2023a)

1822 [Elucidating pollution characteristics, temporal variation and source origins of carbonaceous species](https://doi.org/10.1016/j.atmosenv.2023.119626, 2023a)

1823 [in Xinxiang, a heavily polluted city in North China, Atmospheric Environment, 298, 119626,](https://doi.org/10.1016/j.atmosenv.2023.119626, 2023a)

1824 [https://doi.org/10.1016/j.atmosenv.2023.119626, 2023a.](https://doi.org/10.1016/j.atmosenv.2023.119626, 2023a)

1825 Liu, P., Zhou, H., Chun, X., Wan, Z., Liu, T., Sun, B., Wang, J., and Zhang, W.: Characteristics of fine

1826 carbonaceous aerosols in Wuhai, a resource-based city in Northern China: Insights from energy

1827 efficiency and population density, Environmental Pollution, 292, 118368,

1828 [https://doi.org/10.1016/j.envpol, 2022.](https://doi.org/10.1016/j.envpol, 2022)

1829 Liu, T., Zhao, C., Chen, Q., Li, L., Si, G., Li, L., and Guo, B.: Characteristics and health risk assessment
1830 of heavy metal pollution in atmospheric particulate matter in different regions of the Yellow River
1831 Delta in China, *Environmental Geochemistry and Health*, 45, 2013-2030,
1832 <https://doi.org/10.1007/s10653-022-01318-5>, 2023b.

1833 Liu, W., Hopke, P. K., Han, Y.-J., Yi, S.-M., Holsen, T. M., Cybart, S., Kozlowski, K., and Milligan,
1834 M.: Application of receptor modeling to atmospheric constituents at Potsdam and Stockton, NY,
1835 *Atmospheric Environment*, 37, 4997-5007, <https://doi.org/10.1016/j.atmosenv.2003.08.036>, 2003.

1836 Liu, X., Wang, Y., Liu, R., Zhang, Y., Shao, L., Han, K., and Zhang, Y.: Pollution characteristics, source
1837 identification and potential ecological risk of 50 elements in atmospheric particulate matter during
1838 winter in Qingdao, *Arabian Journal of Geosciences*, 15, [https://doi.org/10.1007/s12517-022-09521-](https://doi.org/10.1007/s12517-022-09521-5)
1839 5, 2022b.

1840 Liu, Y., Liu, G., Yousaf, B., Zhang, J., and Zhou, L.: Carbon fractionation and stable carbon isotopic
1841 fingerprint of road dusts near coal power plant with emphases on coal-related source apportionment,
1842 *Ecotoxicology and Environmental Safety*, 202, 110888, <https://doi.org/10.1016/j.ecoenv.2020a>.

1843 Liu, Y., Wu, G., Duan, A. and Zhang, Q.: New evidence that climate warming in the Tibetan Plateau is a
1844 result of intensified greenhouse gas emissions (in Chinese), *Chinese Science Bulletin*, 51(8), 989-
1845 992, <https://doi.org/10.1360/csb2006-51-8-989>, 2006.

1846 Liu, Y., Zhu, Q., Huang, J., Hua, S., and Jia, R.: Impact of dust-polluted convective clouds over the
1847 Tibetan Plateau on downstream precipitation, *Atmospheric Environment*, 209, 67-77,
1848 <https://doi.org/10.1016/j.atmosenv.2019>.

1849 Liu, Y., Zhu, Q., Hua, S., Alam, K., Dai, T., and Cheng, Y.: Tibetan Plateau driven impact of Taklimakan
1850 dust on northern rainfall, *Atmospheric Environment*, 234, 117583,
1851 <https://doi.org/10.1016/j.atmosenv.2020b>.

1852 Liu, Z. Y., Cheng, J. L., Li, C. Y., Gao, Y., Zhan, C. L., Liu, S., Zhang, J. Q., and Liu, H. X.: Pollution
1853 characteristics and source analysis of carbon components in road dust from Qingshan District,
1854 Wuhan (in Chinese), *Environmental Chemistry*, 40, 772–778, [https://doi.org/10.7524/j.issn.0254-](https://doi.org/10.7524/j.issn.0254-6108.2020061305)
1855 [6108.2020061305](https://doi.org/10.7524/j.issn.0254-6108.2020061305), 2021.

1856 Lonati, G., Ozgen, S., and Giugliano, M.: Primary and secondary carbonaceous species in PM_{2.5} samples
1857 in Milan (Italy), *Atmospheric Environment*, 41, 4599-4610, [https://doi.org/10.1016/j.atmosenv,](https://doi.org/10.1016/j.atmosenv.2007)
1858 2007.

1859 Löw, F., Navratil, P., Kotte, K., Schöler, H. F., and Bubenzer, O.: Remote-sensing-based analysis of
1860 landscape change in the desiccated seabed of the Aral Sea—a potential tool for assessing the hazard
1861 degree of dust and salt storms, *Environmental Monitoring and Assessment*, 185, 8303-8319,
1862 <https://doi.org/10.1007/s10661-013-3174-7>, 2013.

1863 Luo, M., Liu, Y., Zhu, Q., Tang, Y., and Alam, K.: Role and mechanisms of black carbon affecting water
1864 vapor transport to Tibet, *Remote Sensing*, 12(2), 0231, <https://doi.org/10.3390/rs12020231>, 2020.

1865 Ma, Q., Wu, Y., Tao, J., Xia, Y., Liu, X., Zhang, D., Han, Z., Zhang, X., and Zhang, R.: Variations of
1866 chemical composition and source apportionment of PM_{2.5} during winter haze episodes in Beijing,
1867 *Aerosol and Air Quality Research*, 17, 2791-2803, <https://doi.org/10.4209/aaqr.2017.10.0366>, 2017.

1868 Ma, Y., Ji, Y.-Q., Guo, J.-J., Zhao, J.-Q., Li, Y.-Y., Wang, S.-B. and Zhang, L.: Characteristics of
1869 carbon components and source analysis of road dust during spring in Tianjin (in Chinese), *Acta*
1870 *Scientiae Circumstantiae* 40(06), 2540-2545, <https://doi.org/10.13227/j.hjcx>, 2019.

1871 [Mahowald, N. M., Engelstaedter, S., Luo, C., Sealy, A., Artaxo, P., Benitez-Nelson, C., Bonnet, S., Chen,](#)
1872 [Y., Chuang, P. Y., Cohen, D. D., Dulac, F., Herut, B., Johansen, A. M., Kubilay, N., Losno, R.,](#)
1873 [Maenhaut, W., Paytan, A., Prospero, J. M., Shank, L. M., and Siefert, R. L.: Atmospheric iron](#)
1874 [deposition: Global distribution, variability, and human perturbations, *Annual Review of Marine*](#)
1875 [Science, 1, 245-278, <https://doi.org/10.1146/annurev.marine.010908.163727>, 2009.](#)

1876 Manousakas, M., Papaefthymiou, H., Diapouli, E., Migliori, A., Karydas, A. G., Bogdanovic-Radovic,
1877 I., and Eleftheriadis, K.: Assessment of PM_{2.5} sources and their corresponding level of uncertainty
1878 in a coastal urban area using EPA PMF 5.0 enhanced diagnostics, *Science of The Total Environment*,
1879 574, 155-164, <https://doi.org/10.1016/j.scitotenv.2016.09.047>, 2017.

1880 Mbengue, S., Fusek, M., Schwarz, J., Vodička, P., Šmejkalová, A. H., and Holoubek, I.: Four years of
1881 highly time resolved measurements of elemental and organic carbon at a rural background site in
1882 Central Europe, *Atmospheric Environment*, 182, 335-346, <https://doi.org/10.1016/j.atmosenv>, 2018.

1883 [Meng, C. C., Wang, L. T., Zhang, F. F., Wei, Z., Ma, S. M., Ma, X., and Yang, J.: Characteristics of](#)
1884 [concentrations and water-soluble inorganic ions in PM_{2.5} in Handan City, Hebei province, China,](#)
1885 [*Atmospheric Research*, 171, 133-146, <https://doi.org/10.1016/j.atmosres.2015.12.013>, 2016.](#)

1886 Meng, J.-H., Shi, X.-F., Xiang, Y. and Ren, Y.-F.: Current status and sources of heavy metal pollution
1887 in the atmosphere (in Chinese). *Environmental Science and Management* 42(08), 51-53,
1888 <https://doi.org/10.3969/j.issn.1673-1212.2017.08.011>, 2017.

1889 Meng, W., Zhong, Q., Chen, Y., Shen, H., Yun, X., Smith, K. R., Li, B., Liu, J., Wang, X., Ma, J., Cheng,
1890 H., Zeng, E. Y., Guan, D., Russell, A. G., and Tao, S.: Energy and air pollution benefits of household
1891 fuel policies in northern China, *Proceedings of the National Academy of Sciences*, 116, 16773-
1892 16780, <https://doi.org/10.1073/pnas.1904182116>, 2019.

1893 Meng, W., Shen, H., Yun, X., Chen, Y., Zhong, Q., Zhang, W., Yu, X., Xu, H., Ren, Y. a., Shen, G., Ma,
1894 J., Liu, J., Cheng, H., Wang, X., Zhu, D., and Tao, S.: Differentiated-rate clean heating strategy with
1895 superior environmental and health benefits in Northern China, *Environmental Science &*
1896 *Technology*, 54, 13458-13466, <https://doi.org/10.1021/acs.est.0c04019>, 2020.

1897 Miller, M. B., Fine, R., Pierce, A. M., and Gustin, M. S.: Identifying sources of ozone to three rural
1898 locations in Nevada, USA, using ancillary gas pollutants, aerosol chemistry, and mercury, *Science*
1899 *of The Total Environment*, 530-531, 483-492, <https://doi.org/10.1016/j.scitotenv>, 2015.

1900 Millet, D. B., Donahue, N. M., Pandis, S. N., Polidori, A., Stanier, C. O., Turpin, B. J., and Goldstein, A.
1901 H.: Atmospheric volatile organic compound measurements during the Pittsburgh Air Quality Study:
1902 Results, interpretation, and quantification of primary and secondary contributions, *Journal of*
1903 *Geophysical Research: Atmospheres*, 110, <https://doi.org/10.1029/2004JD004601>, 2005.

1904 Ming, J., Xiao, C., Sun, J., Kang, S., and Bonasoni, P.: Carbonaceous particles in the atmosphere and
1905 precipitation of the Nam Co region, central Tibet, *Journal of Environmental Sciences*, 22, 1748-
1906 1756, [https://doi.org/10.1016/S1001-0742\(09\)60315-6](https://doi.org/10.1016/S1001-0742(09)60315-6), 2010.

1907 Mishra, M. and Kulshrestha, U.: Chemical characteristics and deposition fluxes of dust-carbon mixed
1908 coarse aerosols at three sites of Delhi, NCR, *Journal of Atmospheric Chemistry*, 74, 399-421,
1909 <https://doi.org/10.1007/s10874-016-9349-1>, 2017.

1910 Moravek, A., Murphy, J. G., Hrdina, A., Lin, J. C., Pennell, C., Franchin, A., Middlebrook, A. M., Fibiger,
1911 D. L., Womack, C. C., McDuffie, E. E., Martin, R., Moore, K., Baasandorj, M., and Brown, S. S.:
1912 Wintertime spatial distribution of ammonia and its emission sources in the Great Salt Lake region,
1913 *Atmospheric Chemistry and Physics*, 19, 15691-15709, <https://doi.org/10.5194/acp-19-15691-2019>,
1914 2019.

1915 ~~Muller, G.: Index of geoaccumulation in sediments of the rhine river, *GeoJournal*, 2, 108-118, 1969.~~

1916 Munawar, M. E.: Human health and environmental impacts of coal combustion and post-combustion
1917 wastes, *Journal of Sustainable Mining*, 17, 87-96, <https://doi.org/10.1016/j.jsm>, 2018.

1918 Na, K., Sawant, A. A., Song, C., and Cocker, D. R.: Primary and secondary carbonaceous species in the

1919 atmosphere of Western Riverside County, California, *Atmospheric Environment*, 38, 1345-1355,
1920 <https://doi.org/10.1016/j.atmosenv>, 2004.

1921 [Noll, K. E. and Fang, K. Y. P.: Development of a dry deposition model for atmospheric coarse particles,](#)
1922 [Atmospheric Environment \(1967\), 23, 585-594, https://doi.org/10.1016/0004-6981\(89\)90007-3,](#)
1923 [1989.](#)

1924 [Norris, G., Duvall, R., Brown, S., and Bai, S.: EPA Positive Matrix Factorization \(PMF\) 5.0 fundamentals](#)
1925 [and user guide, The United States Environmental Protection Agency, https://www.epa.gov, 2014.](#)

1926 Nuralkyzy, B., Wang, P., Deng, X., An, S., and Huang, Y.: Heavy metal contents and assessment of soil
1927 contamination in different land-use types in the Qaidam Basin, *Sustainability*, 13(21), 12020,
1928 <https://doi.org/10.3390/su132112020>, 2021.

1929 [Offer, Z. Y., Goossens, D., and Shachak, M.: Aeolian deposition of nitrogen to sandy and loessial](#)
1930 [ecosystems in the Negev Desert, Journal of Arid Environments, 23, 355-363,](#)
1931 [https://doi.org/10.1016/S0140-1963\(18\)30609-8](https://doi.org/10.1016/S0140-1963(18)30609-8), 1992.

1932 Oliveira, T., Pio, C., Alves, C., Silvestre, A., Evtyugina, M., Afonso, J., Caseiro, A., and Legrand, M.:
1933 Air quality and organic compounds in aerosols from a coastal rural area in the Western Iberian
1934 Peninsula over a year long period: Characterisation, loads and seasonal trends, *Atmospheric*
1935 *Environment*, 41, 3631-3643, <https://doi.org/10.1016/j.atmosenv>, 2007.

1936 Pacyna, J. M. and Pacyna, E. G.: An assessment of global and regional emissions of trace metals to the
1937 atmosphere from anthropogenic sources worldwide, *Environmental Reviews*, 9, 269-298,
1938 <https://doi.org/10.1139/a01-012>, 2001.

1939 Pandolfi, M., Gonzalez-Castanedo, Y., Alastuey, A., de la Rosa, J. D., Mantilla, E., de la Campa, A. S.,
1940 Querol, X., Pey, J., Amato, F., and Moreno, T.: Source apportionment of PM₁₀ and PM_{2.5} at multiple
1941 sites in the strait of Gibraltar by PMF: impact of shipping emissions, *Environmental Science and*
1942 *Pollution Research*, 18, 260-269, <https://doi.org/10.1007/s11356-010-0373-4>, 2010.

1943 [Parajuli, S. P., Stenchikov, G. L., Ukhov, A., Mostamandi, S., Kucera, P. A., Axisa, D., Gustafson Jr, W.](#)
1944 [I., and Zhu, Y.: Effect of dust on rainfall over the Red Sea coast based on WRF-Chem model](#)
1945 [simulations, Atmospheric Chemistry and Physics, 22, 8659-8682, https://doi.org/10.5194/acp-22-](#)
1946 [8659-2022, 2022.](#)

1947 [Peng, T., Sun, C., Zhang, Y., and Fan, F.: Spatiotemporal variation of anthropogenic heat emission](#)
1948 [landscape pattern in the central urban area of Guangzhou, Journal of South China Normal University](#)

1949 [\(Natural Science Edition\), 53, 92–102, https://doi.org/10.6054/j.jscnun.2021080, 2021.](https://doi.org/10.6054/j.jscnun.2021080)

1950 Pervez, S., Bano, S., Watson, J. G., Chow, J. C., Matawle, J. L., Shrivastava, A., Tiwari, S., and Pervez,

1951 Y. F.: Source profiles for PM_{10-2.5} resuspended dust and vehicle exhaust emissions in Central India,

1952 Aerosol and Air Quality Research, 18, 1660-1672, <https://doi.org/10.4209/aaqr>, 2018.

1953 Phairuang, W., Hongtieab, S., Suwattiga, P., Furuuchi, M., and Hata, M.: Atmospheric Ultrafine

1954 Particulate Matter (PM_{0.1})-bound carbon composition in Bangkok, Thailand, Atmosphere, 13,

1955 <https://doi.org/10.3390/atmos13101676>, 2022.

1956 Pio, C., Cerqueira, M., Harrison, R. M., Nunes, T., Mirante, F., Alves, C., Oliveira, C., Sanchez de la

1957 Campa, A., Artíñano, B., and Matos, M.: OC/EC ratio observations in Europe: Re-thinking the

1958 approach for apportionment between primary and secondary organic carbon, Atmospheric

1959 Environment, 45, 6121-6132, <https://doi.org/10.1016/j.atmosenv>, 2011.

1960 Pipal, A. S., Singh, S., and Satsangi, G. P.: Study on bulk to single particle analysis of atmospheric

1961 aerosols at urban region, Urban Climate, 27, 243-258, <https://doi.org/10.1016/j.uclim.2018.12.008>,

1962 2019.

1963 Popovicheva, O. B., Engling, G., Diapouli, E., Saraga, D., Persiantseva, N. M., Timofeev, M. A., Kireeva,

1964 E. D., Shonija, N. K., Chen, S. -H., Nguyen, D. L., Eleftheriadis, K., and Lee, C. -T.: Impact of

1965 smoke intensity on size-resolved aerosol composition and microstructure during the biomass

1966 burning season in Northwest Vietnam, Aerosol and Air Quality Research, 16, 2635-2654,

1967 <https://doi.org/10.4209/aaqr>, 2016.

1968 [Qi, D. L., Zhao, Q. N., Zhao, H. F., Han, T. F. and Su, W. J.: Temporal and spatial characteristics and](http://www.ghqx.org.cn/CN/Y2018/V36/I6/927)

1969 [regional differences of dust-fall in Qinghai Province from 2004 to 2017 \(in Chinese\), Arid](http://www.ghqx.org.cn/CN/Y2018/V36/I6/927)

1970 [Meteorology, 36\(06\), 927-935, http://www.ghqx.org.cn/CN/Y2018/V36/I6/927, 2018.](http://www.ghqx.org.cn/CN/Y2018/V36/I6/927)

1971 [Qian, G. Q. and Dong, Z. B.: Research on methods and related issues of atmospheric dust collection \(in](https://doi.org/1000-694X9(2004)06-0779-04)

1972 [Chinese\), Chinese Journal of Desert Research, \(06\), 119-122, https://doi.org/1000-](https://doi.org/1000-694X9(2004)06-0779-04)

1973 [694X9\(2004\)06-0779-04, 2014.](https://doi.org/1000-694X9(2004)06-0779-04)

1974 [Qian, Y., Yasunari, T. J., Doherty, S. J., Flanner, M. G., Lau, W. K. M., Ming, J., Wang, H., Wang, M.,](https://doi.org/10.1007/s00376-014-0010-0)

1975 [Warren, S. G., and Zhang, R.: Light-absorbing particles in snow and ice: Measurement and](https://doi.org/10.1007/s00376-014-0010-0)

1976 [modeling of climatic and hydrological impact, Advances in Atmospheric Sciences, 32, 64-91,](https://doi.org/10.1007/s00376-014-0010-0)

1977 [https://doi.org/10.1007/s00376-014-0010-0, 2015.](https://doi.org/10.1007/s00376-014-0010-0)

1978 Qiao, Q., Huang, B., Zhang, C., Piper, J. D. A., Pan, Y., and Sun, Y.: Assessment of heavy metal

1979 contamination of dustfall in northern China from integrated chemical and magnetic investigation,
1980 Atmospheric Environment, 74, 182-193, <https://doi.org/10.1016/j.atmosenv>, 2013.

1981 [Rabha, S., Saikia, B. K., Singh, G. K., and Gupta, T.: Meteorological influence and chemical](#)
1982 [compositions of atmospheric particulate matters in an Indian Urban Area, ACS Earth and Space](#)
1983 [Chemistry, 5, 1686-1694, https://doi.org/10.1021/acsearthspacechem.1c00037, 2021.](#)

1984 [Ramanathan, V. and Carmichael, G.: Global and regional climate changes due to black carbon, Nature](#)
1985 [Geoscience, 1, 221-227, https://doi.org/10.1038/ngeo156, 2008.](#)

1986 Rogge, W. F., Hildemann, L. M., Mazurek, M. A., Cass, G. R., and Simoneit, B. R. T.: Sources of fine
1987 organic aerosol. 3. Road dust, tire debris, and organometallic brake lining dust: roads as sources and
1988 sinks, Environmental Science & Technology, 27, 1892-1904, <https://doi.org/10.1021/es00046a019>,
1989 1993.

1990 [Rörig-Dalgaard, I.: Direct measurements of the deliquescence relative humidity in salt mixtures](#)
1991 [including the contribution from metastable phases, ACS Omega, 6, 16297-16306,](#)
1992 [https://doi.org/10.1021/acsomega.1c00538, 2021.](#)

1993 Safai, P. D., Raju, M. P., Rao, P. S. P., and Pandithurai, G.: Characterization of carbonaceous aerosols
1994 over the urban tropical location and a new approach to evaluate their climatic importance,
1995 Atmospheric Environment, 92, 493-500, <https://doi.org/10.1016/j.atmosenv.2014.04.055>, 2014.

1996 [Saha, A. and Despiiau, S.: Seasonal and diurnal variations of black carbon aerosols over a Mediterranean](#)
1997 [coastal zone, Atmospheric Research, 92, 27-41, https://doi.org/10.1016/j.atmosres.2008.07.007,](#)
1998 [2009.](#)

1999 [Sandrini, S., Fuzzi, S., Piazzalunga, A., Prati, P., Bonasoni, P., Cavalli, F., Bove, M. C., Calvello, M.,](#)
2000 [Cappelletti, D., Colombi, C., Contini, D., de Gennaro, G., Di Gilio, A., Fermo, P., Ferrero, L.,](#)
2001 [Gianelle, V., Giugliano, M., Ielpo, P., Lonati, G., Marinoni, A., Massabò, D., Molteni, U., Moroni,](#)
2002 [B., Pavese, G., Perrino, C., Perrone, M. G., Perrone, M. R., Putaud, J.-P., Sargolini, T., Vecchi, R.,](#)
2003 [and Gilardoni, S.: Spatial and seasonal variability of carbonaceous aerosol across Italy, Atmospheric](#)
2004 [Environment, 99, 587-598, https://doi.org/10.1016/j.atmosenv.2014.10.032, 2014.](#)

2005 [Saraga, D., Maggos, T., Degrendele, C., Klánová, J., Horvat, M., Kocman, D., Kanduč, T., Garcia Dos](#)
2006 [Santos, S., Franco, R., Gómez, P. M., Manousakas, M., Bairachtari, K., Eleftheriadis, K.,](#)
2007 [Kermenidou, M., Karakitsios, S., Gotti, A., and Sarigiannis, D.: Multi-city comparative PM_{2.5}](#)
2008 [source apportionment for fifteen sites in Europe: The ICARUS project, Science of The Total](#)

2009 [Environment, 751, 141855, https://doi.org/10.1016/j.scitotenv.2020.141855, 2021.](https://doi.org/10.1016/j.scitotenv.2020.141855)

2010 [Schepanski, K.: Transport of mineral dust and its impact on climate, Geosciences, 2018, 8\(5\), 151,](https://doi.org/10.3390/geosciences8050151)

2011 [https://doi.org/10.3390/geosciences8050151, 2018.](https://doi.org/10.3390/geosciences8050151)

2012 Schmidl, C., Marr, I. L., Caseiro, A., Kotianová, P., Berner, A., Bauer, H., Kasper-Giebl, A., and Puxbaum,

2013 H.: Chemical characterisation of fine particle emissions from wood stove combustion of common

2014 woods growing in mid-European Alpine regions, Atmospheric Environment, 42, 126-141,

2015 <https://doi.org/10.1016/j.atmosenv>, 2008.

2016 Secrest, M. H., Schauer, J. J., Carter, E. M., and Baumgartner, J.: Particulate matter chemical component

2017 concentrations and sources in settings of household solid fuel use, Indoor Air, 27, 1052-1066,

2018 <https://doi.org/10.1111/ina.12389>, 2017.

2019 Seinfeld, J. H., Pandis, S. N., and Noone, K. J. J. P. T.: Atmospheric chemistry and physics: From air

2020 pollution to climate change, 51, 88-90, 1998.

2021 [Shahram, N., Majid, K., Mehdi, F., Soodabeh, M., and Ahmad, Y.: The origins and sources of dust](https://api.semanticscholar.org/CorpusID:56256748)

2022 [particles, their effects on environment and health, and control strategies: A review, Journal of Air](https://api.semanticscholar.org/CorpusID:56256748)

2023 [Pollution and Health, 1\(2\):137-152, https://api.semanticscholar.org/CorpusID:56256748, 2016.](https://api.semanticscholar.org/CorpusID:56256748)

2024 [Sharma, S., Brook, J. R., Cachier, H., Chow, J., Gaudenzi, A., and Lu, G.: Light absorption and thermal](https://doi.org/10.1029/2002JD002496)

2025 [measurements of black carbon in different regions of Canada, Journal of Geophysical Research:](https://doi.org/10.1029/2002JD002496)

2026 [Atmospheres, 107, AAC 11-11, https://doi.org/10.1029/2002JD002496, 2002.](https://doi.org/10.1029/2002JD002496)

2027 Sheehan, P. E. and Bowman, F. M.: Estimated effects of temperature on secondary organic aerosol

2028 concentrations, Environmental Science & Technology, 35, 2129-2135,

2029 <https://doi.org/10.1021/es001547g>, 2001.

2030 Shen, J. and Dai, B. L.: Development and utilization of salt lake brine lithium resources and its prospects

2031 (in Chinese), Industrial Minerals & Processing, 38, 1-4+7,

2032 <https://doi.org/10.16283/j.cnki.hgkwyjg.2009.04.004>, 2009.

2033 Shen, G.-F., Xiong, R., Cheng, H.-F. and Tao, S.: Estimation of residential energy structure and primary

2034 PM_{2.5} emissions in rural Tibet (in Chinese), Science Bulletin, 66(15), 1900-1911,

2035 <https://doi.org/10.1360/TB-2020-0408>, 2021.

2036 [Shen, L., Wang, H., Kong, X., Zhang, C., Shi, S., and Zhu, B.: Characterization of black carbon aerosol](https://doi.org/10.1016/j.apr.2020.08.035)

2037 [in the Yangtze River Delta, China: Seasonal variation and source apportionment, Atmospheric](https://doi.org/10.1016/j.apr.2020.08.035)

2038 [Pollution Research, 12, 195-209, https://doi.org/10.1016/j.apr.2020.08.035, 2021.](https://doi.org/10.1016/j.apr.2020.08.035)

2039 Shen, Z., Arimoto, R., Cao, J., Zhang, R., Li, X., Du, N., Okuda, T., Nakao, S., and Tanaka, S.: Seasonal
2040 variations and evidence for the effectiveness of pollution controls on water-soluble inorganic species
2041 in total suspended particulates and fine particulate matter from Xi'an, China, *Journal of the Air &*
2042 *Waste Management Association*, 58, 1560-1570, <https://doi.org/10.3155/1047-3289.58.12.1560>,
2043 2008.

2044 [Shen, Z., Zhang, Q., Cao, J., Zhang, L., Lei, Y., Huang, Y., Huang, R. J., Gao, J., Zhao, Z., Zhu, C., Yin,](#)
2045 [X., Zheng, C., Xu, H., and Liu, S.: Optical properties and possible sources of brown carbon in PM_{2.5}](#)
2046 [over Xi'an, China, *Atmospheric Environment*, 150, 322-330,](#)
2047 <https://doi.org/10.1016/j.atmosenv.2016.11.024>, 2017.

2048 Shi, G., Chen, Z., Teng, J., Bi, C., Zhou, D., Sun, C., Li, Y., and Xu, S.: Fluxes, variability and sources
2049 of cadmium, lead, arsenic and mercury in dry atmospheric depositions in urban, suburban and rural
2050 areas, *Environmental Research*, 113, 28-32, <https://doi.org/10.1016/j.envres.2012.01.001>, 2012.

2051 Shi, X., Zhao, Y., Dai, S., Xu, L., Li, Y., Jia, H., and Zhang, Q.: Research on climatic change of Qaidam
2052 Basin since 1961, *Journal of Desert Research*, 25, 123-128,
2053 <http://www.desert.ac.cn/CN/Y2005/V25/I1/123>, 2005.

2054 Shi, Z., Vu, T., Kotthaus, S., Harrison, R. M., Grimmond, S., Yue, S., Zhu, T., Lee, J., Han, Y., Demuzere,
2055 M., Dunmore, R. E., Ren, L., Liu, D., Wang, Y., Wild, O., Allan, J., Acton, W. J., Barlow, J., Barratt,
2056 B., Beddows, D., Bloss, W. J., Calzolari, G., Carruthers, D., Carslaw, D. C., Chan, Q., Chatzidiakou,
2057 L., Chen, Y., Crilley, L., Coe, H., Dai, T., Doherty, R., Duan, F., Fu, P., Ge, B., Ge, M., Guan, D.,
2058 Hamilton, J. F., He, K., Heal, M., Heard, D., Hewitt, C. N., Hollaway, M., Hu, M., Ji, D., Jiang, X.,
2059 Jones, R., Kalberer, M., Kelly, F. J., Kramer, L., Langford, B., Lin, C., Lewis, A. C., Li, J., Li, W.,
2060 Liu, H., Liu, J., Loh, M., Lu, K., Lucarelli, F., Mann, G., McFiggans, G., Miller, M. R., Mills, G.,
2061 Monk, P., Nemitz, E., O'Connor, F., Ouyang, B., Palmer, P. I., Percival, C., Popoola, O., Reeves, C.,
2062 Rickard, A. R., Shao, L., Shi, G., Spracklen, D., Stevenson, D., Sun, Y., Sun, Z., Tao, S., Tong, S.,
2063 Wang, Q., Wang, W., Wang, X., Wang, X., Wang, Z., Wei, L., Whalley, L., Wu, X., Wu, Z., Xie, P.,
2064 Yang, F., Zhang, Q., Zhang, Y., Zhang, Y., and Zheng, M.: Introduction to the special issue "In-depth
2065 study of air pollution sources and processes within Beijing and its surrounding region (APHH-
2066 Beijing)", *Atmospheric Chemistry and Physics*, 19, 7519-7546, [https://doi.org/10.5194/acp-19-](https://doi.org/10.5194/acp-19-7519-2019)
2067 [7519-2019](https://doi.org/10.5194/acp-19-7519-2019), 2019.

2068 [Shrivastava, M., Lou, S., Zelenyuk, A., Easter, R. C., Corley, R. A., Thrall, B. D., Rasch, P. J., Fast, J. D.,](#)

2069 [Massey Simonich, S. L., Shen, H., and Tao, S.: Global long-range transport and lung cancer risk](#)
2070 [from polycyclic aromatic hydrocarbons shielded by coatings of organic aerosol, Proceedings of the](#)
2071 [National Academy of Sciences, 114, 1246-1251, <https://doi.org/10.1073/pnas.1618475114>, 2017.](#)

2072 Simoneit, B. R. T.: Biomass burning — a review of organic tracers for smoke from incomplete
2073 combustion, *Applied Geochemistry*, 17, 129-162, [https://doi.org/10.1016/S0883-2927\(01\)00061-0](https://doi.org/10.1016/S0883-2927(01)00061-0),
2074 2002.

2075 Smichowski, P., Gómez, D., Frazzoli, C., and Caroli, S.: Traffic-related elements in airborne particulate
2076 matter, *Applied Spectroscopy Reviews*, 43, 23-49, <https://doi.org/10.1080/05704920701645886>,
2077 2007.

2078 [Smith, R. M. and Twiss, P. C.: Extensive gaging of dust deposition rates, *Kansas Acad.*, 68:2,](#)
2079 <https://doi.org/10.2307/3626489>, 1965.

2080 Song, P. S., Li, W., Sun, B., Nie, Z., Bu, L. Z., and Wang, Y. S.: Progress in the development and
2081 utilization of salt lake resources (in Chinese), *Journal of Inorganic Chemistry*, 27, 801–815,
2082 2011.

2083 Sow, M., Goossens, D., and Rajot, J. L.: Calibration of the MDCO dust collector and of four versions of
2084 the inverted frisbee dust deposition sampler, *Geomorphology*, 82, 360-375,
2085 <https://doi.org/10.1016/j.geomorph.2006.05.013>, 2006.

2086 Strader, R., Lurmann, F., and Pandis, S. N.: Evaluation of secondary organic aerosol formation in winter,
2087 *Atmospheric Environment*, 33, 4849-4863, [https://doi.org/10.1016/S1352-2310\(99\)00310-6](https://doi.org/10.1016/S1352-2310(99)00310-6), 1999.

2088 Sulong, N. A., Latif, M. T., Sahani, M., Khan, M. F., Fadzil, M. F., Tahir, N. M., Mohamad, N., Sakai,
2089 N., Fujii, Y., Othman, M., and Tohno, S.: Distribution, sources and potential health risks of
2090 polycyclic aromatic hydrocarbons (PAHs) in PM_{2.5} collected during different monsoon seasons and
2091 haze episode in Kuala Lumpur, *Chemosphere*, 219, 1-14, <https://doi.org/10.1016/j.chemosphere>,
2092 2019.

2093 Tang, Y., Han, G. -L. and Xu, Z. -F.: Characteristics of black carbon content in atmospheric dust in
2094 Beijing and its northern regions (in Chinese), *Acta Scientiae Circumstantiae*, 33(02), 332-338,
2095 <https://doi.org/10.13671/j.hjkxxb.2013.02.033>, 2013.

2096 Tao, J., Cheng, T., Zhang, R., Cao, J., Zhu, L., Wang, Q., Luo, L., and Zhang, L.: Chemical composition
2097 of PM_{2.5} at an urban site of Chengdu in southwestern China, *Advances in Atmospheric Sciences*, 30,
2098 1070-1084, <https://doi.org/10.1007/s00376-012-2168-7>, 2013.

2099 Tao, S., Ru, M. Y., Du, W., Zhu, X., Zhong, Q. R., Li, B. G., Shen, G. F., Pan, X. L., Meng, W. J., Chen,
2100 Y. L., Shen, H. Z., Lin, N., Su, S., Zhuo, S. J., Huang, T. B., Xu, Y., Yun, X., Liu, J. F., Wang, X. L.,
2101 Liu, W. X., Cheng, H. F., and Zhu, D. Q.: Quantifying the rural residential energy transition in China
2102 from 1992 to 2012 through a representative national survey, *Nature Energy*, 3, 567-573,
2103 <https://doi.org/10.1038/s41560-018-0158-4>, 2018.

2104 Tian, M., Gao, J., Zhang, L., Zhang, H., Feng, C., and Jia, X.: Effects of dust emissions from wind erosion
2105 of soil on ambient air quality, *Atmospheric Pollution Research*, 12,
2106 <https://doi.org/10.1016/j.apr.2021.101108>, 2021.

2107 Tian, S. L., Pan, Y. P., and Wang, Y. S.: Size-resolved source apportionment of particulate matter in urban
2108 Beijing during haze and non-haze episodes, *Atmospheric Chemistry and Physics*, 16, 1-19,
2109 <https://doi.org/10.5194/acp-16-1-2016>, 2016.

2110 [Tiwari, S., Pandithurai, G., Attri, S. D., Srivastava, A. K., Soni, V. K., Bisht, D. S., Anil Kumar, V., and](#)
2111 [Srivastava, M. K.: Aerosol optical properties and their relationship with meteorological parameters](#)
2112 [during wintertime in Delhi, India, *Atmospheric Research*, 153, 465-479,](#)
2113 [<https://doi.org/10.1016/j.atmosres.2014.10.003>, 2015.](#)

2114 Turpin, B. J. and Huntzicker, J. J.: Identification of secondary organic aerosol episodes and quantitation
2115 of primary and secondary organic aerosol concentrations during SCAQS, *Atmospheric Environment*,
2116 29, 3527-3544, [https://doi.org/10.1016/1352-2310\(94\)00276-Q](https://doi.org/10.1016/1352-2310(94)00276-Q), 1995.

2117 [Turpin, B. J., Huntzicker, J. J., and Hering, S. V.: Investigation of organic aerosol sampling artifacts in](#)
2118 [the los angeles basin, *Atmospheric Environment*, 28, 3061-3071, \[\\[2310\\\(94\\\)00133-6\\]\\(https://doi.org/10.1016/1352-2310\\(94\\)00133-6\\), 1994.\]\(https://doi.org/10.1016/1352-</u>

2119 <a href=\)](#)

2120 VanCuren, R. and Gustin, M. S.: Identification of sources contributing to PM_{2.5} and ozone at elevated
2121 sites in the western U.S. by receptor analysis: Lassen Volcanic National Park, California, and Great
2122 Basin National Park, Nevada, *Science of The Total Environment*, 530-531, 505-518,
2123 <https://doi.org/10.1016/j.scitotenv>, 2015.

2124 Venkataraman, C., Brauer, M., Tibrewal, K., Sadavarte, P., Ma, Q., Cohen, A., Chaliyakunnel, S., Frostad,
2125 J., Klimont, Z., Martin, R. V., Millet, D. B., Philip, S., Walker, K., and Wang, S.: Source influence
2126 on emission pathways and ambient PM_{2.5} pollution over India (2015–2050), *Atmospheric Chemistry*
2127 [and Physics](#), 18, 8017-8039, <https://doi.org/10.5194/acp-18-8017-2018>, 2018.

2128 Wang, F.: The mechanism and timescales of soil formation in the hyper-arid Atacama Desert, Chile,

2129 Purdue University, 2013.

2130 Wang, F., Michalski, G., Seo, J.-h., and Ge, W.: Geochemical, isotopic, and mineralogical constraints on
2131 atmospheric deposition in the hyper-arid Atacama Desert, Chile, *Geochimica et Cosmochimica Acta*,
2132 135, 29-48, <https://doi.org/10.1016/j.gca>, 2014.

2133 Wang, M., Duan, Y., Xu, W., Wang, Q., Zhang, Z., Yuan, Q., Li, X., Han, S., Tong, H., Huo, J., Chen, J.,
2134 Gao, S., Wu, Z., Cui, L., Huang, Y., Xiu, G., Cao, J., Fu, Q., and Lee, S.: Measurement report:
2135 Characterisation and sources of the secondary organic carbon in a Chinese megacity over 5 years
2136 from 2016 to 2020, *Atmospheric Chemistry and Physics*, 22, 12789-12802,
2137 <https://doi.org/10.5194/acp-22-12789-2022>, 2022.

2138 [Watson, J. G., Antony Chen, L. W., Chow, J. C., Doraiswamy, P., and Lowenthal, D. H.: Source](#)
2139 [apportionment: Findings from the U.S. supersites program, *Journal of the Air & Waste Management*](#)
2140 [Association, 58, 265-288, <https://doi.org/10.3155/1047-3289.58.2.265>, 2008.](#)

2141 Wei, C., Bandowe, B. A. M., Han, Y., Cao, J., Zhan, C., and Wilcke, W.: Polycyclic aromatic
2142 hydrocarbons (PAHs) and their derivatives (alkyl-PAHs, oxygenated-PAHs, nitrated-PAHs and
2143 azaarenes) in urban road dusts from Xi'an, Central China, *Chemosphere*, 134, 512-520,
2144 <https://doi.org/10.1016/j.chemosphere.2014.11.052>, 2015.

2145 Wei, T., Dong, Z., Kang, S., Qin, X., and Guo, Z.: Geochemical evidence for sources of surface dust
2146 deposited on the Laohugou glacier, Qilian Mountains, *Applied Geochemistry*, 79, 1-8,
2147 <https://doi.org/10.1016/j.apgeochem>, 2017.

2148 [Wei, Y., Xie, Y., Dang, X., Guo, J., Liu, M., and Wu, H.: Characteristics of atmospheric dust deposition](#)
2149 [and influencing factors in different protection functional areas of the Jilantai Salt Lake Protection](#)
2150 [system, *Research of Soil and Water Conservation*, 30, 201-208,](#)
2151 <https://doi.org/10.13869/j.cnki.rswc.2023.05.027>, 2023.

2152 Wu, C. and Yu, J. Z.: Determination of primary combustion source organic carbon-to-elemental carbon
2153 (OC/EC) ratio using ambient OC and EC measurements: secondary OC-EC correlation
2154 minimization method, *Atmospheric Chemistry and Physics*, 16, 5453-5465,
2155 <https://doi.org/10.5194/acp-16-5453-2016>, 2016.

2156 Wu, C., Wu, D., and Yu, J. Z.: Quantifying black carbon light absorption enhancement with a novel
2157 statistical approach, *Atmospheric Chemistry and Physics*, 18, 289-309, [https://doi.org/10.5194/acp-](https://doi.org/10.5194/acp-18-289-2018)
2158 [18-289-2018](https://doi.org/10.5194/acp-18-289-2018), 2018a.

- 2159 [Wu, Y., Zhang, R., Tian, P., Tao, J., Hsu, S. C., Yan, P., Wang, Q., Cao, J., Zhang, X., and Xia, X.: Effect](#)
2160 [of ambient humidity on the light absorption amplification of black carbon in Beijing during January](#)
2161 [2013, Atmospheric Environment, 124, 217-223, <https://doi.org/10.1016/j.atmosenv.2015.04.041>,](#)
2162 [2016.](#)
- 2163 Xia, X., Zong, X., Cong, Z., Chen, H., Kang, S., and Wang, P.: Baseline continental aerosol over the
2164 central Tibetan plateau and a case study of aerosol transport from South Asia, Atmospheric
2165 Environment, 45, 7370-7378, <https://doi.org/10.1016/j.atmosenv.2011.07.067>, 2011.
- 2166 Xiao, Q., Saikawa, E., Yokelson, R. J., Chen, P., Li, C., and Kang, S.: Indoor air pollution from burning
2167 yak dung as a household fuel in Tibet, Atmospheric Environment, 102, 406-412,
2168 <https://doi.org/10.1016/j.atmosenv>, 2015.
- 2169 Xie, F., Guo, L., Wang, Z., Tian, Y., Yue, C., Zhou, X., Wang, W., Xin, J., and Lu, C.: Geochemical
2170 characteristics and socioeconomic associations of carbonaceous aerosols in coal-fueled cities with
2171 significant seasonal pollution pattern, Environmental International, 179, 108179,
2172 <https://doi.org/10.1016/j.envint.2023.108179>, 2023.
- 2173 Xu, L., Chen, X., Chen, J., Zhang, F., He, C., Zhao, J., and Yin, L.: Seasonal variations and chemical
2174 compositions of PM_{2.5} aerosol in the urban area of Fuzhou, China, Atmospheric Research, 104-
2175 105, 264-272, <https://doi.org/10.1016/j.atmosres>, 2012.
- 2176 Xu, M., Liu, Z., Hu, B., Yan, G., Zou, J., Zhao, S., Zhou, J., Liu, X., Zheng, X., Zhang, X., Cao, J., Guan,
2177 M., Lv, Y., and Zhang, Y.: Chemical characterization and source identification of PM_{2.5} in Luoyang
2178 after the clean air actions, Journal of Environmental Sciences, 115, 265-276,
2179 <https://doi.org/10.1016/j.jes.2021.06.021>, 2022.
- 2180 Xu, R., Tie, X., Li, G., Zhao, S., Cao, J., Feng, T., and Long, X.: Effect of biomass burning on black
2181 carbon (BC) in South Asia and Tibetan Plateau: The analysis of WRF-Chem modeling, Science of
2182 The Total Environment, 645, 901-912, <https://doi.org/10.1016/j.scitotenv.2018.07.165>, 2018b.
- 2183 [Xu, Z., Wang, J., and Han, J.: Ecological vulnerability assessment of the Qaidam Basin based on the SRP](#)
2184 [Model, Salt Lake Research, 32, 53-60, <https://doi.org/10.3724/j.yhyj.2024009>, 2024.](#)
- 2185 [Xu, Z.: Airborne particles in outdoor air: Atmospheric dust, in: Fundamentals of air cleaning technology](#)
2186 [and its application in cleanrooms, Springer Berlin Heidelberg, 47-132, \[https://doi.org/10.1007/978-\]\(https://doi.org/10.1007/978-3-642-39374-7_2\)](#)
2187 [3-642-39374-7_2](#), 2014.
- 2188 Xue, W., Wang, L., Yang, Z., Xiong, Z., Li, X., Xu, Q., and Cai, Z.: Can clean heating effectively alleviate

2189 air pollution: An empirical study based on the plan for cleaner winter heating in northern China,
2190 Applied Energy, 351, 121923, <https://doi.org/10.1016/j.apenergy>, 2023.

2191 Yan, B., Zheng, M., Hu, Y., Ding, X., Sullivan, A. P., Weber, R. J., Baek, J., Edgerton, E. S., and Russell,
2192 A. G.: Roadside, urban, and rural comparison of primary and secondary organic molecular markers
2193 in ambient PM_{2.5}, Environmental Science & Technology, 43, 4287-4293,
2194 <https://doi.org/10.1021/es900316g>, 2009.

2195 Yang, F., He, K., Ye, B., Chen, X., Cha, L., Cadle, S. H., Chan, T., and Mulawa, P. A.: One-year record
2196 of organic and elemental carbon in fine particles in downtown Beijing and Shanghai, Atmospheric
2197 Chemistry and Physics, 5, 1449-1457, <https://doi.org/10.5194/acp-5-1449-2005>, 2005.

2198 Yang, Q.-L., Wang, J.-X. and Zhao, Z.-X.: Temporal and spatial distribution characteristics and source
2199 analysis of heavy metals in atmospheric dust in typical industrial cities in Northeast China during
2200 winter and spring (in Chinese), Acta Scientiae Circumstantiae, 1-9,
2201 <https://doi.org/10.13671/j.hjkxxb.2024.0254>, 2024.

2202 Yao, L., Yang, L., Yuan, Q., Yan, C., Dong, C., Meng, C., Sui, X., Yang, F., Lu, Y., and Wang, W.: Sources
2203 apportionment of PM_{2.5} in a background site in the North China Plain, Science of the Total
2204 Environment, 541, 590-598, <https://doi.org/10.1016/j.scitotenv>, 2016.

2205 Ye, W., Saikawa, E., Avramov, A., Cho, S. H., and Chartier, R.: Household air pollution and personal
2206 exposure from burning firewood and yak dung in summer in the eastern Tibetan Plateau,
2207 Environmental Pollution, 263, 114531, <https://doi.org/10.1016/j.envpol>, 2020.

2208 Yoo, H. Y., Kim, K. A., Kim, Y. P., Jung, C. H., Shin, H. J., Moon, K. J., Park, S. M., and Lee, J. Y.:
2209 Validation of SOC estimation using OC and EC concentration in PM_{2.5} measured at Seoul, Aerosol
2210 and Air Quality Research, 22, 210388, <https://doi.org/10.4209/aaqr.210388>, 2022.

2211 You, S., Yao, Z., Dai, Y., and Wang, C.-H.: A comparison of PM exposure related to emission hotspots
2212 in a hot and humid urban environment: Concentrations, compositions, respiratory deposition, and
2213 potential health risks, Science of The Total Environment, 599-600, 464-473,
2214 <https://doi.org/10.1016/j.scitotenv.2017.04.217>, 2017.

2215 Yu, H., Yang, W., Wang, X., Yin, B., Zhang, X., Wang, J., Gu, C., Ming, J., Geng, C., and Bai, Z.: A
2216 seriously sand storm mixed air-polluted area in the margin of Tarim Basin: Temporal-spatial
2217 distribution and potential sources, Science of The Total Environment, 676, 436-446,
2218 <https://doi.org/10.1016/j.scitotenv>, 2019.

2219 Yu, L.-P., Li, D., Meng, L., Du, C.-Y. and Zhao, P.: Observation and data processing methods for
2220 atmospheric dust deposition (in Chinese), *Anhui Agricultural Sciences*, 44: 185-186,
2221 <https://doi.org/10.13989/j.cnki.0517-6611.2016.31.064>, 2016.

2222 [Yu, L., Wang, G., Zhang, R., Zhang, L., Song, Y., Wu, B., Li, X., An, K., and Chu, J.: Characterization](#)
2223 [and source apportionment of PM_{2.5} in an urban environment in Beijing, *Aerosol and Air Quality*](#)
2224 [Research, 13, 574-583, <https://doi.org/10.4209/aaqr.2012.07.0192>, 2013.](#)

2225 [Yue, D., Zhong, L., Zhang, T., Shen, J., Zhou, Y., Zeng, L., Dong, H., and Ye, S.: Pollution properties of](#)
2226 [water-soluble secondary inorganic ions in atmospheric PM_{2.5} in the Pearl River Delta Region,](#)
2227 [Aerosol and Air Quality Research, 15, 1737-1747, <https://doi.org/10.4209/aaqr.2014.12.0333>, 2015.](#)

2228 [Zan, J., Maher, B. A., Fang, X., Stevens, T., Ning, W., Wu, F., Yang, Y., Kang, J., and Hu, Z.: Global dust](#)
2229 [impacts on biogeochemical cycles and climate, *Nature Reviews Earth & Environment*, 6, 789-807,](#)
2230 [https://doi.org/10.1038/s43017-025-00734-2, 2025.](#)

2231 [Zang, L., Zhang, Y., Zhu, B., Mao, F., Zhang, Y., and Wang, Z.: Characteristics of water-soluble inorganic](#)
2232 [aerosol pollution and its meteorological response in Wuhan, Central China, *Atmospheric Pollution*](#)
2233 [Research, 12, 362-369, <https://doi.org/10.1016/j.apr.2021.01.003>, 2021.](#)

2234 Zhan, C., Han, Y., Cao, J., Wei, C., Zhang, J., and An, Z.: Validation and application of a thermal–optical
2235 reflectance (TOR) method for measuring black carbon in loess sediments, *Chemosphere*, 91, 1462-
2236 1470, <https://doi.org/10.1016/j.chemosphere.2012.12.011>, 2013.

2237 Zhan, C.-L., Zhan, J.-W., Ke, Z.-D., Liu, S., Zhang, J.-Q. and Liu, H.-X.: Pollution characteristics and
2238 source analysis of black carbon in different types of dust in Xiaogan, Hubei (in Chinese),
2239 *Environmental Pollution and Control* 44(01), 14-19 + 26, <https://doi.org/10.15985/j.cnki.1001->
2240 3865, 2022.

2241 Zhan, C.-L., Zhang, J.-Q., Zheng, J.-G., Yao, R.-Z., Xiao, W.-S. and Cao, J.-J.: Pollution
2242 characteristics and source analysis of black carbon in atmospheric dust along National Highway 316
2243 (in Chinese), *Environmental Science and Technology*, 39(04), 154-160, <https://doi.org/10.3969->
2244 [j.issn.1003-6504.20169](#), 2016.

2245 [Zhang, B., Shen, Z., Sun, J., He, K., Zou, H., Zhang, Q., Li, J., Xu, H., Liu, S., Ho, K.-F., and Cao,](#)
2246 [J.: County-level of particle and gases emission inventory for animal dung burning in the](#)
2247 [Qinghai–Tibetan Plateau, China, *Journal of Cleaner Production*, 367,](#)
2248 [https://doi.org/10.1016/j.jclepro.2022.133051, 2022.](#)

2249 Zhang, F.: Study on the dry deposition of organic carbon and elemental carbon in the atmosphere of
2250 Nanchang (in Chinese), Master's Thesis, 2014.

2251 Zhang, F., Wang, Z. W., Cheng, H. R., Lv, X. P., Gong, W., Wang, X. M., and Zhang, G.: Seasonal
2252 variations and chemical characteristics of PM_{2.5} in Wuhan, central China, *Science of the Total*
2253 *Environment*, 518-519, 97-105, <https://doi.org/10.1016/j.scitotenv>, 2015a.

2254 ~~Zhang, J., Liu, H. N., Zheng, Q. P., and Tang, L. J.: Correlation study between particulate matter and~~
2255 ~~visibility in Suzhou, Proceedings of the 7th Annual Conference of Chinese Society of Particuology~~
2256 ~~cum Symposium on Particle Technology across Taiwan Straits, Xi'an, Shaanxi, China, 1, 2010.~~

2257 Zhang, H. and Han, F.: The preliminary remote sensing interpretation of salt lake and its environments
2258 in the Central Qaidam Basin, Northwest China, *Journal of Salt Lake Research*, 10, 28-34, 2002.

2259 ~~Zhang, H., Zhang, F., Song, J., Tan, M. L., Kung, H. T., and Johnson, V. C.: Pollutant source, ecological~~
2260 ~~and human health risks assessment of heavy metals in soils from coal mining areas in Xinjiang,~~
2261 ~~China, Environmental Resesreh, 202, 111702, 10.1016/j.envres.2021.111702, 2021a.~~

2262 Zhang, J., Smith, K. R., Ma, Y., Ye, S., Jiang, F., Qi, W., Liu, P., Khalil, M. A. K., Rasmussen, R. A., and
2263 Thorneloe, S. A.: Greenhouse gases and other airborne pollutants from household stoves in China:
2264 a database for emission factors, *Atmospheric Environment*, 34, 4537-4549,
2265 [https://doi.org/10.1016/S1352-2310\(99\)00450-1](https://doi.org/10.1016/S1352-2310(99)00450-1), 2000.

2266 Zhang, J., Huang, X., Li, J., Chen, L., Zhao, R., Wang, R., Sun, W., Chen, C., Su, Y., Wang, F., Huang,
2267 Y., and Lin, C.: Chemical composition, sources and evolution of PM_{2.5} during wintertime in the city
2268 cluster of southern Sichuan, China, *Atmospheric Pollution Research*, 14, 101635,
2269 <https://doi.org/10.1016/j.apr.2022.101635>, 2023.

2270 Zhang, K., Shang, X., Herrmann, H., Meng, F., Mo, Z., Chen, J., and Lv, W.: Approaches for identifying
2271 PM_{2.5} source types and source areas at a remote background site of South China in spring, *Science*
2272 *of The Total Environment*, 691, 1320-1327, <https://doi.org/10.1016/j.scitotenv>, 2019.

2273 Zhang, N., Cao, J., Liu, S., Zhao, Z., Xu, H., and Xiao, S.: Chemical composition and sources of PM_{2.5}
2274 and TSP collected at Qinghai Lake during summertime, *Atmospheric Research*, 138, 213-222,
2275 <https://doi.org/10.1016/j.atmosres>, 2014.

2276 Zhang, P.-X.: Salt lakes in the Qaidam Basin (in Chinese), Beijing: Science Press, 1987.

2277 Zhang, R., Wang, H., Qian, Y., Rasch, P. J., Easter, R. C., Ma, P. L., Singh, B., Huang, J., and Fu, Q.:
2278 Quantifying sources, transport, deposition, and radiative forcing of black carbon over the Himalayas

2279 and Tibetan Plateau, *Atmospheric Chemistry and Physics*, 15, 6205-6223,
2280 <https://doi.org/10.5194/acp-15-6205-2015>, 2015b.

2281 [Zhang, R., Jing, J., Tao, J., Hsu, S. C., Wang, G., Cao, J., Lee, C. S. L., Zhu, L., Chen, Z., Zhao, Y., and](#)
2282 [Shen, Z.: Chemical characterization and source apportionment of PM_{2.5} in Beijing: seasonal](#)
2283 [perspective, *Atmospheric Chemistry and Physics*, 13, 7053-7074, \[https://doi.org/10.5194/acp-13-\]\(https://doi.org/10.5194/acp-13-7053-2013\)](#)
2284 [7053-2013, 2013.](#)

2285 [Zhang, S.: Spatial and temporal variation characteristics of atmospheric dust deposition flux in Hebei](#)
2286 [Province over the Recent 20 Years, Master's thesis, Hebei Normal University, 2010.](#)

2287 Zhang, X. Y., Wang, Y. Q., Zhang, X. C., Guo, W., and Gong, S. L.: Carbonaceous aerosol composition
2288 over various regions of China during 2006, *Journal of Geophysical Research: Atmospheres*, 113,
2289 <https://doi.org/10.1029/2007jd009525>, 2008.

2290 Zhang, X. Y., Wang, Y. Q., Wang, D., Gong, S. L., Arimoto, R., Mao, L. J., and Li, J.: Characterization
2291 and sources of regional-scale transported carbonaceous and dust aerosols from different pathways
2292 in coastal and sandy land areas of China, *Journal of Geophysical Research: Atmospheres*, 110,
2293 <https://doi.org/10.1029/2004jd005457>, 2005.

2294 [Zhang, Y.: Satellite Observation and ground validation of volatile organic compounds emissions from](#)
2295 [biomass combustion, Master's thesis, Yunnan University,](#)
2296 <https://doi.org/10.27456/d.cnki.gyndu.2024.002784>, 2024.

2297 Zhang, Z., Zhou, Y., Zhao, N., Li, H., Tohniyaz, B., Mperejekumana, P., Hong, Q., Wu, R., Li, G., Sultan,
2298 M., Zayan, A. M. I., Cao, J., Ahmad, R., and Dong, R.: Clean heating during winter season in
2299 Northern China: A review, *Renewable and Sustainable Energy Reviews*, 149, 111339,
2300 [https://doi.org/10.1016/j.rser, 2021b](https://doi.org/10.1016/j.rser.2021b).

2301 Zhang, Z.-C., Xie, Y.-Q., Zhang, Z.-J., Gao, G.-S., Xu, B., Tian, X., Xu, H., Wie, Y.-T., Shi, G.-L.
2302 and Feng, Y.-C.: Source analysis and seasonal variation characteristics of atmospheric dust
2303 deposition in Taiyuan City based on two receptor models (in Chinese), *China Environmental*
2304 *Science*, 42, 2577-2586, <https://doi.org/10.3969/j.issn.1000-6923>, 2022.

2305 Zhao, Z., Cao, J., Shen, Z., Xu, B., Zhu, C., Chen, L. W. A., Su, X., Liu, S., Han, Y., Wang, G., and Ho,
2306 K.: Aerosol particles at a high-altitude site on the Southeast Tibetan Plateau, China: Implications
2307 for pollution transport from South Asia, *Journal of Geophysical Research: Atmospheres*, 118,
2308 <https://doi.org/10.1002/jgrd.50599>, 2013.

2309 Zheng, J., Hu, M., Du, Z., Shang, D., Gong, Z., Qin, Y., Fang, J., Gu, F., Li, M., Peng, J., Li, J., Zhang,
2310 Y., Huang, X., He, L., Wu, Y., and Guo, S.: Influence of biomass burning from South Asia at a high-
2311 altitude mountain receptor site in China, *Atmospheric Chemistry and Physics*, 17, 6853-6864,
2312 <https://doi.org/10.5194/acp-17-6853-2017>, 2017.

2313 Zheng, K., Li, Y., Li, Z., and Huang, J.: Provenance tracing of dust using rare earth elements in recent
2314 snow deposited during the pre-monsoon season from mountain glaciers in the central to northern
2315 Tibetan Plateau, *Environmental Science and Pollution Research*, 28, 45765-45779,
2316 <https://doi.org/10.1007/s11356-021-13561-x>, 2021.

2317 Zheng, M.-P.: Geological report on salt lake resources and ecological environment in China (in Chinese),
2318 *Acta Geologica Sinica*, 84: 1613-1622. <https://doi.org/DOI-10.19762/j.cnki.dizhixuebao>, 2017.

2319 Zhou, Y., Gao, X., and Lei, J.: Characteristics of dust weather in the Tarim Basin from 1989 to 2021 and
2320 its impact on the atmospheric environment, <https://doi.org/10.3390/rs15071804>, 2023.

2321 Zhou, Y., Yang, J., Kang, S., Hu, Y., Chen, X., Xu, M., and Ma, M.: Black carbon aerosols impact
2322 snowfall over the Tibetan Plateau, *Geoscience Frontiers*, 16, 101978, <https://doi.org/10.1016/j.gsf>,
2323 2025.

2324 Zhu, C.-S., Chen, C.-C., Cao, J.-J., Tsai, C.-J., Chou, C. C. K., Liu, S.-C., and Roam, G.-D.:
2325 Characterization of carbon fractions for atmospheric fine particles and nanoparticles in a highway
2326 tunnel, *Atmospheric Environment*, 44, 2668-2673, <https://doi.org/10.1016/j.atmosenv>, 2010.

2327 Zhu, H., Li, W., Kong, X., and Zhang, X.: Overlooked contribution of salt lake emissions: A case study
2328 of dust deposition from the Qinghai-Xizang Plateau, *Journal of Geophysical Research: Atmospheres*,
2329 130, e2024JD042693, <https://doi.org/10.1029/2024JD042693>, 2025.

2330 Zhu, H.-X.: The dust deposition data of the Qaidam Basin [Data—set]. Zenodo.
2331 <https://doi.org/10.5281/zenodo.14382853>, 2024.

2332 [Zhu, X., Zhu, K., Xie, M., Huang, A., Ouyang, Y., Chen, F., and Zhao, W.: Analysis of current](https://doi.org/10.1007/s11356-016-15171-2)
2333 [situation and future trend of anthropogenic heat emissions in Jiangsu Province, *Climatic and*](https://doi.org/10.1007/s11356-016-15171-2)
2334 [*Environmental Research*, 21, 306-312, <https://doi.org/10.3878/j.issn.1006-9585.2016.15171>,](https://doi.org/10.1007/s11356-016-15171-2)
2335 [2016.](https://doi.org/10.3878/j.issn.1006-9585.2016.15171)